Effect of DNA Damage and Repair Mechanisms in Human Haematopoiesis and their role in Chemoresistance of Acute Myeloid Leukaemia

Amy Bradburn

University College London

and

The Francis Crick Institute

PhD Supervisor: Prof. Dominique Bonnet

A thesis submitted for the degree of

Doctor of Philosophy

University College London

September 2016

Declaration

I Amy Bradburn confirm that the work presented in this thesis is my own. Where information has been derived from other sources, I confirm that this has been indicated in the thesis.

Abstract

Most standard AML chemotherapy regimes utilize Ara-C, a cytotoxic compound inflicting DNA damage in proliferating cells and inducing cell death. Comparing normal and malignant haematopoietic cells in their response to Ara-C will determine whether differing responses to DNA damage and activation of DNA repair mechanisms contribute to chemoresistance. Moreover, DNA repair in primitive human haematopoiesis and LIC's is still not well established.

Using AML cell lines, cord blood and CD34+ AML patient samples, a characterization of the DNA damage response post Ara-C treatment was performed. AML cell lines were shown to have a range of sensitivities with significant increases in DNA damage after Ara-C exposure. However, cell lines resistant to Ara-C, were quicker to recover their DNA damage, with a faster revival of cell numbers and reduction in apoptosis. Similar findings were also observed when using ionizing radiation as a source of DNA damage. Analysis of the DNA repair mechanisms non-homologous end joining (NHEJ) and homologous recombination (HR) by 53BP1 and RAD51 localization respectively, showed NHEJ was preferentially used in response to Ara-C, with low rates of HR.

Normal haematopoietic stem and progenitor populations were compared with leukaemia initiating and tumour populations of CD34+ AML patient samples *in vivo*. Normal stem populations showed significant increases in apoptosis with enrichment in cells in G0 after exposure to Ara-C. Progenitor cells were more refractory to treatment and displayed a G1/S-phase accumulation. When observing AML patient samples it appeared they either behaved in a progenitor, or a stem like manner, showing heterogeneous responses overall. Just like the AML cell lines NHEJ was primarily observed, with some basal level of activation. Overall there are differences in normal stem progenitor and cells in response to Ara-C, with AML patient samples displaying a more heterogeneous response to DNA damage.

Acknowledgement

I would like to thank my supervisor Dr Dominique Bonnet for giving me the opportunity to work in her lab and for the support and guidance in managing my project. Special thanks to Fernando Anjos-Afonso for taking me under his wing and giving me lots of encouragement and cake over the years.

To all past and present members of the HSC lab, you have made this experience unforgettable and it's been a great pleasure to work with you all. Even if my accent confused you at times…

Thank you to the core facilities, especially the FACs lab, who went above and beyond with my laborious cell sorts.

And lastly, thank you to all my friends and family for their invaluable love and support. I can finally say I'm done at last!

Table of Contents

Table of figures

List of tables

Abbreviations

2HG	2-hydroxyglutarate
AML	Acute Myeloid Leukaemia
ASPP1	Apoptosis stimulating protein of p53
ATM	Ataxia Telangiectasia mutated Serine/Threonine Kinase
ATR	Ataxia Telangiectasia and Rad3-related
BER	Base excision repair
BM	Bone marrow
BSA	Bovine Serum Albumin
CB	Cord blood
CDK	Cyclin Dependent Kinase
cDNA	Complementary deoxyribose nucleic acid
CFU	Colony forming unit
CLP	Common lymphoid progenitor
CMP	Common myeloid progenitor
DAPI	4', 6'-diamidino-2-phenylindole
DDR	DNA damage response
DMSO	Dimethyl sulfoxide
DNA	Deoxyribose Nucleic Acid
DNA-PK	DNA-dependent protein kinase
DSB	Double strand breaks
FA	Fanconi Anaemia
FACS	Fluorescence activated cell sorting
FBS	Foetal Bovine Serum
FL	Foetal Liver
Flt3	FMS-like tyrosine kinase 3
GCSF	Growth factor colony stimulating factor
GMP	Granulocyte macrophage progenitor
HPC	Haematopoietic progenitor cells
HR	Homologous recombination
HSC	Haematopoietic stem cell
HSPC	Haematopoietic stem and progenitor cells

IDH1/2	Isocitrate dehydrogenase 1/2
IF	Immunofluorescence
IMDM	Iscove's Modified Dulbeccos's medium
ITD	Internal tandem duplications
i.v	Intravenous injection
LIC	Leukaemia initiating cell
LIG3	DNA Ligase III
LIG4	DNA Ligase IV
LMPP	Lymphoid primed multipotent progenitor
LSC	Leukaemic stem cell
LSK	Lineage-, Sca-1+, C-Kit-
LT-HSC	Long-term haematopoietic stem cell
MDS	Myelodysplastic Syndrome
MEP	Megakaryocyte-erythroid progenitor
MLP	Myeloid lymphoid Progenitor
MMR	Mismatch Repair
MNC	Mononuclear cells
MPP	Multipotent progenitor
MRN	MRE11-RAD50-NBS1 complex
NER	Nucleotide Excision Repair
NHEJ	Non-homologous end joining
NOD	Non-obese diabetic
NSG	NOD SCID gamma
PBS	Phosphate buffered saline
PCR	Polymerase chain reaction
PFA	Paraformaldehyde
RAD51	Homolog of RecA
RNA	Ribonucleic acid
ROS	Reactive Oxygen Species
RPMI	Roswell Park Memorial Institute
RT	Room temperature
SCID	Severe combined immune deficient
SCF	Stem cell factor
SSB	Singe-strand breaks

ST-HSC	Short term haematopoietic stem cell
TF	Transcription factor
TKD	Tyrosine Kinase Domain
TPO	Thrombopoietin
UCB	Umbilical cord blood

Chapter 1. Introduction

1.1 Normal Haematopoiesis

Within the mammalian body, blood is one of the most highly regenerated tissues with ~10 billion of new cells being produced on a daily basis in a human adult. For systems with such high cellular turnover, stem cells and their self-renewal properties are paramount to the on-going regeneration, maintenance and function of their resulting organs. The haematopoietic system is one of the most established and researched adult stem cell hierarchies. It was over a century ago that biologists began to hypothesise that all blood lineages were organised in a hierarchical nature deriving from a common precursor, which would be coined the haematopoietic stem cell (HSC) (Maximow, 1909). However definitive proof of the existence of such a blood stem cell wouldn't be discovered until decades later when the more advanced methods available showed that HSC's had multi-lineage potential using *in vivo* repopulation assays (Becker et al., 1963, Till and McCulloch, 1961). These seminal studies opened the gateway into the study and characterisation of the haematopoietic hierarchy, which places the HSC at the apex and mature terminally differentiated erythrocytes, lymphoid cells and myeloid cells at the ends of the hierarchy branches (Eaves, 2015).

Significant breakthroughs in the architecture of the haematopoietic system and its regulation would not have been possible without vertebrate models, such as zebrafish and the mouse. Knowledge gained from these animal studies has been translated to better aid our understanding of the human system, where understandably direct human experimentation cannot be performed. It has only been through clinical observations and major technological advances with *in vitro* assays and *in vivo* xenograft models where huge progress has been made in the ability to directly study human haematopoiesis (Doulatov et al., 2012).

1.1.1 Haematopoietic Hierarchy

At the top of the haematopoietic hierarchy lays the long-term HSC (LT-HSC). This precious reservoir of cells is retained throughout the lifetime of the individual and is

largely quiescent. However, to create the full haematopoietic system, while maintaining their own numbers, LT-HSC must divide asymmetrically and self-renew. Thus this creates new pools of differentiated progeny termed the short-term HSC (ST-HSC) and multipotent progenitors (MPP). These populations have decreased self-renewal ability and higher proliferative capacity compared to the LT-HSC, allowing the LT-HSC to maintain its integrity. This means the ST-HSC/MPP's are the real powerhouses of the haematopoietic system, as they retain multi-potency and can give rise to abundant numbers of differentiated oligopotent progenitors.

To be able to accurately replenish the high turnover of erythrocytes and balance the amount of myeloid and lymphoid cells in the bone marrow and periphery, the hierarchy needs to be a tightly regulated homeostatic process. This relies on very specific cell autonomous and environmental queues where during times of stress, such as infection or bleeding, the haematopoietic system must be able to quickly and accurately mount an appropriate response. This may require producing more of a certain mature blood cell to ensure homeostasis is maintained. Therefore, the hierarchical nature of the blood system is a robust and efficient way to ensure regeneration while protecting the valuable pool of HSC's.

1.1.2 Haematopoietic stem cells

HSC are typically identified from other haematopoietic cells by the expression of certain immunogenic surface markers and by their functional capacity to self-renew and reconstitute multiple mature blood lineages. Although much progress has been made in the ability to directly study human haematopoiesis, many questions can still only be feasibly answered by examining the murine haematopoietic system. This means the need for in depth characterisation of the murine LT-HSC and resulting progeny. Mature populations are first excluded based on a combination of surface markers exclusively expressed on lineage-committed cells. The resulting lineage negative cells can be further purified for functional HSC's by expression of Sca-1 (Stem cells antigen-1) (Spangrude et al., 1988) and c-Kit (receptor tyrosine kinase; CD117) (Morrison and Weissman, 1994). Known as the LSK population, this is a mixture of LT-HSC, ST-HSC and MPPs with heterogeneous self-renewal

ability where 100 cells have been shown to have long-term repopulating ability in lethally irradiated murine hosts (Okada et al., 1992). Further enrichment for more purified stem populations were later characterised by negative expression of CD34 and Flt3 (Fms-like receptor tyrosine kinase 3; CD135) (LSK-CD34$^-$Flt3$^-$) (Osawa et al., 1996, Adolfsson et al., 2001, Yang et al., 2005). However, more recently an alternative way using antigens from the Slam family of markers, CD48 and CD150 (LSK-CD150$^+$CD48$^-$), has produced functionally similar populations of LT-HSC (Kiel et al., 2005).

Although characterisation of the human LT-HSC has been challenging due to experimental limitations, there has been great success over the decades in refining a highly purified stem population. Key to this has been the use of the xenograft model and the development of fluorescence activated cell sorting (FACS) technologies. This relies on the transplantation of populations of human haematopoietic cells in limiting dilution, which have been purified by FACS based on surface marker expression, to help assess multi-lineage repopulating ability. One of the first widely accepted molecules for identification of immature haematopoietic cells was the CD34 antigen (Civin et al., 1984). Although its exact function has not been fully elucidated it is believed to be involved in cell-cell adhesion and attachment to the bone extracellular matrix (Nielsen and McNagny, 2009). CD34+ cells make up a mixture of haematopoietic stem and progenitor cells (HSPC), which constitute 1-4% of bone marrow mononuclear cells (MNC) (Civin et al., 1984) and approximately 2% of umbilical cord blood (UCB) (Fritsch et al., 1996). Primitive populations were further defined by discovery of the CD90 (Thy-1) antigen, where Lin-CD34+CD90+ cells were able to repopulate SCID mice with both myeloid and lymphoid lineage engraftment (Baum, 1993). Additional refinement was also attained by the negative selection of the CD38 glycoprotein (Bhatia et al., 1997) and CD45RA markers (Lansdorp et al., 1990).

Hence, the human HSC was primarily identified as Lin-CD34+CD38-CD90+CD45RA-, with Majeti et al., showing long-term multi-lineage engraftment in a third of NSG (*non-obese* diabetic (NOD)-severe combined immunodeficient (scid) IL2rγ (null)) mice engrafted with as little as 10 cells (Majeti et al., 2007b). It was anticipated that the loss of CD90 would characterise the more differentiated MPP,

however CD34+CD90- cells were still able to serially transplant, even if diminished in their ability compared to the CD90+ HSCs (Majeti et al., 2007b). This led the need to find the closest progeny to the HSC where self-renewal was properly diminished, based on something further than negative and positive CD90 expression. Integrin's were a prime candidate as it had already been shown in the murine HSC that expression of integrin α2 (CD49b) allowed the differentiation between ST-HSC and LT-HSC (Benveniste et al., 2010). This led to the discovery that integrin α6 (CD49f) surface marker expression, on purified human single cells injected intra-bone, were able to engraft long-term with multi-lineage output with successful secondary transplantation (Notta et al., 2011). Therefore overall, it's widely accepted that Lin-CD34+CD38-CD90+CD45RA-CD49f+ defines a very pure human LT-HSC population.

Recent studies have provided evidence for another layer on top of the human hierarchy, beyond a CD34+ stem cell, which reflects the murine CD34- HSC. CD34- cells purified from UCB were shown to give rise to CD34+ cells and multi-lineage engraftments when injected intra-bone into SCID mice (Ishii et al., 2011). Attempts to find additional surface markers for better identification of these cells uncovered expression of CD93 or CD133 (promonin-1) as good candidates for further purification (Takahashi et al., 2014, Danet et al., 2002). As well, using serial transplantation assays, they appear to possess greater self-renewal capacity than CD34+ HSC. Evidence suggests these cells are able to differentiate into CD34+ cells providing a strong case for an additional layer at the top of the haematopoietic hierarchy (Anjos-Afonso et al., 2013).

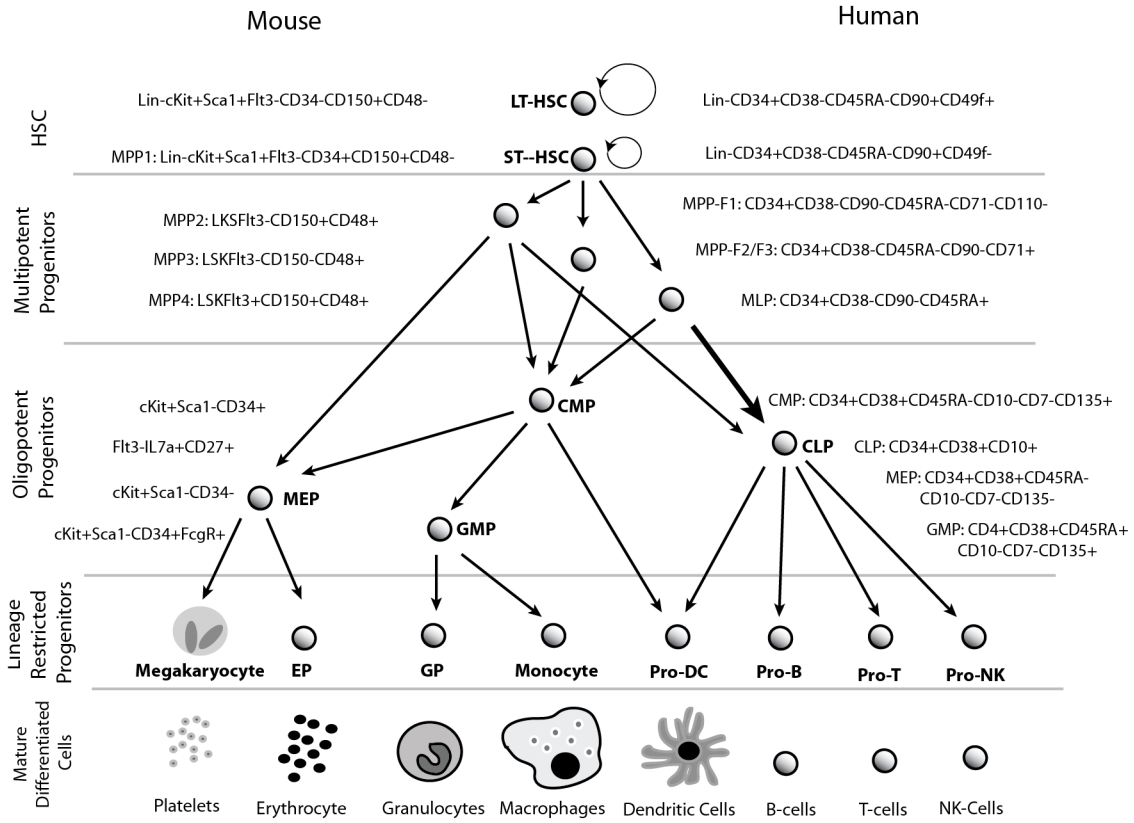

Figure 1.1 The human and murine haematopoietic hierarchy.

1.1.3 Multi-potent progenitors

Directly beyond the HSC in the hierarchy lies the MPP, which are characterised with decreased self-renewal but retention of full differentiation capacity. In the mouse this was defined as the CD34+Flt3+LSK population, which retains multi-potency but with reduction in self-renewal capacity (Adolfsson et al., 2001). This helped support the idea that decreasing self-renewal gives way to increasing lineage commitment. However, efforts over the last few years have further defined the murine MPP into functionally different subpopulations. It was observed previously that in LSK, high expression of Flt3+ outlined cells that were still multipotent but possessed lymphoid bias (Adolfsson et al., 2005). These were dubbed lymphoid-primed MPP (LMPP), only to be renamed a couple of years later to MPP4 when evidence of myeloid biased subpopulations MPP2 (Flt3-CD150+CD48+LSK) and MPP3 (Flt3-CD150-CD48+LSK) emerged, primarily distinguished by their negative expression of Flt3 (Wilson et al., 2008). In this analogy MPP1 refers to a metabolically active murine HSC, unlike the quiescent

CD34- HSC (Cabezas-Wallscheid et al., 2014). In depth functionality studies comparing the different MPPs, by individually transplanting each population, showed each was produced independently by the HSC and gave rise to multi-potent engraftment up to 4 weeks (Pietras et al., 2015). Yet the different MPP were biased, as respectively described before, in their generation of mature cells.

In the human system the MPP population was previously distinguished as Lin-CD34+CD38-CD45RA-CD90-CD49f- and when transplanted into NSG mice, gave a transient short-term multi-potent engraftment, which peaked at 4 weeks and became indiscernible by 16 weeks (Majeti et al., 2007a). Again, this reflected that the MPP could be defined as having multi-potent potential yet reduced self-renewal compared to the HSC. More recently they were sub-fractionated, based on the expression of CD71 (Transferrin receptor) and CD110 (Thrombopoietin receptor), into MPP F1, F2 and F3 (Notta et al., 2016). Just like the murine MPP populations, these were shown to display early lineage bias with F1 able to give rise to predominantly megakaryocytes and F2/F3 cells being more biased towards erythroid lineages. A comparison of these populations was undertaken through different development stages of haematopoiesis by analysing foetal liver (FL), CB and adult BM. It could be seen that there was a fundamental developmental shift as FL presented more oligopotent progenitors whereas the adult BM held primarily unipotent progenitors, appearing to come directly from MPPs. This could potentially redefine adult haematopoiesis as being a ‘two-tier’ system, unlike the current widely accepted model of a hierarchy with progressively differentiated populations (Figure 2).

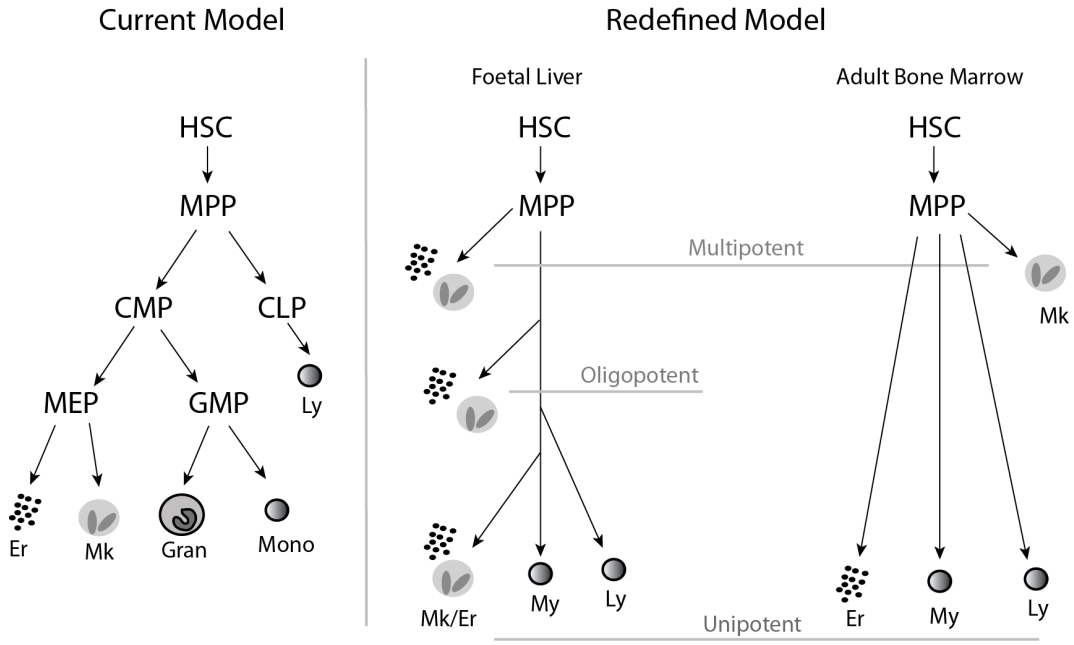

Figure 1.2 Redefined model of human haematopoiesis.

The current still widely accepted model of haematopoiesis states that cells mature through a number of differentiation stages, with intermediate progenitor cells, which progressively lose potency to eventually reach mature unipotent haematopoietic cells. However Notta et al., showed that in adult bone marrow unipotent cells can arise directly from multipotent progeny, suggesting the oligopotent step in between is not required, therefore creating a two-tier system in adult haematopoiesis instead of a hierarchy.

1.1.4 Progenitors

Downstream of the MPPs lies the lineage restricted progenitors that reside in the Lin-CD34+CD38+ fraction of human CB and bone marrow. The CD45RA and CD123 (IL-3Rα) surface markers can primarily define the myeloid hierarchy into the common myeloid progenitor (CMP), which gives rise to the granulocyte/macrophage progenitors (GMP), and in turn differentiates into the megakaryocyte/erythrocyte progenitors (MEPs). These progenitors allow the production of granulocytes, dendritic cells, monocytes (GMP), megakaryocytes and erythrocytes (MEP) (Manz et al., 2002).

The standard human hierarchical model states that the separation of myeloid and lymphoid lineages occurs at the split between CMP and the common lymphoid progenitor (CLP), creating the first lineage commitment step. As described in the previous section, this is now under dispute with evidence of early lineage biasing

taking place before differentiation into lineage commitment. A multi-lymphoid progenitor (MLP) population, described as CD34+CD38-CD90-CD45RA+CD10+, gave rise to all lymphoid lineages and possessed some myeloid potential, but no erythroid or granulocytic segregation (Doulatov et al., 2010). As well, in comparison to the murine LMPP, a human counterpart in UCB was described as CD34+CD38-CD45RA+CD10-, which had the added ability to produce granulocytes compared to the MLP (Goardon et al., 2011a). This showed that expression of CD10+ was required for lymphoid differentiation whereas CD10- cells were chiefly myeloid. However, these studies were preformed using UCB and analysis of adult BM showed that the LMPP population is actually within the CD38+ fraction and expresses high levels of CD62L (L-selectin) (Kohn et al., 2012). Work by Yamamoto et al has even described a “myeloid bypass model’ wherein the murine HSC can asymmetrically divide to directly produce a fully lineage committed myeloid precursor with long-term repopulating ability (Yamamoto et al., 2013). Evidently there’s not a clear-cut delineation between myeloid and lymphoid commitment as previously thought.

1.1.5 In vivo Assays – Xenograft Model

As eluded too in previous sections, use of the xenograft model has been paramount in the study of human haematopoiesis. The expression of certain panels of surface markers on haematopoietic cells does not guarantee they behave in a homogenous manner, meaning functionality must be tested by assessing long-term and multi-lineage engraftment potential of purified cells injected into immunodeficient mice.

Success of the xenograft model relies on three key principles:

1. The recipient mouse must be sufficiently immune deficient to reduce the possibility of graft rejection.
2. There must be a suitable niche for accommodation of human cells.
3. The niche must be able to support the human haematopoietic cells over a long period of time.

One of the first widely used models was the server combined immunodeficient (SCID) mouse, which lack T and B lymphocytes, and must to be irradiated pre-

engraftment to clear the bone marrow of murine cells and provide niche spaces for human HSC (McCune et al., 1988). This model however requires larges numbers of donor cells to be injected and still holds an innate immune system, with presence of natural killer (NK) cells and macrophages impeding engraftment.

To solve the problem of residual macrophages, the SCID model was crossed with mice on the non-obese diabetic (NOD) background, providing immune deficient mice whose macrophages can tolerate human material (Pflumio et al., 1996). Irradiated NOD/SCID mice permit the engraftment of small numbers of human CD34+ cells and are able to reconstitute a multi-lineage engraftment (Shultz et al., 2005).

Nevertheless, the NOD/SCID model does not come without its caveats. With a high occurrence of thymic lymphoma and the prevalence of natural killer (NK) cells, long-term engraftment studies were a struggle to perform (Prochazka et al., 1992). To achieve disruption of NK cells, the IL-2 receptor common gamma chain (IL-2Rγ) was deleted to interfere with cytokine signalling downstream of IL-15, a crucial cytokine needed for NK development (Ito et al., 2002). This resulted in the NOD/SCID/ IL-2Rγnull (NSG) model, devoid of B, T and NK cells with tolerant macrophages, which is now one of the most commonly used models for xenograft studies.

Additionally, attempts to humanize the mouse, ensuring sufficient homing, maintenance and differentiation of the human HSC, have been undertaken. Expression of the human cytokines thrombopoietin (TPO); IL-3; granulocyte-macrophage colony stimulating factor (GM-CSF) and stem cell factor (SCF) have all been achieved in the murine system (Chen et al., 2009). They help create a more hospitable environment, by creating a deficiency in the murine cytokines thus causing impairment of the host HSC and macrophages (Willinger et al., 2011).

All these improvements have helped the maintenance and differentiation of human HSPC post engraftment and have been so far invaluable in the study of human haematopoiesis. However, the xenograft models still do not come without their limitations. While primitive populations are well recapitulated in NOD/SCID and

NSG mice, the differentiation into mature lineages is largely impaired. Development of functional myeloid and NK cells is limited with a bias towards production of lymphoid B cells, which is not reflective of the human situation (Manz, 2007). The NSG-SGM3 model, which expresses SCF, GM-CSF and IL-3, was specifically designed to aid the engraftment and support of myeloid/lymphoid cells. Although this provides higher engraftment levels, it comes at the expense of early exhaustion of the HSC (Nicolini et al., 2004). This leads to another drawback in delineating the appropriate time-point to assess the end-point of engraftment. This is of particularly importance as engraftment of HSPC is transient, with ST-HSC providing multi-lineage engraftment from 6-12 weeks wherein LT-HSC begin to take over and enable engraftment beyond into 6 months. Most investigators implement a 12-week engraftment window for their analysis.

Despite its drawbacks the immune deficient mouse model is still the best assay available for evaluating human haematopoietic cell functionality.

1.1.6 In vitro assays

In vitro assays are another widely used method for analysing haematopoietic stem and progenitor cells. They provide a system for the easy manipulation of culture conditions allowing assessment of numerous parameters such as interactions with the microenvironment and responses to drug treatments (Barnett et al., 1991). Crucially, the long-term culture of primitive haematopoietic cells requires an adherent stromal cell layer for sufficient support and maintenance over time. This feeder layer aids in mimicking the bone marrow microenvironment and pioneering studies originally utilized mesenchymal cells purified from bone marrow (Sutherland et al., 1989). Currently, most cultures are done with the immortalized murine stromal cell line MS-5 which are able to support human HSC and allow differentiation of primitive progenitors (Issaad et al., 1993, Kanai et al., 2000).

1.2 Acute Myeloid Leukaemia

1.2.1 Leukaemia: The Disease

Acute myeloid leukaemia (AML) is a severe malignancy of the myeloid compartment resulting in excesses of immature heterogeneous myeloid cells that are unable to differentiate. The uncontrolled growth of leukaemic cells infiltrates the bone marrow and spills out into the peripheral blood. Current data shows that patients under the age of 60 have a 35-40% cure rate, however for patients >60 years of age this is only 5-15%, showing the outlook for older AML patients still remains extremely poor (Dohner et al., 2010).

Prognosis	Cytogenetic Abnormality
Good	t(15;17)(q22;q21) PML/RARA
	t(8;21)(q22;q22) AML1-ETO
	inv(16)(p13q22)/t(16;16)(p13;q22)
Intermediate	Normal Karyotype
	Or karyotypes not otherwise categorised as good or poor prognosis.
Poor	inv(3)(q21q26)/t(3;3)(q21;q26)
	add(5q), del(5q), -5
	-7, add(7q)/del(7q)
	t(6;11)(q27;q23) KMT2A/MLLT4
	t(10;11)(p11~13;q23)
	t(9;22)(q34;q11)
	Complex (≥4 unrelated abnormalities)
	-17/abn(17p)
	abn(3q)

Table 1.1 MRC prognostic classification of AML based on karyotypes.
Adapted from (Grimwade et al., 2010).

AML is categorised into prognostic categories based on cytogenetic abnormalities, which help predict the outcome and best treatment strategy upon initial screening (Byrd et al., 2002). Chromosomal abnormalities have long been recognised as key

drivers that cause and promote the leukaemic disease. Good prognosis karyotypes consist of the onco-fusion proteins AML1/ETO and PML/RARA and inversions on chromosome 16. Cytogenetically normal patients, who make up approximately 40-50% of cases, are categorised as intermediate risk due to the difficulty to predict clinical outcome based on obvious karyotypes and the heterogeneity displayed in response to therapy. Lastly, poor risk groups include complex karyotypes with >4 aberrations and certain specific karyotypes as outlined in Table 1.1.

Due to the advent of deep sequencing techniques the heterogeneous response of normal karyotype AML samples was unravelled when it was found that there were several gene specific mutations potentially being harboured in each patient (CancerGenomeAtlasResearch, 2013), even though compared to other malignancies, the mutational burden is quite low (Table 1.2). Many of these mutations are now themselves being used as predictive markers and have helped shed light on the molecular control of AML, even becoming direct targets for novel chemotherapies.

NPM1 is the most commonly mutated gene, present in approximately 30% of patients. Mutations result in the abnormal expression of the *NPM1* protein within the cytoplasm, which helps fuel proliferation (Cheng et al., 2010). Expression predicts a favourable outcome and is associated with chemo-sensitivity. However, this effect is revoked in the presence of a Fms-Like Tyrosine Kinase 3 (*FLT3)* mutation (Döhner et al., 2005).

Mutations in *FLT3* come in two forms: internal tandem duplications (ITD) in the juxta-membrane domain or mutations in the second tyrosine kinase domain (TKD). Both cause constitutive activation of FLT3 signalling, which promotes blast proliferation (Kelly et al., 2002). FLT3-ITD is associated with an increased incidence of relapse and the degree to which it acts as a marker for poor prognosis relies on the allelic burden and whether the ITD is present in the juxta-membrane domain (Gale et al., 2008, Pratcorona et al., 2013).

Gene	Overall Frequency
FLT3	19-28% (FLT3-ITD) and 5-10% (FLT3-TKD)
NPM1	27-35%
DNMT3A	26%
NRAS	8-9%
ASXL1	17-19%
CEBPA	4-6%
TET2	8-9%
WT1	6-7%
IDH2	8-9%
IDH1	9%
KIT	2-4%
RUNX1	5-10%
MLL-PTD	5%
NRAS	8-9%
PHF6	3%
KRAS	2-4%
TP53	2-8%
EZH2	2%
JAK2	1-3%

Table 1.2 Frequency of gene mutations in AML.
Adapted from Molecular therapy for acute myeloid leukaemia (Coombs et al., 2016).

Mutations in *DNMT3A*, *IDH1/IDH2* and *TET2* are all involved in epigenetic changes. *DNMT3A,* which codes for a DNA methyltransferase, conveys an adverse prognosis after acquisition of missense mutations (Marcucci et al., 2012). Mutations in the isocitrate dehydrogenase 1 and 2 genes cause gain-of-functions of the enzymes they code for which acquire the new ability to catalyse the reduction of α-KG to 2-hydroxyglutarate (2HG) (Cairns and Mak, 2013). 2HG is an oncometabolite with the ability to inhibit TET enzymes resulting in hypermethylation phenotypes. As well as the effect of *IDH1* on TET enzymes, loss of function mutations in *TET2* are

evident, however the prognostic significance of this is still unclear (Chou et al., 2011, Metzeler et al., 2011).

1.2.2 Leukaemic Initiating Cells: The Hierarchy

Just like their normal counterparts, AML cells are arranged in a hierarchical nature with stem-like leukaemia initiating cells (LIC) at the apex, giving rise to more differentiated tumour cells. Thus creating a malignant mimicry of the normal haematopoietic system.

The original model established stated that all LICs were contained within the CD34+CD38- compartment (Bonnet and Dick, 1997), similar to normal HSC hierarchy. However this paradigm was challenged when it was observed that using the anti-CD38 antibody during population sorting was inhibiting the engraftment of CD38+ samples into mice, in both AML and normal cord blood samples (Taussig et al., 2008). This led to the discovery that LICs could also be CD34+CD38+, revealing a more heterogeneous nature to LICs then realized before. Yet repopulating cells weren't just restricted to the CD34+ compartment as improved xenograft models showed CD34- AML cells could also have LIC activity (Martelli et al., 2010, Sarry et al., 2011). As well, it is now known that specifically LIC can arise from normal LMPP and GMP populations, and coexist in the same sample (Goardon et al., 2011b).

It is generally believed that the LIC is the main contributor to relapse of AML post treatment due to the expression of a stem-like gene signature causing the LIC to have a more quiescent state than its blast progeny (Eppert et al., 2011, Kreso and Dick, 2014). Indeed gene signatures of LSC from the study by Eppert et al. were found to most closely resemble that of normal healthy HSC. However Goardan et al. showed that CD34+ LSC more closely correlated with progenitor gene signatures, with the acquisition of expression of self-renewal genes (Goardon et al., 2011a).

While indeed these studies helped to shed light onto the heterogeneous origin of the LIC and how it might be regulated, over the last few years evidence of a 'pre-

leukaemic stem cell', with mutations in NPM1 and TET2 was described (Jan et al., 2012). Work by Shlush et al. also defined a population of pre-leukaemic stem cells, which held *DNMT3A* mutation, but had not yet progressed to a full leukaemic disease (Shlush et al., 2014). Highly purified HSC, progenitors and mature hematopoietic cells from the blood of an AML patient showed the presence of *DNMT3A* mutation at high allele frequency, but no *NPM1* mutation, which was present within the AML blasts of the same patient. The *DNMT3A* mutant HSC had multi-lineage potential when engrafted into mice and showed a repopulation advantage over healthy HSC counterparts and when the patient was in remission, clones were still present in the bone marrow. These pre-leukaemic HSC have helped to show a role for commonly observed mutations in initiation of AML.

1.2.3 Therapeutic Regimes

The backbone of treatment for AML has remained relatively unchanged for decades. Standard induction therapy for AML utilises the "7+3" regime of 3 days of anthracycline treatment from either daunorubicin or idarubicin and seven days of continuous Ara-C treatment (Cheson et al., 2003). This system is able to achieve a complete remission in around 65%–73% of young patients and only 38%–62% of patients over 60 years of age. As these regimes can be quite harsh, elderly patients require having their fitness tested first and if deemed unfit will be put on a lower dose regime.

To prevent relapse and eliminate minimal residual disease after a remission has been achieved, patients under go consolidation therapy, which uses intermediate dose Ara-C twice daily on a cycle every 2 days (Byrd et al., 2002). This has shown to be an effective regimen for good risk patients under 60 years of age. However, for intermediate and high-risk patients allogeneic bone marrow transplant remains the most effective long-term cure (Popat et al., 2012). Indeed, upon relapse many patients become refractory to treatment and a bone marrow transplant is the only hope for these patients.

1.3 DNA Damage Response and DNA Repair Mechanisms

DNA is essential for the on-going development, maintenance and reproduction of all life forms. Each day the cells in the human body receive masses of DNA lesions, which if left unchecked can endanger the viability of the cell or whole organism through mutations or larger genomic aberrations. These insults to DNA can come from multiple sources such as replicative stress, exposure to UV light, ionizing radiation or reactive oxygen species to name but a few. Lesions most commonly come in the form of single-strand DNA breaks (SSBs) and in more severe cases double strand DNA breaks (DSBs), which are more lethal and difficult for the cell to repair. Fortunately cells have formed highly effective DNA damage response and repair mechanisms to aid in combatting the diverse range of ways DNA lesions can arise and to protect from the daily onslaught of stresses. However, any alterations in these pathways can lead to the creation of mutations, which may aid in the formation and progression of diseases such as cancer. Therefore it is in the cells best interest to effectively manage and repair any DNA damage occurred and maintain genomic integrity for the health of the organism.

1.3.1 DNA Damage Response

The DNA damage response is a highly evolved and concerted mechanism for the detection of DNA damage. From the recognition of DNA damage to the promotion of repair, it orchestrates a wide range of signals to ensure the appropriate response is achieved. Key molecules in the process are the serine/threonine kinases ATM and ATR, which are activated by the presence of DSBs and SSBs respectively (Cimprich and Cortez, 2008, Shiloh, 2003). DSBs are recognised by the MRN complex (formed of MRE11-RAD50-NBS1), which helps act as a bridge between the DSB and recruits ATM. This allows ATM to phosphorylate many downstream targets, such as the histone H2A variant on serine 139, which acts as a good experimental marker for DSBs (Savic et al., 2009). Whereas SSBs recruit ATR through the recognition of RPA proteins binding to ssDNA (Zou and Elledge, 2003). In response to DNA damage two of the main molecules that ATR and ATM activate are CHK1 and CHK2 respectively (Shiloh, 2003), however evidence has suggested that this is not a mutually exclusive activation an there is overlap between the

pathways (Abraham, 2001). These protein kinases help reduce levels of cyclin-dependent kinases (CDKs) so cells with DNA damage will halt cycling at key cell cycle checkpoints and allow themselves time to repair (Bartek and Lukas, 2007). One way they do this is by phosphorylating the phosphatase Cdc25A, which targets it for proteolytic degradation, thus stopping it promoting the G1/S phase transition by dephosphorylating Cdk2 or the G2/M transition by dehosphorylating Cdc2 (Donzelli and Draetta, 2003, Molinari et al., 2000).

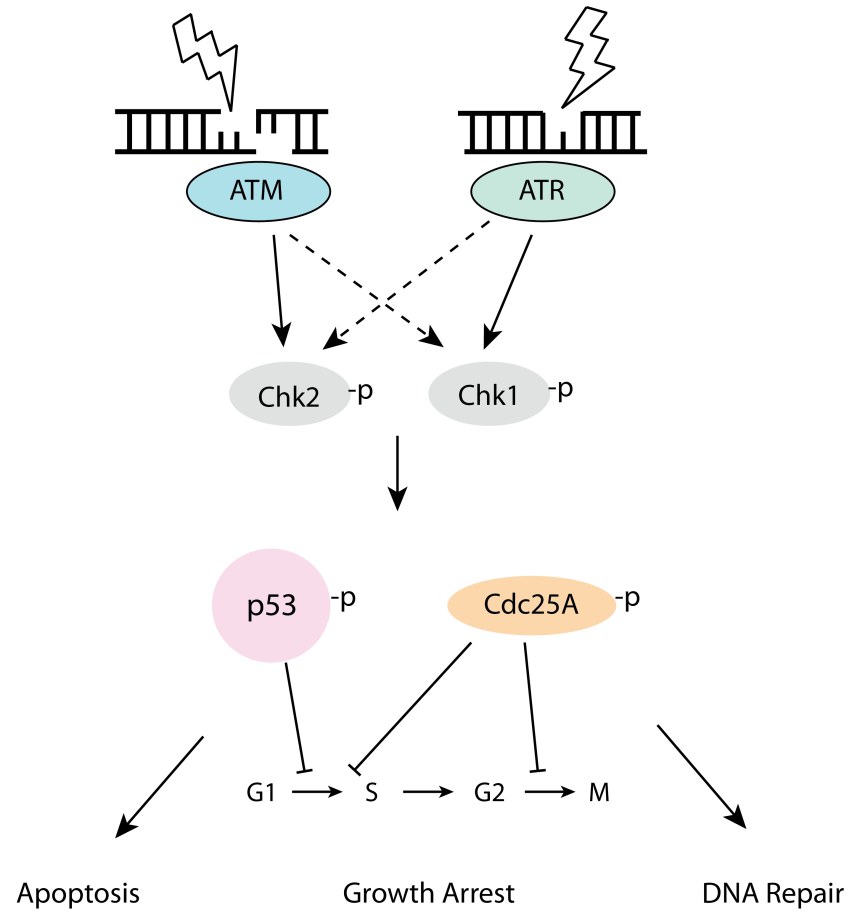

Figure 1.3 Components of the DNA Damage response.

DNA breaks are recognised by the serine/threonine protein kinases ATM and ATR. They phosphorylate Chk1 and Chk2 proteins which act as transducers to activate effectors such as p53 and Cdc25A to exert their effects on cell cycle checkpoints and co-ordinate how the cell overcomes the DNA damage.

The CHK1/2 proteins have also been shown to mediate part of their effect through phosphorylation of p53, a well-studied and integral player in the DNA damage response often called the 'Guardian of the Genome' (Shieh et al., 2000, Lane,

1992). Upon activation, p53 can orchestrate an extremely vast and complex set of responses to DNA damage through its action as a transcription factor and aids the cell in the decision to either repair any DNA damage incurred or to initiate apoptosis making it a potent tumour suppressor. Two of the most well recognised genes that have been implicated in this process, and are transcriptionally regulated by p53, are p21 and *PUMA*. PUMA (p53–up-regulated modulator of apoptosis) is a BH3 family protein, which induces apoptosis through the mitochondrial pathway (Yu and Zhang, 2003), while expression of p21 induces a growth arrest at the G1/S phase, allowing time for the decision to enter into DNA repair or senescence (Barboza et al., 2006). However, in what way p53 fully mediates these effects and the downstream pathways it influences in the decision between DNA repair and apoptosis are still under intensive investigation.

1.3.2 DNA Repair Mechanisms

There are several mechanisms of DNA repair to deal with the different types of lesions DNA can acquire. Base excision repair (BER) excises single nucleotide bases that have become chemically damaged, such as 8-oxoguanine, and relies on DNA glycosylases to 'flip' the damaged base out from the DNA (Hitomi et al., 2007). Mismatch repair (MMR) corrects the misincorporation of bases during DNA replication and any insertion/deletion loops formed by slippage of the polymerase during repetitive sequences. This process is highly conserved from *E.coli* to humans and is regulated primarily by the MutS and MutL components (Li, 2008). Nucleotide excision repair (NER) differs from BER in that it primarily repairs bulky adducts that distort the DNA helix. These can be caused by 6-4 photoproducts from UV damage, pyrimidine dimers and DNA crosslinks (Costa et al., 2003).

Double strand breaks are prepared by either homologous recombination (HR) non-homologous end joining (NHEJ). HR repair is the restricted to the S-G2 phases of the cycle and uses the undamaged sister chromatid as a template for accurate repair (Li and Heyer, 2008). Upon the detection of DNA damage the MRN complex

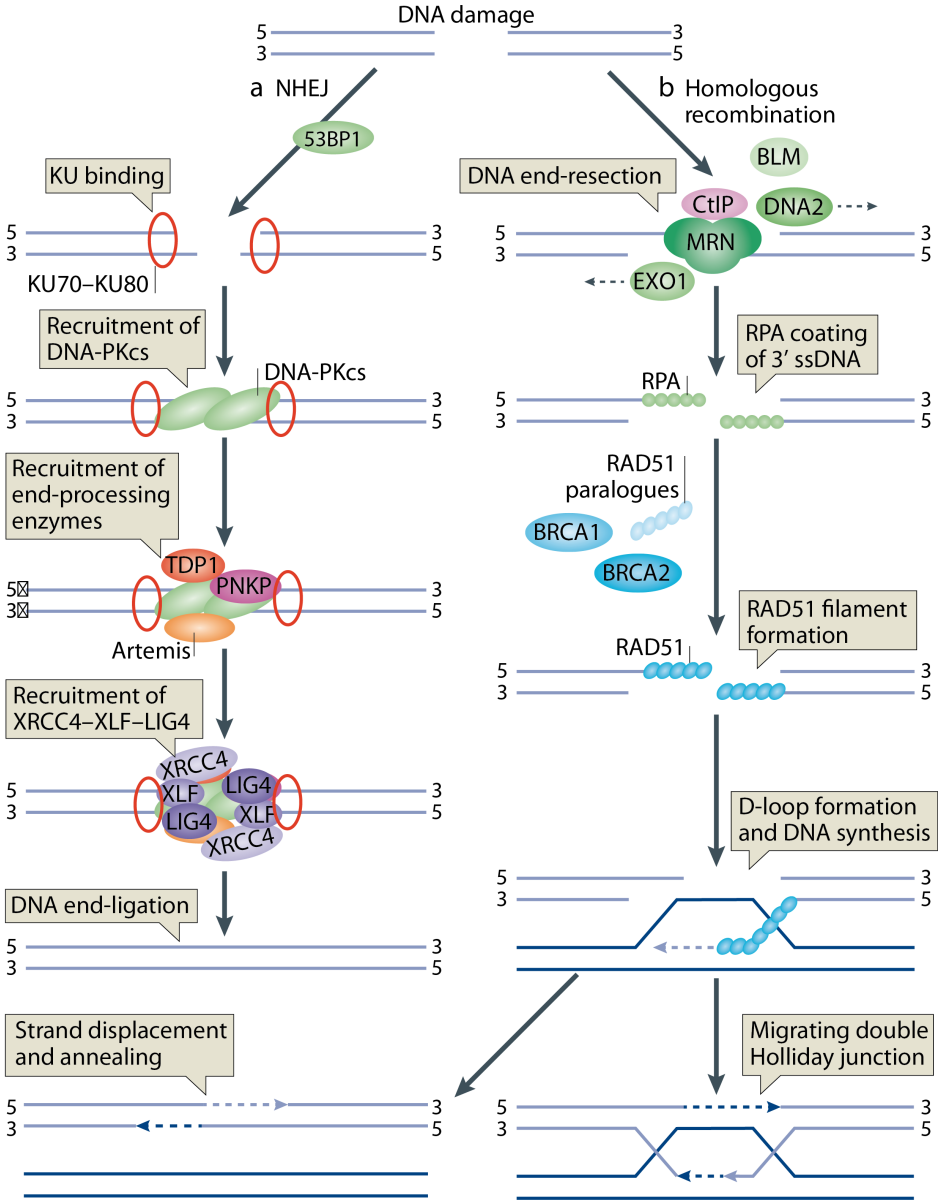

Figure 1.4 DNA double strand break repair mechanisms: Non-homologous end joining and homologous recombination.

Adapted from 'Double-strand break repair: 53BP1 comes into focus.' (Panier and Boulton, 2014).

recruits the exonuclease Exo1, which resects the ends of the DNA breaks to single strands that become coated with RPA protein. Mediated by BRCA2 and Rad52, the RAD51 recombinase is recruited to the DNA break to begin strand invasion of the sister chromatid and the damaged DNA is re-copied from the undamaged template (Sugiyama and Kowalczykowski, 2002). On the other hand NHEJ is a more error-

prone form of repair, which directly ligates the DNA break back together with minimal end processing (Lieber, 2010b). This process can take place during any phase of the cell cycle. The Ku70/Ku80 heterodimer binds directly to the exposed DNA ends and recruits the catalytic subunit DNA-PKcs that holds the DNA together and recruits end-processing factors, which may result in the loss of some DNA bases. The final step requires recruitment of the XRCC4/DNA Ligase IV complex, which ligates the DNA back together (Ahnesorg et al., 2006).

1.3.3 DNA Damage Response and Repair in the Haematopoietic System

The blood is a highly regenerative tissue compartment and the HSC must function throughout its life to sustain an on-going haematopoiesis. Preceding the discovery of the HSC it was observed that survivors of the Hiroshima bombings, who were exposed to persistent low doses of irradiation, most often died of haematopoietic failures. This led to work in bone marrow transplants and development of assays for studying the radio-sensitivity of haematopoietic cells (Jacobson et al., 1950). While it has been known for decades that primitive haematopoietic cells in the BM are exquisitely sensitive to DNA damage insult by irradiation, the mechanisms surrounding this are only beginning to be unravelled. For their on-going function it is paramount HSC ensure they maintain genomic integrity as any mutations or DNA damage incurred can be passed down to more differentiated daughter cells.

A number of protective properties have been shown to aid in avoiding the accumulation of DNA damage in HSCs. Such as HSC are known to reside in hypoxic niches and maintain low levels of metabolic rates, which limits exposure to reactive oxygen species (ROS) (Kocabas et al., 2012, Suda et al., 2011) and are primarily quiescent, which reduces replicative stress (Wilson et al., 2008).

In response to irradiation it has been shown that human CB cells presented differential responses when comparing HSC and progenitor populations (Lin-CD34+CD38+) (Milyavsky et al., 2010). HSC underwent apoptosis more readily than progenitors and displayed persistence of γH2AX foci. This was shown to be exerted via a p53-dependent mechanism, as knockdown of p53 or up-regulation of

Bcl-2 abrogated this effect. Analysis of global expression profiles highlighted the expression of a molecular regulator of p53, known as ASPP1 (apoptosis-stimulating protein of p53), that was more highly expressed in the HSC than progenitor populations and was responsible for the priming of human HSC to apoptosis (Milyavsky et al., 2010).

At the same time a study on the murine HSC response to irradiation was also published which showed the opposite result, however they compared HSPC with myeloid progenitors CMP and GMPs (Mohrin et al., 2010). The myeloid progenitors were shown to have a higher induction of apoptosis compared to HSPCs and increased expression of pro-apoptotic genes, thus making them more primed for cell death in response to DNA damage. Analysis of p53 showed it was active in all the populations in response to irradiation, yet was causing a p21 mediated growth arrest in HSPC and inducing apoptosis in the myeloid progenitors, showing a dual role for p53 in murine haematopoietic cells.

Another study went deeper into the murine phenotype and saw that murine LT-HSCs, in response to irradiation, was also apoptosis resistant. However in contrast to the previously described study, they did not activate p53 (Insinga et al., 2013). There was also a large increase in p21 expression, which was upregulated in a p53-independent manner, and induced symmetric division. As the previous study by Mohrin et al., only analysed HSPC populations, this p53-independent mechanism was no doubt masked by the heterogeneity of the populations being analysed. However recent work by Yamashita et al., added another layer of complexity onto this story by showing the murine LT-HSC predominantly expressed Aspp1 compared to progenitors and underwent apoptosis mediated by p53 (Yamashita et al., 2015). While this falls in line with what was observed in the human CB model, there still appears to be many discrepancies as to how primitive haematopoietic cells respond to insult from DNA damage by irradiation.

Although there are conflicts as to whether HSCs should survive in response to DNA damage, it is also shown that DNA repair mechanisms are playing an important role in HSC genomic maintenance. In the same study by Mohrin et al., analysis of DNA repair mechanisms showed that quiescent HSPC populations had enhanced

NHEJ repair compared to progenitors and when pushed to cycle, HR repair was preferentially used (Mohrin et al., 2010). As NHEJ is an error-prone form of repair this allowed for the acquisition of mutations and chromosomal aberrations in quiescent cells. However cells that were pushed to cycle acquired fewer mutations due to the use of the higher-fidelity HR repair.

One of the markers of an aged HSC is the accumulation of DNA damage evidenced by persistent γH2AX foci (Rossi et al., 2007, Rube et al., 2011). Beerman et al., showed that during quiescence expression of DNA repair and response genes were attenuated, however upon entry into cell cycle aged HSC repaired their accrual DNA damage and up-regulated a DNA repair gene signature (Beerman et al., 2014). It appears that aged HSC are able to persist in a quiescent state with accrual DNA damage, apparently going against what is believed about HSCs aiming to protect their genomic integrity for the sake of the haematopoietic system. As well, recent work by Moehrle et al. has show that the integrity of DNA repair between young and aged mice is the same, with HSC being resilient to acquiring mutations, something that does not change in the aged HSC (Moehrle et al., 2015). Therefore the paradigm of aging, which posits that DNA damage persistence in quiescent cells is leading to age-associated mutations that are seen in myelodysplastic syndrome (MDS) and AML (Jan et al., 2012, Will et al., 2012), requires further investigation.

Mutations or deletions in DNA repair and response genes have been shown to have negative effects on HSC function. Fanconi Anaemia (FA) is a rare inherited condition where there can be mutations in any one of up to 12 FA proteins, including BRCA2, all of which are involved in DNA repair from damage caused by cross-linking agents or ROS (D'Andrea and Grompe, 2003). Patients present with progressive bone marrow failure and pancytopenia and display a high risk of developing neoplasms such as MDS and AML (Mathew, 2006). MDS itself is a genomic disability disorder with a high propensity for developing into AML with the sequential acquisition of co-operating mutations (Zhou et al., 2013). Recurrent mutations in genes involved in histone modifications such as EZH2 or DNA methylation such as TET2, show as well a potential link for epigenetic regulation of progression of the disease into AML (Graubert and Walter, 2011).

1.3.4 DNA Damage and Repair in Acute Myeloid Leukaemia

It's clear to see that DNA damage plays an integral role in the disease progression of AML. As outlined in the previous sections on AML, the disease is categorised based on chromosomal aberrations and mutational status due to their influence on prognosis and overall survival. Components of the DDR are very rarely mutated in AMLs yet an increasing amount of evidence is showing that aberrant epigenetic control, based on chromosomal translocations often involving epigenetic regulators and transcription factors (TF), create global gene expression changes which can influence DDR genes (Cheung and So, 2011, Krivtsov and Armstrong, 2007).

The AML1/ETO fusion onco-protein exerts it epigenetic effects by recruiting HDAC complexes to its AML-1 TF binding sites (Davis et al., 2003). It has been shown that presence of AML1/ETO alone is not enough to induce a malignancy, and other genetic alterations are required for a full disease initiation. Alcalay et al. showed that genes involved in BER, such as *OGG1,* are down regulated by AML1/ETO, as well as *ATM*, an important mediator of the DDR (Alcalay et al., 2003).

PML/RARA is another fusion onco-protein that exerts effects on the transcription of DNA repair genes via histone modifications (Casorelli et al., 2006). There is down regulation of a number of components involved in HR and NHEJ repair such as *BRCA1* and *DNA-PK*. The fusion partner PML is also known to have a functional role in HR as a stabiliser of RAD51 (Boichuk et al., 2011), and leukaemia's with PML/RARA were revealed to have a reduction in the activity of HR repair, potentially leading to genome instability and accounting for the accumulation of DNA damage see in these cells (Viale et al., 2009). There is also strong p21 expression, independent of p53, in both PML/RARA and AML/ETO leukaemia's, which provides protection from further accumulation of the high amounts of DNA damage they already display. This oncogenic cell cycle restriction is believed to help maintain leukaemic populations and protect from DNA damage induced apoptosis (Viale et al., 2009).

Within MLL rearranged leukaemia's, there are dozens of different fusion partners, with many involved in recruitment of chromatin re-modellers such as the histone methyltransferase DOT1L (Deshpande et al., 2013). MLL fusion proteins have been shown to suppress p53 transcriptional activity by preventing its acetylation upon DNA damage, meaning p21 cannot be induced and DNA will accrue un-repaired (Wiederschain et al., 2005).

However it's not just AML patients with genomic rearrangements that are manipulating DDR to their advantage. Presence of the FLT3-ITD mutation has been shown to confer resistance to cytotoxic agents, potentially due to up regulation of *RAD51* (Bagrintseva et al., 2005). As well, mutant IDH1, a common driver of AML, usually exerts its effects through inhibition of TET2. Yet it was recently shown that IDH1 can provide it's own influences by down regulating the expression of *ATM* thus impairing DNA repair activation and increasing sensitivity to DNA damage (Inoue et al., 2016).

Complex karyotype AML samples are particularly refractory to chemotherapeutic treatment. One of the most common genomic abnormalities in this subgroup is the loss of 5q, which accounts for the reduced expression of two important DDR genes *RAD50*, part of the MRN complex, and *XRCC4* (Lindvall et al., 2004). When DNA damage was analysed in a large panel of complex karyotype AML samples these patients were found to have high levels of constitutive DNA damage and activated Chk1 (Cavelier et al., 2009). This aberrant checkpoint activation provided increased resistance to Ara-C treatment that could be abrogated upon inhibition of Chk1.

DNA damage response and repair mechanisms in AML are clearly intertwined with epigenetic events. Compromised DDR is evidently helping to promote leukaemic transformation, aid disease progression and resistance to chemotherapy.

Chapter 2. Materials & Methods

2.1 General Lab Equipment

Suppliers of materials and reagents are provided below in the relevant methods sections. All plastic ware and tissue culture vessels were purchased from Becton Dickinson (Plymouth, UK) and Corning Life Sciences. Centrifugation of cell suspensions were performed in either an Allegra 6R or Allegra X-12 Beckman Coulter centrifuges.

2.2 Cell Culture

2.2.1 Cell line Maintenance

All cells were cultured at 37^{o}C and 5% CO_2 in humidified incubators. All human leukaemic cell lines were maintained in RPMI (Gibco) supplemented with 10% foetal bovine serum (FBS) (Gibco) and 1% penicillin/streptomycin (Gibco). Cells were passaged every 2-3 days to maintain them at optimal density. Murine MS5 cells were maintained in IMDM (Gibco) with 10% FBS and 1% penicillin/streptomycin. Adherent cells were passaged by trypsinisation and maintained at sub-confluency.

2.2.2 Freezing and Thawing Stocks

Cells for cryopreservation were harvested at low passage number, pelleted at 300xg and resuspended in 500 µl FBS in a cryotube. An equal volume of FBS with 20% dimethylsulfoxide (DMSO) was added and mixed by pipetting. Cryotubes were placed into a cryobox containing isopropanol and placed at -80^{o}C for a minimum 3 days. For long-term storage cells were then subsequently transferred to liquid nitrogen.

Frozen vials were thawed in 37^{o}C water bath and cell suspension was added drop-wise to warm complete medium in a 15ml falcon to dilute the DMSO. Cells were then centrifuged and resuspended in an appropriate volume.

2.3 Umbilical Cord Blood Cells

2.3.1 Source of Samples

Umbilical cord blood was collected from mothers giving birth at the Royal London Hospital, in accordance with a protocol approved by the East London and Research Ethics Committee. Informed and written consent was obtained prior to collection of samples.

2.3.2 Separation of mononuclear cells by Ficoll density centrifugation

Cord blood samples were pooled and diluted 1:2 with PBS. 15 ml of Ficoll (GE Healthcare) was dispensed into 50 ml Falcon tubes and 35 ml of diluted cord blood was slowly layered over the Ficoll. The tubes were then centrifuged at 1600 RPM for 30 minutes at room temperature with slow deceleration.
The layer of mononuclear (MNC) cells was carefully removed with a plastic Pasteur pipette and transferred to a new 50 ml Falcon tube containing 25 ml of 2% FBS/PBS solution to dilute the remaining Ficoll and centrifuged (300xg for 5 minutes). Remaining erythrocytes were lysed with ammonium chloride for 10 minutes at room temperature and the reaction stopped with the addition of FBS. The mononuclear cells were pelleted and resuspended in PBS with 2% FBS for counting using a haemocytometer.

Cells were then either frozen or purified based on immunogenic markers.

2.3.3 CD34 Positive Purification

Fresh MNC that had been separated from cord blood were selected for CD34+ cells using EasySep Human CD34 Positive Selection kit (Stem Cell Technologies, Vancouver) according to manufacturers instructions. All steps were performed using 2% FBS/PBS. Cells were first incubated with EasySep Positive Selection Cocktail at room temperature for 15 minutes and then with EasySep Magnetic nanoparticles at RT for 10 minutes. The stained cells were then placed into an EasySep Magnet for 5 minutes before unselected cells were discarded and CD34+ remained magnetically held to the inside of the tube. The tube was then removed from the magnet and cells resuspended. This was repeated at least 5 times to

ensure a high purity of CD34+ cells. Purity checks were done by FACS before freezing down the cells down in aliquots.

2.4 Acute Myeloid Leukaemia Samples

AML cells were obtained after informed consent from patients attending St Bartholomew's Hospital, London, under a protocol approved by the East London and City Research Ethics Committee. Frozen samples were thawed as described in the previous section.

2.5 In vitro assays

2.5.1 Culture of primary haematopoietic cells

If culturing cells longer than one-week culture dishes were coated with collagen solution (0.3 mg/ml), left to dry then rinsed with PBS. MS-5 cells could then be plated in IMDM (supplemented with 10% FBS, 1% PenStrep) and left to reach sub-confluency before irradiation with 6.8 Gy from a ^{137}Caesium source (IBL 637 Gamma Irradiator) to inhibit further growth.

Freshly thawed positively selected CD34+ UCB cells were resuspended and cultured in Myelocult™H5100 media (Stemcell Technologies) containing 1% PenStrep. Cells were counted on a haemocytometer with trypan blue exclusion and before plating on the MS-5 stromal layers at a density of 1-2x10^3 cell/cm^2. Cultures were left for a minimum of 3 days before any assays were performed. Ara-C (Sigma Aldrich) was diluted in H_2O and added directly to cultures at a final concentration of 500 nM.

2.5.2 Culture of primary acute myeloid leukaemia samples

Stromal layers were prepared as described above. AML samples were thawed (as previously described) and suspended in Myelocult™ H5100 medium (1% PenStrep) for counting with trypan blue exclusion using a haemocytometer. Cells were resuspended to appropriate volume in Myelocult™ supplemented with a

cocktail of cytokines: 20 ng/ml IL-3, 20ng/ml GCSF and 20 ng/ml TPO (PeproTech, London, UK). Samples were plated onto stromal layers at a density of 2.5-5x10^5 cell/ml. For drug treatments, Ara-C (Sigma Aldrich) was diluted in H_2O and added directly to cultures at a final concentration of 500 nM.

2.6 In vivo assays

2.6.1 Mice

All work was performed in accordance with Home Office regulations with the approval of the Francis Cricks Institutes ethics committee. NOD.Cg-*Prkdc*^{scid} *Il2rg*^{tm1Wjl}/SzJ (NOD/SCID/IL2 receptor 2 gamma chain null, NSG) mice were bred at the Clare Hall Laboratories, Francis Crick Institute. Mice were transferred to the animal facility at 7-8 weeks old and housed in sterile conditions and fed acidified water.

2.6.2 Primary Transplantation

24 hours prior to transplantation 8-12 week old mice were sublethally irradiated with 3.75 Gy from a ^{137}Caesium source (IBL 637 Gamma Irradiator). The mice were administered prophylactic antibiotics (Baytril 2.5% via drinking water) three times per week for two weeks after irradiation.
Samples were prepared in 2% FBS/PBS with DNase to inhibit cell clumping. For purified CD34+ cells, 50,000 cells per mouse in a volume of 150 ul were injected. Human AML patient samples were depleted for CD3+ cells prior to injection by using the Okt3 antibody (BioXCell) at a concentration of 1 ug per 1x10^6 of cells. The sample was incubated at room temperature for 30 minutes and taken directly for injection.

Mice were first warmed in a heat box to 38^{o}C to dilate the tail vein and cells were injected intravenously with a 30 G needle and 0.5 ml syringe.

2.6.3 Analysis of human engraftment

Engraftment of human cells in the murine bone marrow was assessed 12 weeks post injection. Mice were sacrificed by cervical dislocation and tibia, femur and ilium dissected bilaterally. Bone marrow was harvesting by flushing the bone cavity with 2% FBS/PBS using a 30 G needle and 1 ml syringe, each mouse was processed individually. Remaining erythrocytes were lysed with 2-3 ml of ammonium chloride for 3 minutes at room temperature. The reaction was stopped by addition of 500 ul FBS and cell were pelleted. The sample was then processed for FACs analysis as described in the next section. Antibodies used are listed in Appendix 7.2.

2.7 Flow Cytometry

2.7.1 Extracellular Staining and Analysis Parameters

Cells were incubated with antibodies at room temperature for 15 minutes, or 4^{o}C for 30 minutes, in the dark in 50 µl 2% FBS/PBS. Samples were subsequently washed and suspended in DAPI (4', 6'-diamidino-2-phenylindole) at concentration 100 ng/ml in 2% FBS/PBS and analysed on a LSRII flow cytometer (BD Biosciences).
For multicolour experiments single colour controls of stained OneComp compensation beads (eBiosciences) were used for compensation of flourochromes. Gates were set to exclude non-viable cells, debris and doublets during analysis. CountBright™ Absolute Count beads (Life Technologies) were used to quantify different populations. A minimum of 10^4 events from the gate of interest was recorded for each sample.

2.7.2 AnnexinV Staining

Cells were first stained for extracellular antigens as previously described, if required. Cells were washed in PBS and resuspended in 30-50 µl AnnexinV staining buffer 10x (BD Pharmingen) diluted 1:10 in distilled water. 5 µl of anti-AnnexinV-APC was added and cells incubated in the dark at room temperature for 15 minutes. Cells were not washed and 300 µl of 1 x Annexin Staining buffer with DAPI 100 ng/ml was added to the sample and analysed straight away. An unlabelled sample was used as a negative control. Live cells undergoing apoptosis

were identified as DAPI negative and AnnexinV positive. DAPI and AnnexinV double positive cells were classed as dead.

2.7.3 Intracellular Staining

Cells were first stained for extracellular markers, washed with PBS and fixed with PFA (Para-formaldehyde) at room temperature for 10 minutes. Cells were washed in PBS and permeabilised with PBS containing 0.1% Triton-X100 for 10 minutes at room temperature. The reaction was stopped by washing with 2% FBS/PBS. Samples were split into two and stained with appropriate isotype control and target antibody for 1 hour at 4^{o}C. Cells were washed with 2% FBS/PBS and resuspended in DAPI 1 µg/ml with 2% FBS/PBS and analysed.

2.7.3.1 γH2AX Staining

For analysis of phosphorylation of H2AX cells were fixed at 37^{o}C for 10 minutes using PFA. Cells were washed with PBS and permeabilized with 0.1% Triton X-100 for 10 minutes at room temperature. Samples were split in two and stained with either 1 µl γH2AX-Alexa647 or 0.5 µl isotype control Alexa647 for 1 hour at 4^{o}C in 2% FBS/PBS. Cells were washed and resuspended in 300 µl 2% FBS/PBS with DAPI 1 µg/ml.

2.7.3.2 Ki67 Staining

For cell cycle analysis cells were fixed and permeabilised as described and stained with 10 µl of anti-Ki67- FITC or isotype control conjugated to FITC. Staining was performed for 1 hour at 4^{o}C. Cells were washed in 2% FBS/PBS and resuspended in 300 µl 2% FBS/PBS with DAPI 1 µg/ml.

2.7.4 Cell Sorting

Cells were stained as previously described and as appropriate for the assay. Samples were resuspended in 1 ml DAPI 100 ng/ml in 2% FBS/PBS and filtered through a 70 µm mesh filter (BD Biosciences) to remove clumps and samples kept on ice. Sorting was performed on either MoFlo XDP (Beckman Coulter), BD FACS Aria or BD Influx sorters using a 100 µm nozzle. Collection tubes contained 2% FCS/PBS and purity checks were performed to check sort quality.

2.8 Molecular Biology

2.8.1 RNA Extraction

Cells were washed in PBS to remove residual serum spun down. RNA was extracted using the Qiagen RNeasy kit according to manufacturers protocol. The RNeasy Microkit was used for samples below $5x10^5$ cells and the RNeasy Mini kit for samples up to $1x10^7$ cells. RNA was eluted in RNase-free distilled water. The RNA concentration and purity was quantified on the Nanodrop 2000c Spectrophotometer (Thermo Scientific) by measuring absorbance at 230 nm, 260 nm and 280 nm. Samples were stored at -80^{o}C.

2.8.2 Reverse Transcription

RNA was reverse transcribed to cDNA using Superscript III M-MLV reverse transcriptase (Invitrogen), according to manufacturers protocol. A maximum of 5 µg of total RNA and oligodT_{20} primers were used per 20 µl reaction. The reaction was incubated for one hour at 50^{o}C, and then inactivated at 70^{o}C for 15 minutes. cDNA was stored at -20^{o}C.

2.8.3 Quantitative real-time PCR

All quantitative PCR (QPCR) was performed with SybrGreen. Reactions were performed in 10 µl reactions with the following components: 5-100 ng cDNA, forward and reverse primers at 300 nM each, 5 µl of SYBR® Green Mastermix (Applied Biosystems) and distilled water to 10 µl. Reactions were run in duplicate or duplicate in 384-well plates. B-Actin was used as normalization control. Thermal cycling was performed in a ViiA™7 Real-Time PCR System (Applied Biosystems).

The run method was as follows:
Hold Stage - 95.0^{o}C 10:00 minutes
Cycle x 40 – Denature 95.0^{o}C 15 seconds, Anneal/extend 60.0^{o}C 1 minute.
Melt Curve – 60^{o}C to 95^{o}C continuous.
Data was analysed using QuantStudio™ Real-Time PCR software (Applied Biosystems).

2.8.4 RT2 Profiler PCR Array

The RT^2 Profiler PCR array (Qaigen) is a 384-well array that has primers for SybrGreen based qPCR pre-loaded into each well. The array contained primers for human DNA repair genes and the house keeping genes, ACTB, B2M, GAPDH, HPRT1 and RPLP0. Targeted wells were arranged in quadruplicate allowing for the analysis of two samples in duplicate on each array plate.

PR reactions were prepared as described before, in 10 µl volume, and pipetted directly into the plate before sealing and centrifuging and running on ViiA™7 Real-Time PCR System (Applied Biosystems) under the conditions described previously. Data was analysed with the aid of the Qiagen GeneGlobe Data analysis centre.

2.8.5 Relative Quantification using $2^{-\Delta\Delta Ct}$

Relative gene expression was expressed as fold change relative to the control sample with samples normalised to a housekeeping gene. Briefly described, the Ct value for the target gene is subtracted from the Ct value of the housekeeping control giving the ΔCt. The ΔCt of the test sample is subtracted from that of the control sample to give the ΔΔCt. Subsequently the ΔΔCt of the test sample is normalised to the control sample and the value is transformed from a logarithmic value to linear and expressed as $2^{-\Delta\Delta Ct}$.

2.9 Immunoflourescence

Purified cells (2000-50,000) were pipetted onto polysine slides (Thermoscientific) and incubated for 20 minutes. Cell were fixed with 2% PFA for 10 minutes at RT, then washed with PBS, before permeabilisation with 0.1% Triton X-100 for 10 minutes at RT. Samples were then blocked for 1 hour at RT in blocking solution (see appendix 7.1). Primary antibodies (see appendix 7.2), either used alone or in combination were diluted in blocking solution and pipetted onto the slide for overnight incubation at 4°C. Slides were washed 3 times with PBS and stained with secondary antibodies in blocking solution for 45 minutes at RT, protected from light. After a final 3 rounds of PBS washes, slides were mounted with fluorescent

mounting medium (Dako) containing 500 ng/ml DAPI and placed with coverslips. Until analysis slides were kept at 4^{o}C in the dark.

2.10 Microscopy

2.10.1 Foci Scoring

Fixed and mounted cells were analysed for foci on an Axioplan2 microscope (Zeiss) using 100x magnification. 100 cells were scored by eye per condition in each experiment.

2.10.2 Confocal Microscopy

Images were captured using the Zeiss LSM710 upright confocal microscope with ZEN software (Zeiss) and processed using Imaris (Bitplane) and Adobe Photoshop CS5.1 and ImageJ.

2.11 Comet Assay

Alkaline comet assay was performed using Trevigen CometSlides. Each slide was prepared by coating with 1.5% normal melting point agarose and dried overnight. Purified cells were resuspended to 1x10^{6} cells per ml in PBS on ice. Positive controls were then irradiated at 10 Gy. 20 µl of cell suspension was transferred to 240 µl of 0.5% low melting point agarose preheated to 37^{o}C. 120 µl of the agarose/cell solution was dropped onto each circle of the slide then covered with a circular coverslip. The agarose was allowed to set at room temperature for 10 minutes then coverslips were removed. Slides were placed in cold lysing solution at 4^{o}C overnight in the dark. A horizontal electrophoresis tank was set up at 4^{o}C in the dark and filled with cold electrophoresis buffer. Slides were placed into the tank in the same orientation and left for 60 minutes, protected from light, for the DNA to unwind. They were run at 20 V constant and 300 mA for 30mins. Post electrophoresis slides were neutralized with neutralization buffer for 3 rounds of 5 minutes. They were then dehydrated in absolute ethanol for 10 minutes and edges of the slides were coated with clear lacquer to inhibit the peeling of the agarose and

left overnight to dry. Cells were stained with ethidium bromide (10 µg/ml) and visualized using Zeiss Axioscope microscope at 40x magnification using Comet Assay IV software (Perceptive Instruments). 50 cells were randomly scored per circle on each slide. Comet tail moment was calculated as DNA migration x Tail intensity. See Appendix 7.1 for buffer recipes.

2.12 Statistical Analysis

The results shown were mean, median or standard deviation values as stated. All statistical analyses were performed using GraphPad Prism software. The Student's t-test was used unless indicated otherwise. A p-value <0.05 was considered significant.

Chapter 3. Results 1: Response of Acute Myeloid Leukaemia Cell Lines to Ara-C Treatment

3.1 Introduction

Since its introduction into clinics in the 1960s, Ara-C has been a mainstay in treatment of AML and is still widely used in most treatment regimes to this day (Short and Ravandi, 2016). This acts as a testament to its effectiveness as a chemotherapeutic drug, which has helped improve the poor clinical outcome of AML patients, with most now able to attain a complete remission. However, long-term outlook for these patients still remains dismal with a 5 year survival rate of 25% due to relapse (Howlader N, 2014). Upon relapse the majority of patients become refractory to previously used treatments and succumb to their disease, with a haematopoietic stem cell transplant usually being the last option available.

Many studies in the past have tried to pinpoint a definitive mechanism for how AML cells develop resistance to Ara-C, with much focus being taken on cellular uptake and metabolism of the drug. Ara-C is a nucleoside analogue which targets proliferating cells by incorporating itself into the cells DNA as the cell replicates leading to chain termination and an unstable replication fork which eventually breaks down and cause double strand breaks (DSBs) (Robak, 2003). Low expression of the human equilibrative transporter (hENT1) (Gati et al., 1997, Gati et al., 1998, Wiley et al., 1982), which influxs the drugs. Reduction in activity of deoxycytidine kinase (dCK) (Bhalla et al., 1984, Stegmann et al., 1993), which phosphorylates Ara-C to it's active form Ara-CTP. Or even increase in cytidine deaminase (CDA) expression (Schroder et al., 1996), which inactivates Ara-C to Ara-U. So far all have been suggested as contributing factors to chemoresistance based on assessment in cell lines and clinical samples. While these studies have presented correlations to adverse drug responses, it appears that no conclusive or targetable mechanisms have come to light and resistance is most likely due to the contribution of many factors.

Deregulation of DNA damage response and repair mechanisms are observed in most malignancies, wherein defects in these pathways are exploited by many cancer therapies, which utilise DNA damaging approaches, and have been heavily implicated in chemotherapy response and resistance (Bouwman and Jonkers, 2012). These irregularities are particularly evident in leukaemia's which inherently accumulate chromosomal aberrations. Ara-C primarily works by its cytotoxic effects of incorporating into DNA at the S-phase of the cell cycle, blocking replication and damaging DNA (Kufe et al., 1980). Thus in its ability to cause DNA damage, a possible factor in resistance to Ara-C treatment could potentially be found by studying DNA damage response and repair mechanisms.

The use of AML cell lines was therefore deployed as an initial study into the effect of Ara-C on normal and malignant haematopoietic cells and DNA damage responses.

3.2 Results

3.2.1 Survival of AML cell lines post Ara-C treatment

As an initial screen AML cell lines were utilised due to the abundance of cells available and for easy optimisation of techniques without wasting valuable primary material. As well, all *in vitro* assays were performed on MS-5 stromal layers to better mimic the bone marrow environment creating a more physiologically relevant assay. Previous work has shown that the stroma has a protective effect on leukaemic cells in response to chemotherapy (Konopleva, 2002), however for the scope of this study the microenvironment interactions will not be assessed as the focus will be on more cell intrinsic properties of DNA damage response.

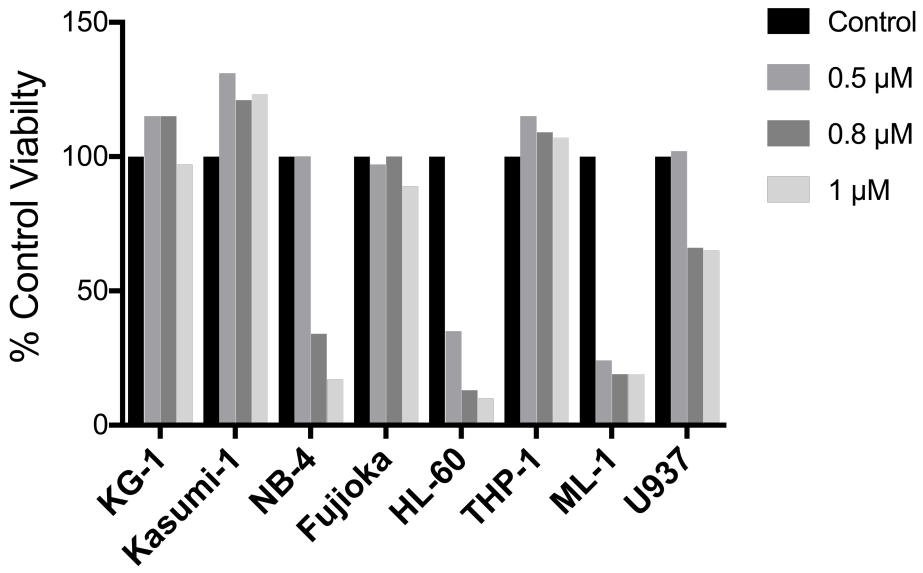

Figure 3.1 Viability screen of a cohort of acute myeloid leukaemia cell lines post Ara-C treatment.

Measurement of viability by XTT assay, 24 hours post varying doses of Ara-C treatment *in vitro*. Normalised to untreated control. (n=2).

After a pre-screening of several AML cell lines, a cohort of three was selected based on their viability after varying doses of Ara-C treatment (Figure 3.1). The HL-60 cell line is an acute promyelocytic cell line with a complex karyotype and amplified c-myc expression (Favera et al., 1982). ML-1 is a myeloblastic cell line harbouring a MLL-AF6 chromosomal translocation (Strout et al., 1996) and the

U937 cell line, although originating from a histiocytic lymphoma (Sundstrom and Nilsson, 1976), displays myelomonocytic characteristics with presence of the leukaemic fusion oncogene CALM/AF10 (Dreyling et al., 1996) and is often used in studies of AML.

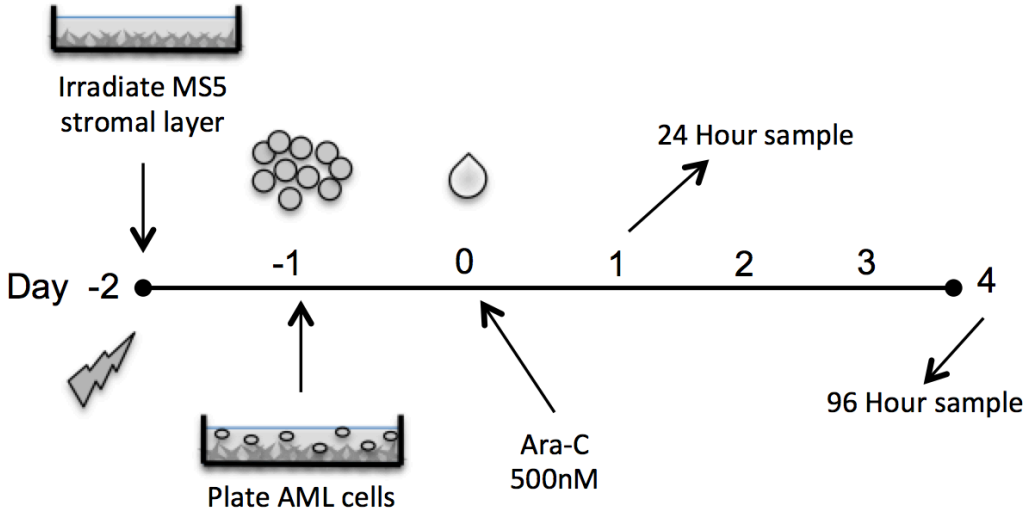

Figure 3.2 Schematic of in vitro treatment protocol for acute myeloid leukaemia cell lines.

Cell lines were plated on MS-5 stromal cell layers before treatment with Ara-C. Samples were taken at 24 and 96 hours post treatment.

Outlined in Figure 3.2 is the treatment protocol created to examine how AML cell lines respond to treatment of Ara-C *in vitro*. Irradiated MS-5 stromal layers were prepared for pre-plating of cell lines, which undergo overnight incubation on stroma, before addition of Ara-C.

It has been shown clinically that patient plasma levels of Ara-C, after a standard dose regime, can reach the range of 0.5-1 μM (Weinstein et al., 1982). Therefore, various doses of Ara-C were tested (Figure 3.1) before resolving on the lower concentration of 0.5 μM, which provided a dose in which adequate material could be collected for analysis post treatment.

As Ara-C works through its incorporation into proliferating cells, it is important to compare two time points, of early (24 hours) and late (96 hours), to ensure sufficient exposure of the drug.

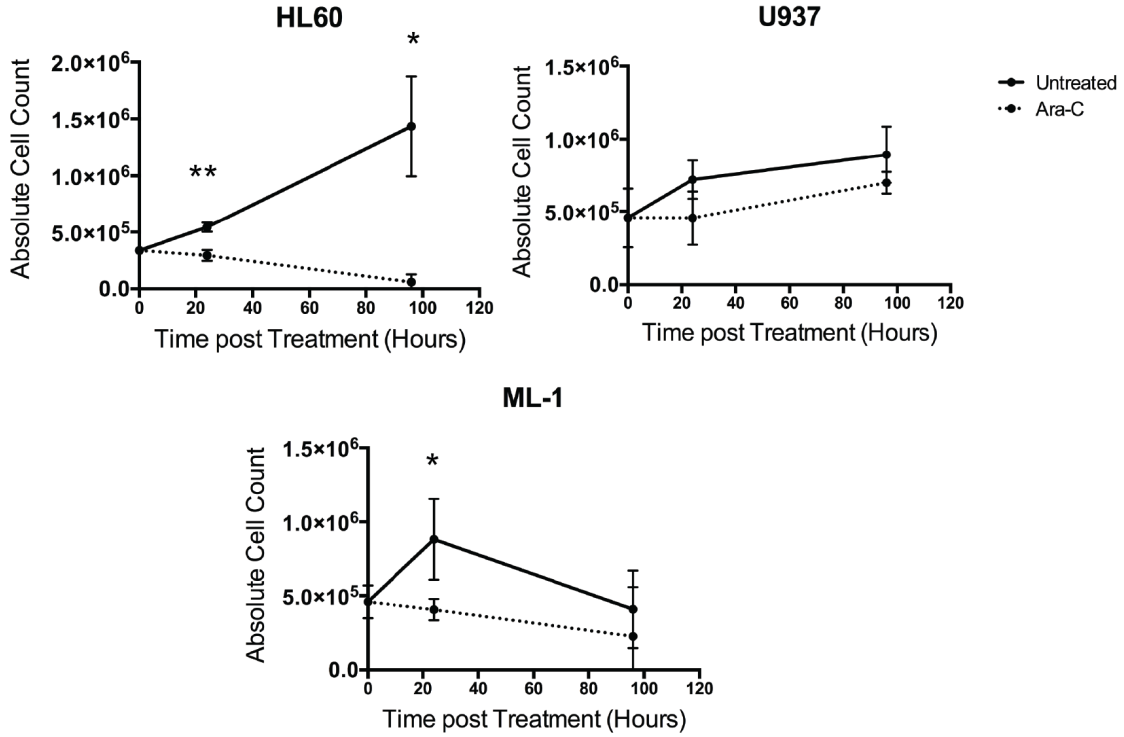

Figure 3.3 Cell count of AML cell lines post Ara-C treatment.

Cell counts at 24 and 96 hours for AML cell lines co-cultured on MS-5 stromal cells in treated (Ara-C 500 nM) or untreated conditions (n=3). *p<0.05, **p<0.005. Error bars are ± S.D (standard deviation of the mean).

After treatment under the conditions outlined, analysis of cell number by FACS (flow cytometry) compared to untreated showed varying reductions up to 96 hours across the panel (Figure 3.3). While the majority of the cell lines showed a continual reduction over time in cell number in the Ara-C treated cells, U937 cell line was much less responsive showing no significant differences compared to untreated (24 hours: p=0.119, 96 hours: p=0.22). All the other cell lines showed varying reductions in cell number, with HL60 cells appearing to be the most sensitive, with the former becoming almost completely diminished by 96 hours. Even though ML-1 cells showed a significant reduction in cell number at 24 hours (*p=0.03), the untreated sample appears to reach a growth plateau by 96 hours.

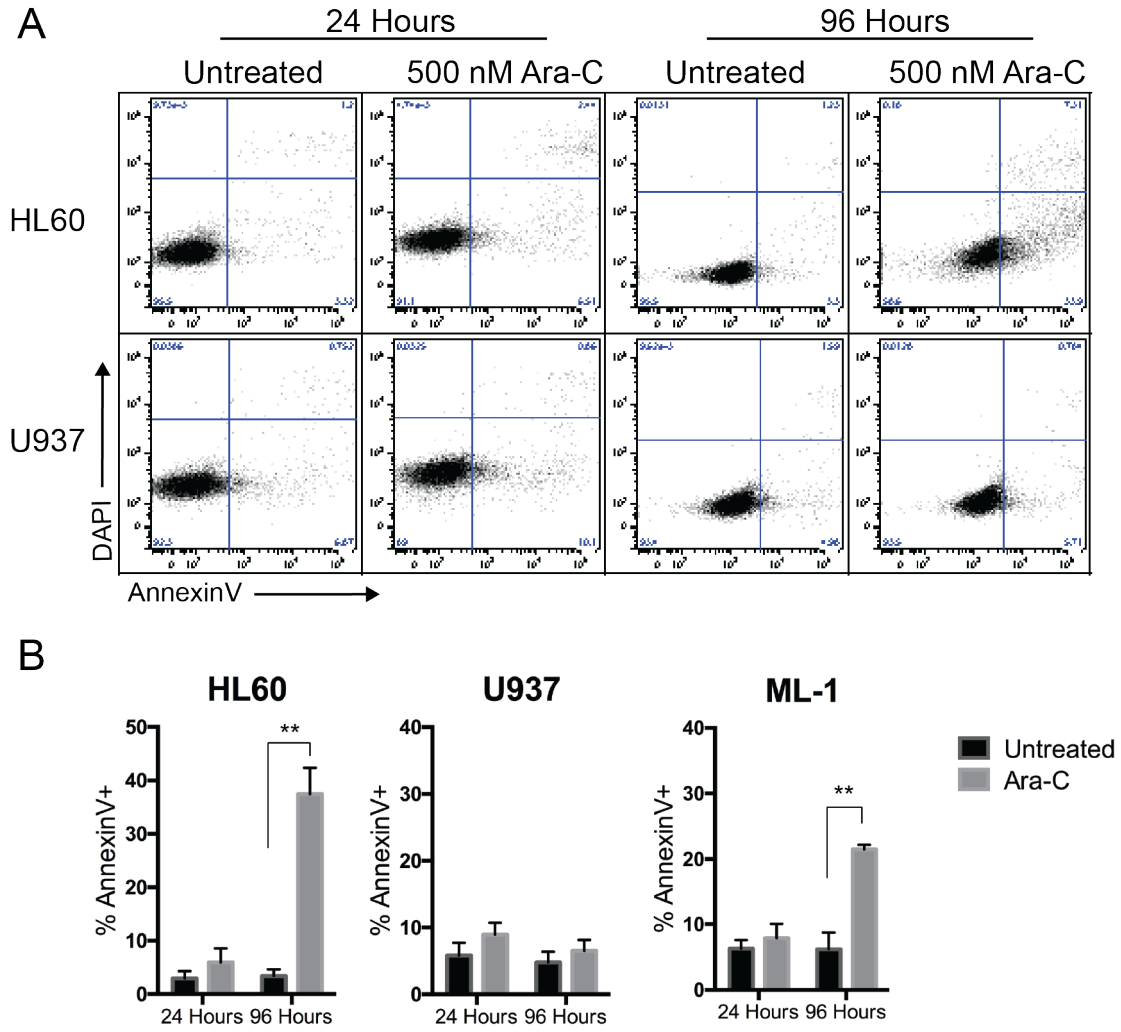

Figure 3.4 AnnexinV+ expression post Ara-C treatment in leukaemic cell lines.

(A) Representative flow cytometry plot of AnnexinV+ and DAPI stained HL60 and U397 cell lines under different timepoints and conditions as stated. (B) Quantification of frequency of AnnexinV positive and DAPI negative stained AML cell lines. Culture conditions were on stromal cell layers over 96 hours in presence of Ara-C 500 nM or untreated. ±S.D (n=3), **p<0.005.

Induction of apoptosis, as shown by AnnexinV+ staining, appeared to reflect these results (Figure 3.4A). Initially, at 24 hours, slight increases but no significant changes can be seen across the panel of cell lines (Figure 3.4B). Yet by 96 hours, HL60 and ML-1 cells displayed an almost 4-fold (**p=0.004) and 2-fold (**p=0.005) increase in apoptosis respectively. This is in sharp contrast to U937 which displayed no significant differences in either AnnexinV staining (p=0.257) or reduction in cell numbers.

These results suggest AML cell lines display different sensitivities to Ara-C based on survival post treatment. However, as the action if Ara-C is dependent on the rate of proliferation, it is important to determine the cell cycle status of these cells.

3.2.2 Cell cycle profile of AML cell lines post Ara-C treatment

As shown in section 3.2.1, differences in survival of the AML cell lines in exposure to Ara-C treatment could potentially be determined by cell cycle status as action of Ara-C is dependent on the cell being in the S-phase.

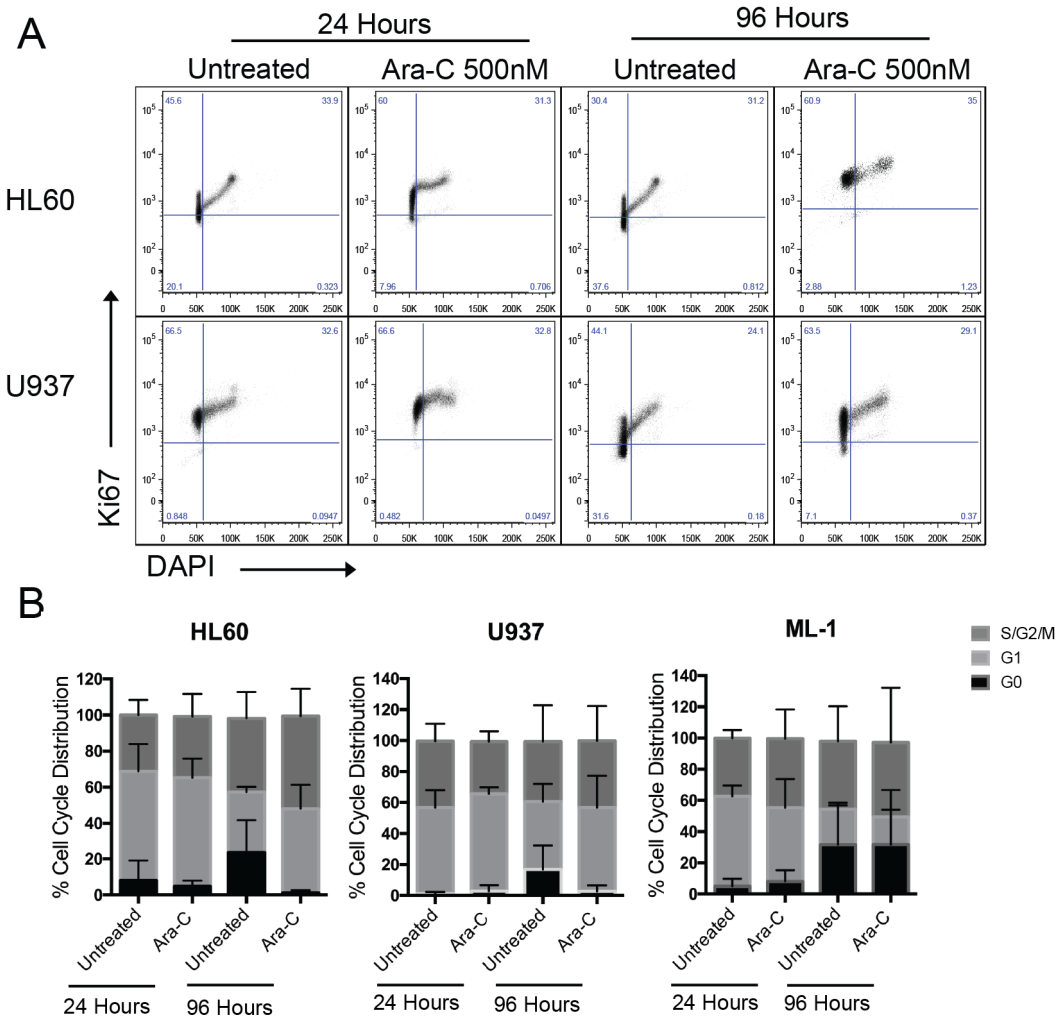

Figure 3.5 Cell cycle profile of Ara-C treated leukaemic cell lines.

(A) Representative flow cytometry plots of Ki67 and DAPI stained HL60 and U937 cell lines at indicated conditions. (B) Quantification of Ki67 and DAPI stained AML cell lines for analysis of cell cycle profile. Culture conditions were on stromal cell layers over 96 hours in presence of Ara-C 500 nM or untreated. ±S.D (n = 3).

Using the same treatment protocol as previously, the different phases of the cell cycle were determined by examining Ki67 and DAPI content by FACS (Figure 3.5A).

Across all cell lines approximately 40% of the cells were within the S-phase at any one time, showing equal opportunity for the effect of Ara-C (Figure 3.5B). HL60 cells appeared to be the only sample, at 24 vs 96 hours Ara-C treated, that showed a slight S-phase increase however it was not significant (p=0.8). It has been previously shown that Ara-C can cause a block and accumulation of cells in the S-phase, and frequency of G0 decreases as cells are recruited into active cell cycle only to become blocked (van Pelt et al., 2005). At 96 hours in both HL60 and U937 cells, although not statistically significant, there was a slight reduction in frequency of G0 cells in the Ara-C treated compared to untreated (p=0.16) and (p=0.2) cells respectively. Unusually ML-1 cells showed minimal if any changes in cell cycle status, reflective of the proliferation observed in Figure 3.2.

This data suggests that as the cell lines react in a similar manner regarding cell cycle status post Ara-C treatment, with a trend towards reduction in frequency of G0 (albeit not significant), other downstream mechanisms may be affecting their differential responses to Ara-C.

3.2.3 Ara-C Induces DNA damage in AML cell lines

As previously outlined, Ara-C is a cytotoxic agent capable of inflicting DNA damage through it's incorporation into replicating DNA causing the destabilisation of replication forks and the formation of double strand breaks. Thus, one of the most sensitive ways to assess DNA damage is by measuring phosphorylation of the histone H2AX on Ser139, which marks a double-strand break (DSB) (Savic et al., 2009). For easy quantification of DNA damage on low numbers of cells, measurement of total levels of γH2AX by intracellular FACS is an extremely useful tool (Figure 3.6A).

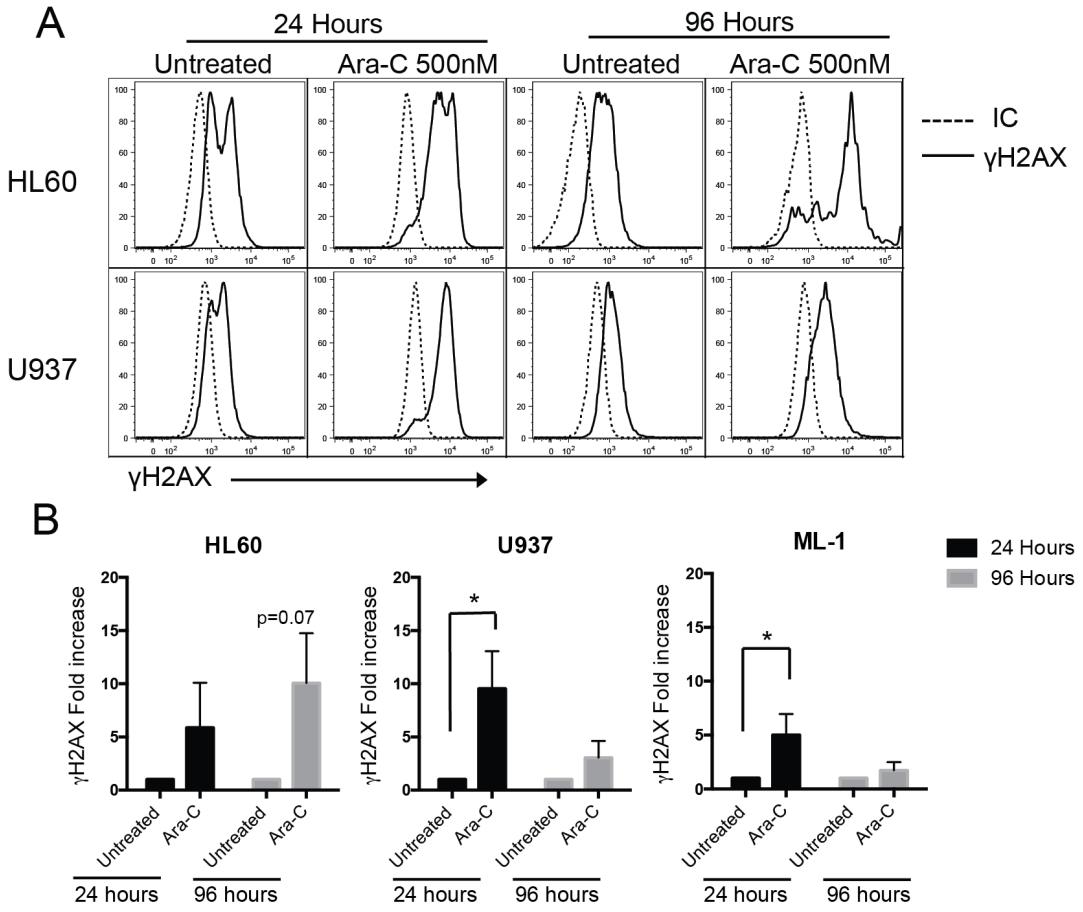

Figure 3.6 Measurement of γH2AX by intracellular FACS post Ara-C treatment in AML cell lines.

(A) Representative phospho-flow cytometry histogram for intracellular staining of γH2AX in HL60 and U397 cell lines under different time points and conditions as stated. (B) Quantification of γH2AX MFI (mean fluorescent intensity) by geometric mean represented as fold difference normalized to untreated. Culture conditions were on stromal cell layers over 96 hours in presence of Ara-C 500nM or untreated. Error bars represent ± S.D (n=3) *p<0.05.

Using this method AML cell lines were analysed using the same treatment schematic outlined in Figure 3.1. At 24 hours post Ara-C treatment all cell lines displayed increases in γH2AX signalling (HL60: p=0.1, U937: *p=0.012, ML-1: *p=0.02) (Figure 3.6B). By 96 hours this had decreased to insignificance in U937 and ML-1 cells (p=0.15, p=0.24 respectively), analogous with observations from section 3.2.1 where by 96 hours the effect of Ara-C is not as striking as when compared to HL60 cells at the same time point.

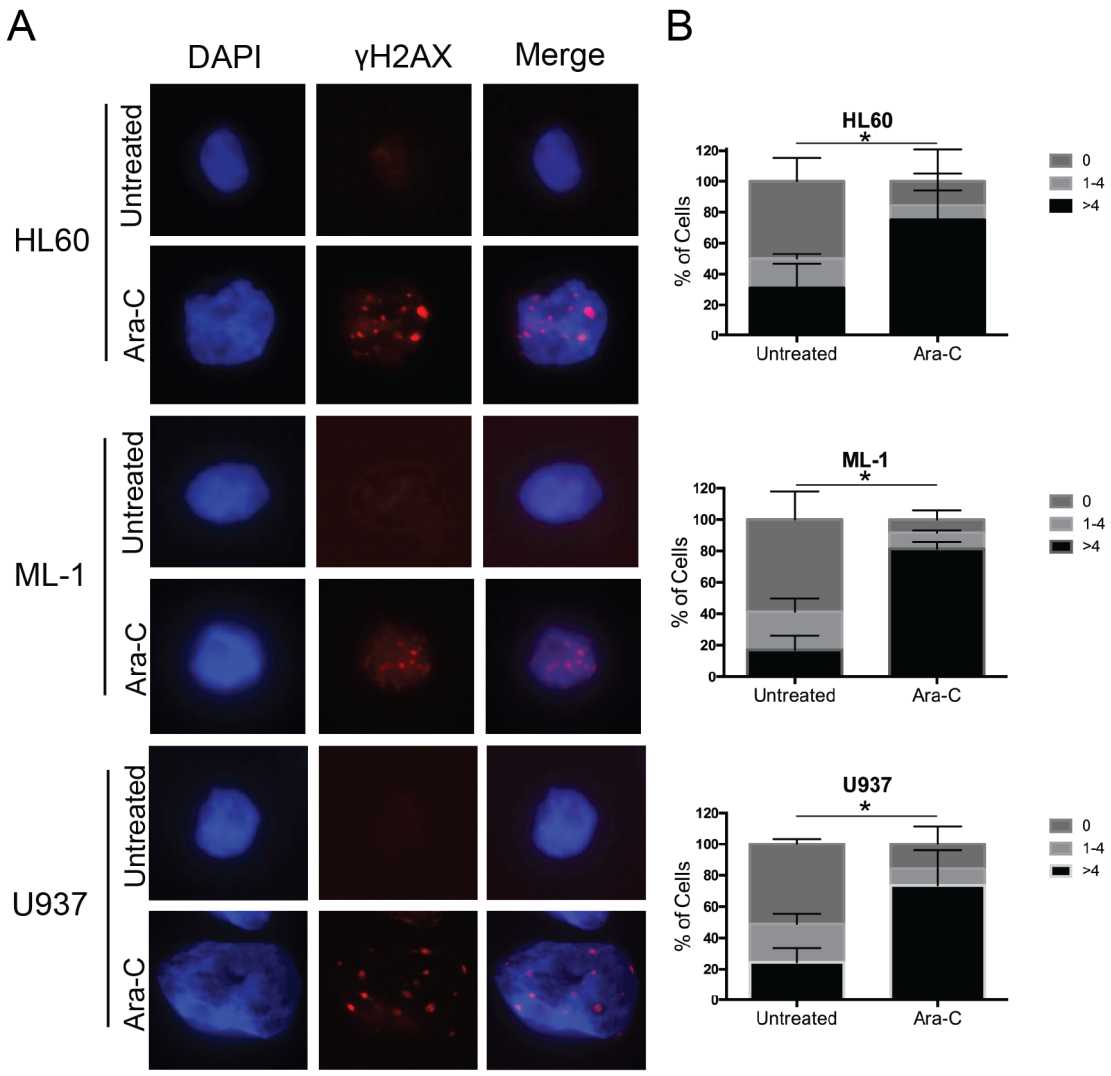

Figure 3.7 γH2AX foci counts post Ara-C treatment.

(A) Representative immunofluorescence staining of γH2AX foci (red) and DNA (blue) by DAPI in leukaemic cell lines post Ara-C treatment on stroma. 100x magnification. (B) Quantification of number of foci per nucleus 24 hours post Ara-C treatment. 100 nuclei were scored for each condition. *$p<0.05$ (n=3). Error bars represent ±S.D.

A more qualitative way of measuring DNA damage is by immunofluorescence and visualisation of γH2AX stained foci within the nucleus (Figure 3.7A). Counting the foci per nucleus permits a spectrum of how damaged the cell is. In this study a score of 0 foci = undamaged, 1-4 = increasingly damaged and >4 = very damaged was used to quantify the foci. After 24 hours all samples treated with Ara-C showed a significant increase in being 'very damaged' (>4 foci/nucleus), compared to

untreated (Figure 3.7B) (HL60: *p=0.04, U937: *p=0.024, ML-1: *p=0.012). This is comparable to when γH2AX is detected by FACS (Figure 3.6) at the same time point.

As analysis of γH2AX is only a marker of DNA damage, to be certain of actual direct DNA damage, this can be measured by the alkaline comet assay (Figure 3.8A). As expected significant increases in DNA damage were detected across the board, with damage persisting in U937 and ML-1 cells up to 96 hours despite reduction in γH2AX by FACS (Figure 3.6B).

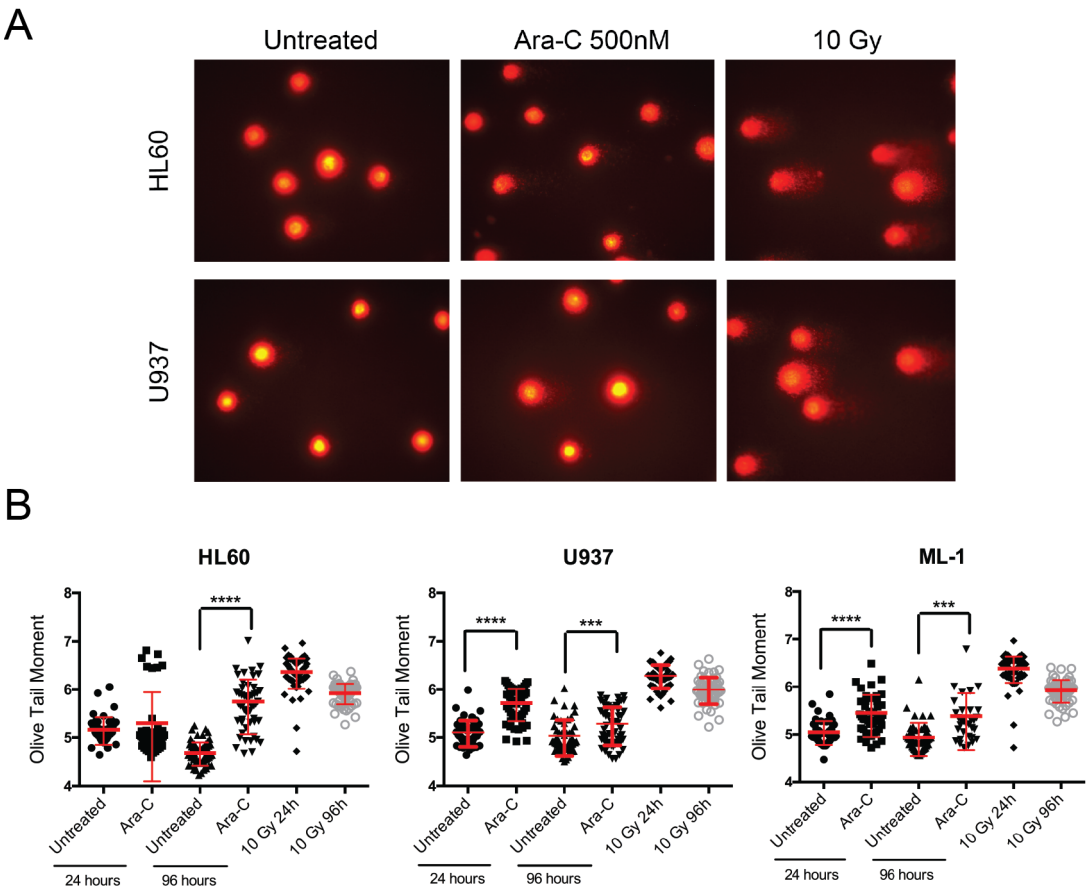

Figure 3.8 Measurement of direct DNA damage by alkaline comet assay of Ara-C treated AML cell lines.

(A) Representative images of DNA comet tails stained with ethidium bromide under different treatment conditions. 10 Gy acts as positive control. (B) Quantification of comet tails done by olive tail moment, a measurement of DNA migration x DNA density of the comet tail. Leukaemic cells were treated with Ara-C over 96 hours on stroma. 100 cells were scored per slide. Error bars represent ±S.D. ***p<0.0005. ****p<0.0001.

Overall there is direct evidence that Ara-C induces DNA damage in AML cell lines. In U937 and ML-1 cells this appears to be in similar levels as evidenced by γH2AX and comet assay. HL60 cells however failed to show an as comparably significant evidence of DNA damage; this may be due to the increased apoptosis and markedly reduced cell number post Ara-C treatment compared to the other cell lines, which means cells are lost during the assay. It appears that even though Ara-C inflicts DNA damage upon U937 cells, it can tolerate this damage much better as it displays no significant reduction in apoptosis or cell number.

3.2.4 Response of AML cell lines to irradiation induced DNA damage.

As AML cell lines display different responses to Ara-C it was next investigated whether inflicting DNA damage from another source, such as irradiation, would elicit similar effects in cell death and resolution of γH2AX. As irradiation induced DNA damage is not dependent on proliferation, a shorter time frame of 0 to 48 was observed. A dose of 2Gy was chosen as was previously used in haematopoietic cell studies (Milyavsky et al., 2010).

Post irradiation a reduction in cell number can be observed in all the cell lines (Figure 3.9A) however, much like when treated with Ara-C, HL60 cell line has a

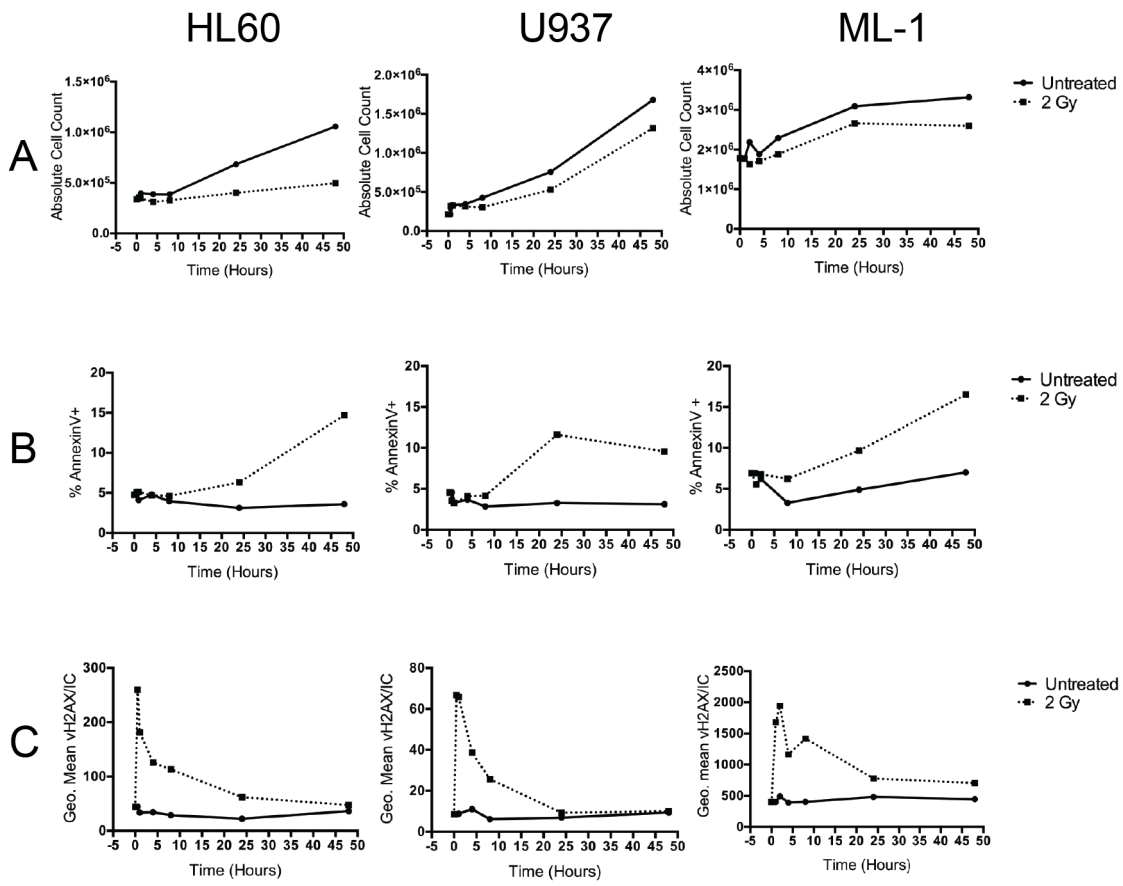

Figure 3.9 Effect of DNA damage by irradiation on AML cell lines.

AML cell lines, grown on stromal cell layers were irradiated with 2 Gy and analysed at 0, 0.5, 2, 4, 8, 24 and 48 hours post treatment. (A) Absolute cell count by FACS (B) frequency of AnnexinV+ cells (C) Intracellular FACS staining for γH2AX normalised to IC (isotype control).

greater decline in numbers than U937 and ML-1 cells, with the latter cell lines showing a stronger kinetic of growth recovery.

The onset of apoptosis, as measured by AnnexinV staining, mirrored the kinetics of reduction in cell number (Figure 3.9B). U937 cells, after showing an initial peak at 24 hours, started to show a decline of apoptosis by 48 hours. HL60 cells showed a growing rate of apoptosis up to 48 hours, as did ML-1 cells. Measurement of γH2AX by FACS (Figure 3.9C) again showed the U937 cell line was faster at responding to irradiation by reducing levels of γH2AX back to untreated by 24 hours. In contrast, HL60 and ML-1 cells lagged behind taking an extra 24 hours to return to near untreated levels of γH2AX.

Overall this shows that DNA damage induced by irradiation produces a similar response in AML cell lines to DNA damage that has been inflicted by Ara-C. The U937 cell line appears to be impervious and more able to tolerate DNA damage, while HL60 cells are more sensitive. ML-1 cells are more difficult to conclude a comprehensive answer from, as at times it appears to behave sensitively similar to HL60 cells and other times, it responds just like U937 cells.

3.2.5 AML cell lines initiate DNA Repair in response to Ara-C treatment.

As mentioned previously γH2AX foci are most primarily symptomatic of DNA DSBs (Savic et al., 2009). Analysis by comet assay showed direct DNA damage being inflicted by Ara-C treatment as well as increase in γH2AX foci (See Section 3.2.3). This ability of Ara-C to create DNA damage by DSBs, yet incur varying survival rates between the cell lines, suggests a possible role for DNA repair.

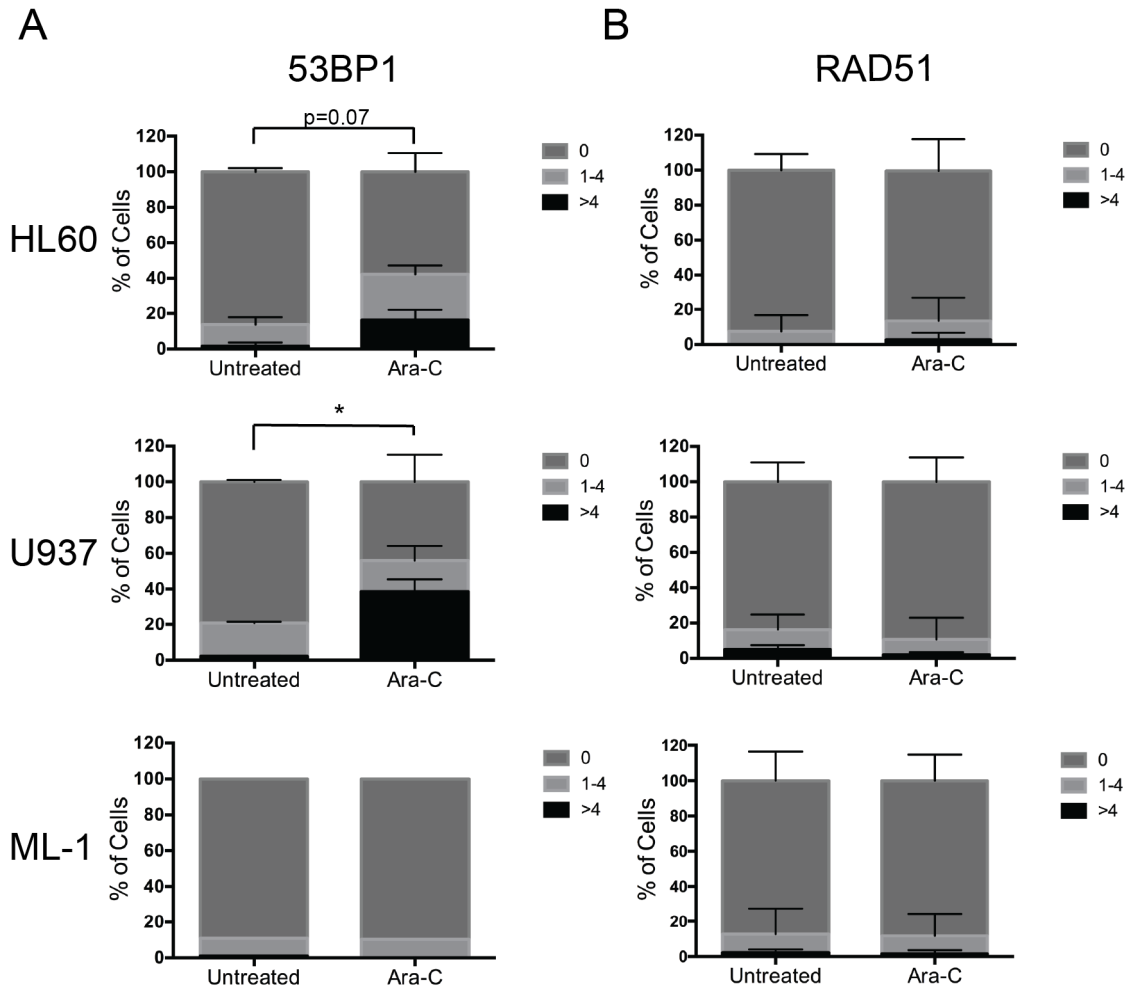

Figure 3.10 DNA Repair Mechanisms post Ara-C Treatment.

Quantification of number of foci per nucleus, 24 hours post Ara-C treatment. 100 nuclei were scored for each condition. Error bars represent ± S.D. (n=2-3) *p<0.05. (A) Foci counts/nuclei of 53BP1 localisation showing activation of Non-homologous end joining repair. (B) Foci counts/nuclei of RAD51 localisation showing activation of homologous recombination repair.

The two primary pathways for DSB DNA repair are non-homologous end joining (NHEJ) and homologous recombination (HR). To detect their activity, immunofluorescence for the nuclear localisation of key proteins 53BP1 for NHEJ and RAD51 for HR was performed. These protein form foci at DSBs and are indicative of activation of the DSB repair mechanisms. This is a classical way to report on the early functions of each pathway and to show which mechanism is preferentially used by the cells.

Quantification of foci was done using the same scoring system as for the γH2AX immunostaining (0 foci = undamaged, 1-4 = increasingly damaged and >4 = very damaged).

Quantification of 53BP1 foci formation post Ara-C treatment only showed significant localisation (>4 foci/nuclei) in U937 cells (*p=0.017) in approximately 40% of cells (Figure 3.10A). There was evidence of activation of NHEJ repair in HL60 cells, however this was insignificant at both high levels (>4 foci/nuclei: p=0.07) and low levels (1-4 foci/nuclei: p=0.09) of localisation. ML-1 cells showed no indication of repair after exposure to Ara-C. On the other hand, analysis of RAD51 foci formation post Ara-C treatment showed no indication of activation of HR repair (Figure 3.10B) in any of the cell lines tested.

These results appear to be strong evidence that U937 cells can utilize DNA repair mechanisms to potentially overcome the DNA damaging effect of Ara-C.

3.3 Discussion

As a first port of call, leukaemic cell lines were used to discern the response of chemotherapeutic treatment with Ara-C, specifically looking at activation of DNA damage and repair mechanisms.

It was initially observed that by culturing *in vitro* in presence of Ara-C, cell lines displayed differing degrees of sensitivity with cell number and apoptosis complimenting each other. While HL60 and ML-1 cells had significant reduction in cell numbers and induction of apoptosis, U937 cells only had a mild response to Ara-C, with an initial small decrease in cell number but this recovered at the later time point with no apparent induction of apoptosis. This showed that HL60 and ML-1 cell lines were more sensitive to Ara-C than U937, which appeared refractory to treatment.

Cell cycle status across the different cell lines was similar showing a high frequency of cells in the cycling phases, which were slightly perturbed when adding Ara-C causing a small but insignificant block of cells within the S-phase. This shows that all cell lines should be incorporating Ara-C at comparable rates, even though as evidenced, they responded differently. However it can be noted that leukaemia cell lines by their very nature are highly proliferative due to their immortalisation and oncogenic status, meaning changes in cell cycle should be interpreted with caution.

To resolve how leukaemic cell lines, with their similar cell cycle statuses could respond differently to Ara-C, induction of DNA damage was examined. As shown, all cell lines displayed initial increases in DNA damage by analysis of γH2AX and direct damage as measured by comet assay. By 96 hours in U937 and ML-1 cells this had began to fall, with HL60 cells continuing to increase their DNA damage after Ara-C exposure. It could be seen as well that there was an observable level of endogenous damage within the untreated condition. With such a low frequency of cells in G0, the cells are rapidly dividing causing potential replicative stress, which leads to genomic instability and activation of DNA response mechanisms (Hills and

Diffley, 2014). This could also suggest that leukaemic cell lines have a tolerance to DNA damage, as they appear to bypass levels of endogenous damage in normal culture conditions. When using irradiation as a second form of DNA damage, again HL60 and ML-1 cells were shown to be more sensitive to DNA damaging treatments, and U937 cells were able to recover faster. Overall this showed that again there are differing responses between the cell lines to DNA damage, even when damage was inflicted by different methods.

It is important to note that both HL60 and U937 cells possess mutant p53 with no levels of p53 protein (Sugimoto et al., 1992, Prokocimer et al., 1986) and ML-1 cells are p53 wildtype (Smardova et al., 2005). p53 is a tumour suppressor and co-ordinates responses to several cellular stresses, including DNA damage, and is one of the most commonly mutated proteins in oncogenic diseases. Typically, loss of p53 means that cells cannot co-ordinate an appropriate response to DNA damage. This means that where usually a p53 wildtype cell would undergo apoptosis in response to DNA damage, a p53 mutant would carry on proliferating regardless of damaged acquired (Muller and Vousden, 2013). Interestingly, only 10% of AML patients appear to possess a mutant p53 (Trecca et al., 1994), in contrast to the majority of other cancers where p53 mutation rates are approximately 50% (Soussi et al., 2006). This would imply that HL60 and U937 cells should behave in a similar manner post Ara-C treatment, as they have a similar p53 status, however the differences in responses to Ara-C shown must be due to other downstream mechanisms which are independent of p53.

As DNA damage is induced upon Ara-C treatment in all the cell lines, it was next examined whether DNA repair could be a factor in the cell lines differing responses to Ara-C. While U937 and HL60 cells showed activation of NHEJ, ML-1 cells did not and none of the cell lines showed activation of HR repair. U937 cells had the highest level of activation of NHEJ repair appearing to correlate with their ability to maintain a refractory response to Ara-C treatment. Indeed it could have been expected that as the cell lines are highly proliferative and HR works as the cell is cycling, that this would have been the preferred method of repair (Mohrin et al., 2010). However, NHEJ appears to be the preferred choice of DNA repair suggesting the cell lines may favour a quick fix over an accurate repair. Unusually,

HL60 cells induced NHEJ post Ara-C treatment, contrary to its more sensitive phenotype, suggesting that U937 cells may have a more efficient, overactive repair mechanism. Moreover ML-1 cells displayed no indication of activation of DNA repair suggesting that overall they are preferentially led to apoptosis as evidenced by reduction in cell number and increase in AnnexinV staining.

One future perspective would be to utilise the DNA repair reporter constructs developed to measure the efficiency and quality of the two DSB DNA repair mechanisms (Seluanov et al., 2010). Fluorescent reporter constructs, engineered for both HR and NHEJ activity, are linearised *in vitro* and transfected into cells. Successful re-joining and repair of the linearised construct allows for the expression of GFP and detection by flow cytometry, making this a very sensitive assay. Using these it would be extremely useful to observe and quantify any differences between the activity and rates of DNA repair between the cell lines.

In summary this chapter shows that AML cell lines responses to Ara-C are heterogeneous. Although all cell lines display increase in DNA damage post Ara-C treatment, how they responded to treatment was diverse.

Chapter 4. Results 2: Effect of Ara-C on Normal Cord Blood Haematopoietic Cells

4.1 Introduction

While understandably the majority of studies on chemotherapeutic drugs revolve around their effect on malignant cells, it is also of equal importance to assess their influence on normal tissues. As Ara-C is one of the most widely used drugs in the clinic for the treatment of AML there are a copious amount of studies into its effect on leukaemic cells. However, what is frequently understudied is how normal haematopoietic cells respond to Ara-C treatment. Particularly pertinent is the question: how do normal haematopoietic cells survive chemotherapeutic treatment to resurrect and maintain a normal haematopoiesis post therapy? While this question opens up numerous avenues to explore, regarding the results in Chapter 3, it would be interesting to assess how normal haematopoietic cells respond to Ara-C regarding their DNA damage response and repair mechanisms.

Recent years have seen a flurry of studies into the regulation of DNA damage in the HSC, with key findings showing that when comparing the HSC and progenitor populations they present differential responses to DNA damage by ionizing radiation (Milyavsky et al., 2010, Mohrin et al., 2010). While the murine system shows a preferential survival of HSC, with loss of progenitors, the opposite was shown to be true in the human HSC. Thus presenting remaining discrepancies between the murine and human systems as to which response to DNA damage entails.

Hence it is of interest to investigate how Ara-C treatment may fit into the paradigm of what is already known about DNA damage response in the human haematopoietic system.

For the study of the effect of Ara-C on normal primitive haematopoietic cells, material purified from umbilical cord blood (UCB) was utilized. UCB provides a cheap and abundant source of primitive material. Therefore, CD34+ cells purified from UBC blood were used as a comparison of both the *in vitro* and *in vivo* response of primitive haematopoietic stem and progenitor populations to Ara-C.

4.2 Results – *in vitro*

For *in vitro* analysis, CD34+ UCB cells were cultured on irradiated MS-5 stromal layers for at least 3 days before any treatment to allow sufficient time for recovery from thawing. As well, the use of stromal cells is essential in the long-term maintenance of primary haematopoietic cells for *in vitro* cultures. As outlined in the previous chapter, the *in vitro* experimental procedure for Ara-C treatment utilised a window of 24 and 96 hours exposure to Ara-C to enable an early and late time-point of exposure.

To compare HSC and progenitors, the populations were fractionated by way of flow cytometry as shown in Figure 4.1. Haematopoietic progenitor cells (HPCs) were defined as CD34+/CD38+ and haematopoietic stem and progenitor cells (HSPCs) as CD34+/CD38-. The HSPC population still remains a relatively heterogeneous population that can be further sub-fractionated into LT-HSC, ST-HSC and MPPs. However, it was necessary to have a primitive population with sufficient material available for analysis post chemotherapeutic treatment, so further refinement was not undertaken.

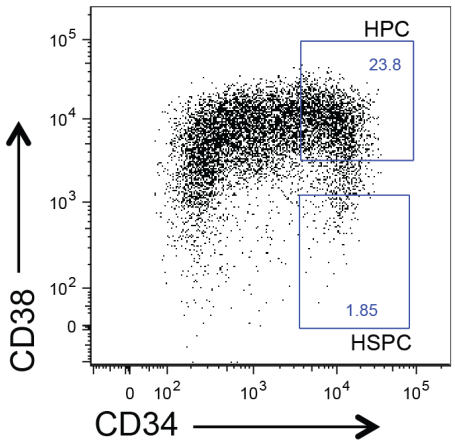

Figure 4.1 FACS gating strategy for UCB stem and progenitor populations.

Haematopoietic stem and progenitor populations (HSPC) (CD34+/CD38-) and haematopoietic progenitor populations (HPC) (CD34+/CD38+) FACS gates for *in vitro* cultures of CD34+ UCB cells on MS-5 stromal layers.

4.2.1 Survival of normal CD34+ stem and progenitor populations post Ara-C treatment.

After Ara-C exposure, HPC and HSPC population cell numbers were analysed by FACS (Figure 4.2A). Initially both populations showed a slight but insignificant reduction in cell numbers, which by 96 hours had decreased dramatically. The greatest effect could be seen in the HSPC population which had a 5-fold decrease compared to the HPCs, which displayed on average 3-fold reduction in cell number.

Induction of apoptosis as demonstrated by AnnexinV staining was moderately increased across all populations (Figure 4.2B). HSPCs showed the most significant apoptosis at 24 hours (p=0.0065), which appears to precede the sizeable reduction in cell number at 96 hours. Evidence of apoptosis was still maintained in HSPC at 96 hours (p=0.025).

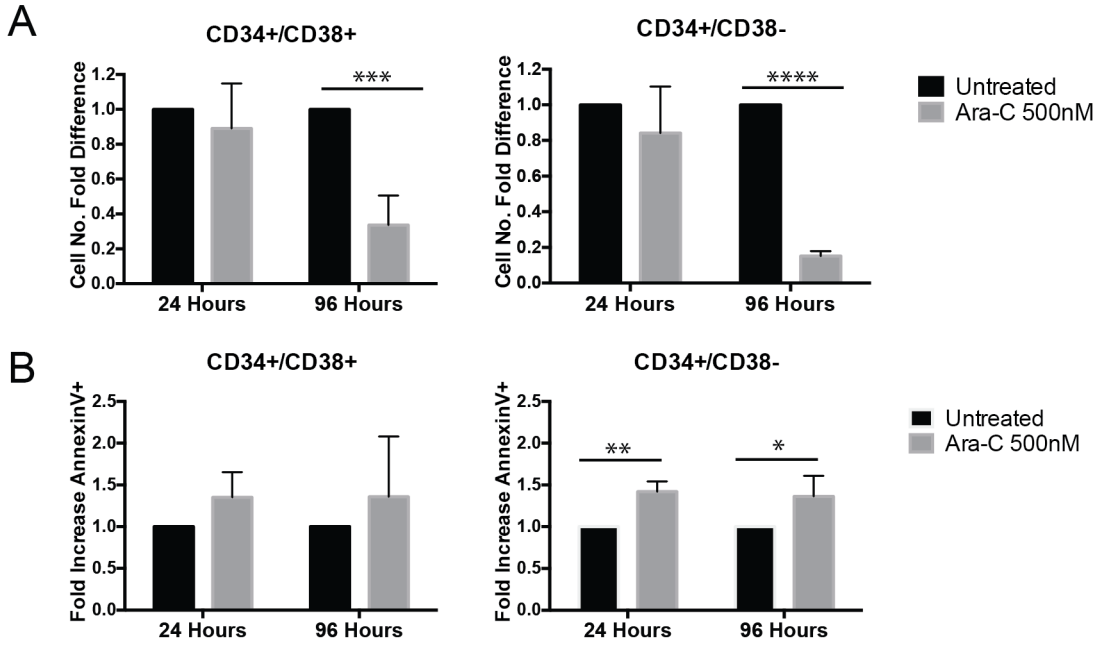

Figure 4.2 Cell counts and AnnexinV+ FACS analysis post Ara-C Treatment of CD34+ cord blood cells *in vitro.*

(A) Fold change in cell number of HPCs (CD34+/CD38+) and HSPCs (CD34+CD38-) CB cells grown on MS-5 stromal cell layers 24 and 96 hours post Ara-C treatment *in vitro* compared to untreated as analysed by FACS (n=7) ***p<0.0005, ****p<0.0001. Error bars are ± S.D. (B) Fold change of frequency of AnnexinV staining 24 and 96 post Ara-C treatment of CD34+ CD cells *in vitro.* *p<0.05, ** p<0.01 (n=4) error bars are ± S.D.

Although there was slight increase in apoptosis in the HPCs, this was never able to reach significance. These results initially suggest that the more primitive HSPCs are more prone to the effect of Ara-C treatment than progenitor populations.

This observation appears to go against what is inherently know about the nature of progenitor and stem cell populations concerning their cell cycle status. As the action of Ara-C relies on the cell entering the S-phase it would seem the most obvious scenario would be the proliferative progenitor populations would be most effected by Ara-C, than compared to the more quiescent stem cell populations.

4.2.2 Cell cycle status of stem and progenitor cells post Ara-C

To compare the cell cycle status of the HSPC and HPCs cultured *in vitro*, cells were analysed by FACS for Ki67 and DAPI profiles. Both populations showed a relatively equal frequency of cells within G0, however HPCs had twice as many cells in the S/G2/M cycling phases compared to HSPCs (32% versus 15% respectively) (Figure 4.3) within the untreated condition.

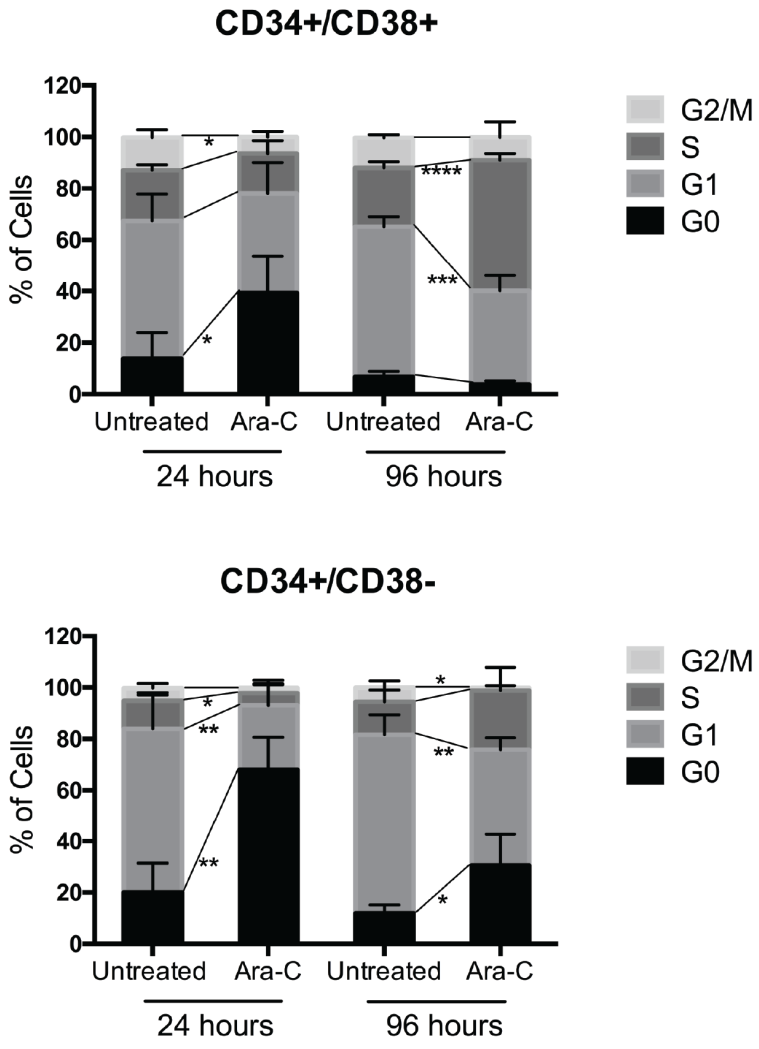

Figure 4.3 Cell cycle Ki67 intracellular staining in CD34+ cord blood cells in *vitro* post Ara-C.

Analysis and quantification of cell cycle profiles of CD34+ populations HPC (CD34+/CD38+) and HSPC (CD34+/CD38-) *in vitro* 24 and 96 hours post Ara-C treatment by staining with Ki67 and DAPI for DNA content. Represented as frequency of cells. *p<0.05, **p<0.005, ***p<0.0005, ****p<0.0001 (n=4). Error bars are ± S.D.

After 24 hours Ara-C treatment the most evident change was the significant enrichment in the frequency of cells within the resting G0 phase in both populations; HPCs doubled ($p=0.03$) and HSPCs almost tripled the amount of cells in G0 ($p=0.001$). In hand with this, there were significant reductions in the cycling phases, with HSPCs showing the most pronounced alterations. This suggests that when Ara-C is first added, any proliferating cells succumb rapidly to the treatment, initially sparing the more quiescent populations.

However, by 96 hours, the scenario had changed quite dramatically in response to Ara-C. HPCs showed significant decreases in G1 ($p=0.0009$) and increases in S-phase frequencies ($p<0.0001$), with only approximately 5% of cell within G0 compared to untreated. HSPCs as well showed a reduced amount of quiescent cells, as compared to 24 hours Ara-C treated condition, but still retained 30% of cells within G0. Nonetheless, HSPCs still displayed the significant decrease in G1 ($p=0.0016$) and increase in S-phase ($p=0.09$), seen in HPCs. As well, there was an almost complete abolishment of G2/M phase within HSPCs ($p=0.018$).

At the early time point of treatment it is evident that there is enrichment of cells in G0 across the populations as Ara-C takes its first effects. However at the later time point, when cells were exiting quiescence to continue cycling, there was an apparent blocking of cells within the S-phase as previously described by van Pelt et al. and previously shown in the AML cell lines treated with Ara-C (Chapter 3). This is particularly noticeable in HSPCs, which show no G2/M at 96 hours post Ara-C treatment.

4.2.3 DNA damage is induced by Ara-C in normal CD34+ stem and progenitor cells

Previously in this study it was shown that Ara-C induces DNA damage in AML cell lines so it stands to reason that Ara-C is also inflicting damage upon normal haematopoietic cells *in vitro*. CD34+ cells were cultured on MS-5 stromal layers and treated with Ara-C 500 nM before analysis of DNA damage, by measuring the phosphorylation of H2AX by FACS, 24 and 96 hours post treatment (Figure 4.4A).

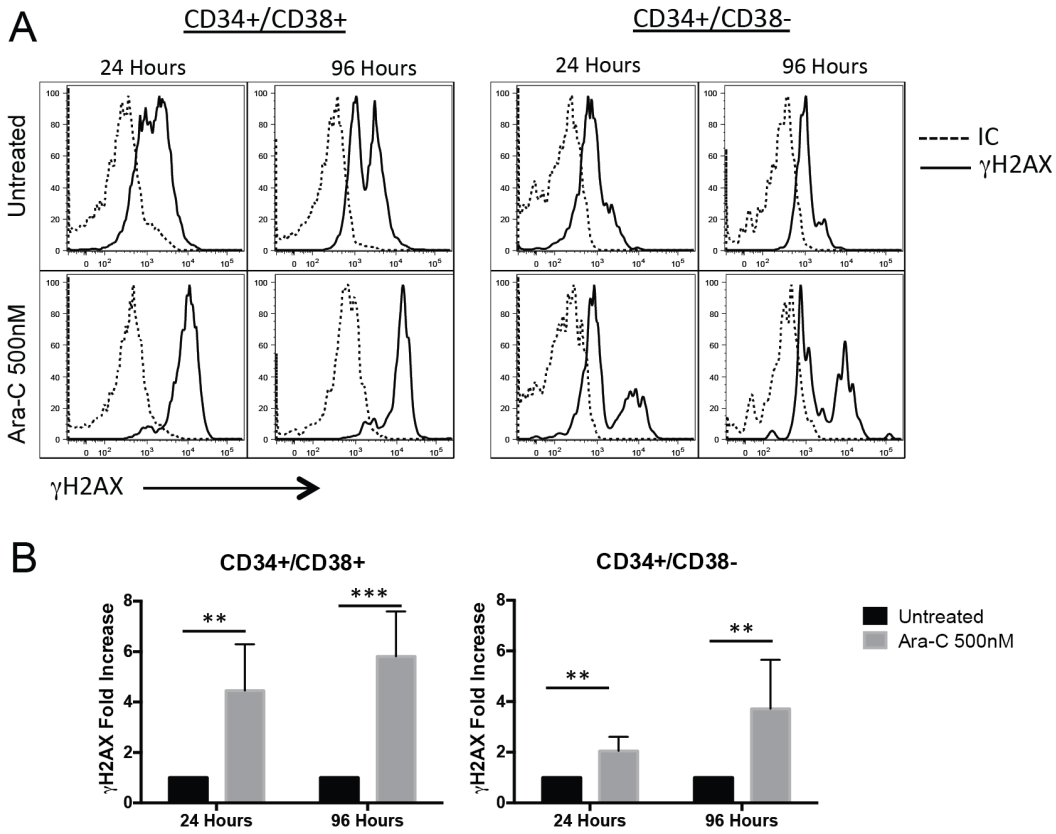

Figure 4.4 Levels of γH2AX measured by intracellular FACS post Ara-C treatment in CD34+ *in vitro*.

(A) Representative histogram of phospho-flow cytometry for intracellular staining of γH2AX in CD34+ CB cells *in vitro* grown on MS-5 stromal cell layers under conditions stated. (B) Quantification of γH2AX by fold difference of MFI by geometric mean normalized to untreated. CD34+ CB were cultured in presence of Ara-C 500 nM or untreated condition and analyzed at 24 and 96 hours post treatment by FACS. **p<0.01, ***p<0.0005 (n=8). Error bars are ± S.D.

All CD34+ populations displayed significant increases in γH2AX post Ara-C treatment (Figure 4.4B). HPCs showed initially, at 24 hours, a 4-fold increase in

damage which further increased to 6-fold at 96 hours. On the other hand, HSPCs showed only a 2-fold increase in γH2AX at 24 hours, with this doubling by 96 hours. As could be anticipated, HPC gained more DNA damage from Ara-C than HSPC, which is comparable to their proliferation statuses, with progenitors cycling more than stem populations (Figure 4.3).

As performed previously on the AML cell lines, visualization of γH2AX nuclear foci by immunofluorescence (IF) was used as a more qualitative way to quantify DNA damage (Figure 4.5A). HSPCs and HPCs were sorted from MS-5 stromal layers 24 hours and 96 hours post Ara-C treatment. Foci were scored as described previously (0 foci = undamaged, 1-4 = increasingly damaged and >4 = very damaged).

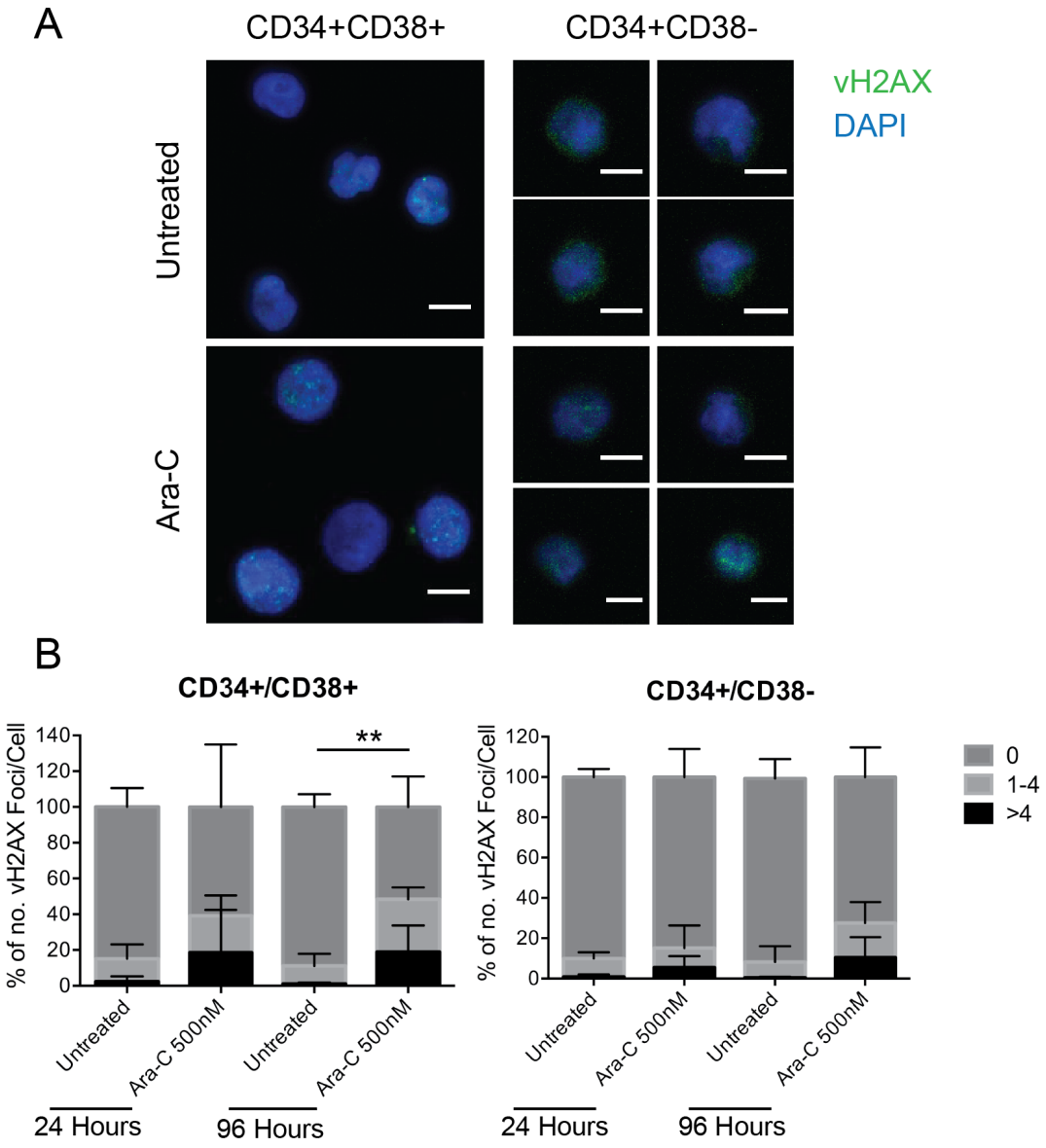

Figure 4.5 Foci counts of γH2AX post Ara-C treatment in CD34+ cells *in vitro*.

(A) Representative immunofluorescence staining of γH2AX foci (green) and DNA (blue) by DAPI in CD34+ CB HSPC and HPC populations post Ara-C treatment grown on MS-5 stromal cell layers *in vitro*. Scale bar, 10 μm. (B) Quantification of number of foci per cell represented as frequency of cells with either 0, 1-4 or >4.foci per cell. 100 cells were counted per condition **p<0.01 (n=4). Error bars are ± S.D.

By this method all samples showed increased numbers of γH2AX foci in the Ara-C treated condition (Figure 4.5B). 50% of HPCs showed a significant amount of γH2AX displaying 1-4 foci/nucleus at 96 hours (**p=0.007) and >4 foci/nucleus (p=0.05). The effect on HSPCs was milder, with no significant changes and small increases in nuclear foci counts. While the onset of DNA damage by Ara-C was not

as marked when quantifying by foci counts, it showed a similar trend to γH2AX FACS, which measures overall intensity.

To define if there was indeed direct DNA damage, using the same *in vitro* procedure, HPCs and HSPCs were sorted from MS-5 stromal layers for analysis by alkaline comet assay (Figure 4.6). HPCs showed a significant increase in olive tail moment at 96 hours (p=0.024) post Ara-C treatment, comparable to γH2AX IF data (Figure 4.5B). Unusually, 24 hours post Ara-C treatment HSPC showed significant increases in olive tail moment (p=0.035) with no changes compared to untreated at 96 hours.

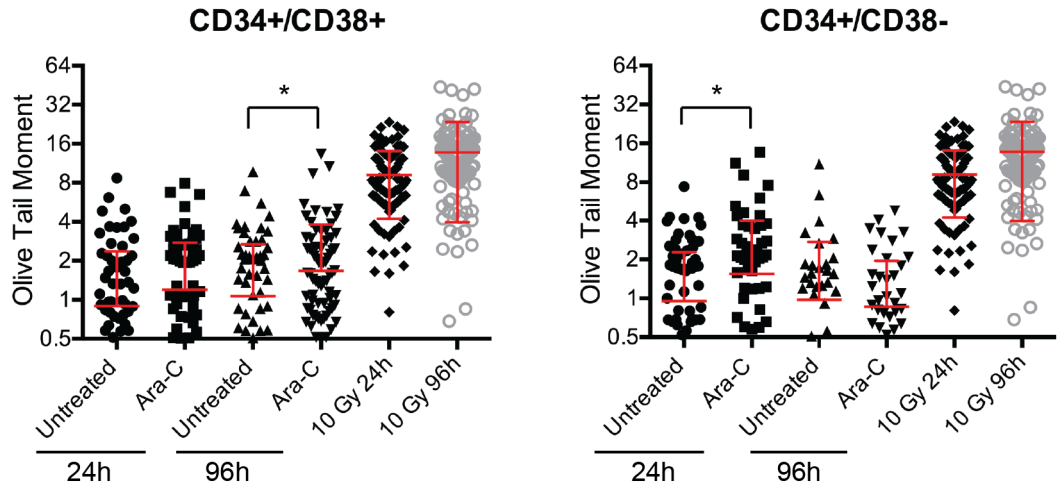

Figure 4.6 Alkaline comet assay of CD34+ cells treated with Ara-C *in vitro*.

Quantification of direct damage by olive tail moment, a measurement of DNA tail migration x comet tail DNA density. CD34+ HSPC and HPC populations were sorted from MS-5 stromal layers at 24 and 96 hours post Ara-C 500nM treatment *in vitro*. 100 cells were scored per slide where possible. *p<0.05 (n=2). Error bars (in red) are ± S.D.

Overall there is evidence for generation of DNA damage by treatment with Ara-C in normal CD34+ stem and progenitor populations. DNA damage is inflicted at a greater rate in HPCs, which correlates with their increased proliferation compared to HSPCs.

4.2.4 Activation of DNA repair mechanism post Ara-C treatment

In Chapter 3 it was shown that AML cell lines were able to initiate DNA repair mechanism in response to Ara-C treatment (Section 3.2.9). To investigate whether the same holds true for normal CD34+ populations, IF staining was performed for the nuclear localisation of 53BP1 and RAD51 (Figure 4.7A and 4.8A) for analysis of NHEJ and HR repair respectively.

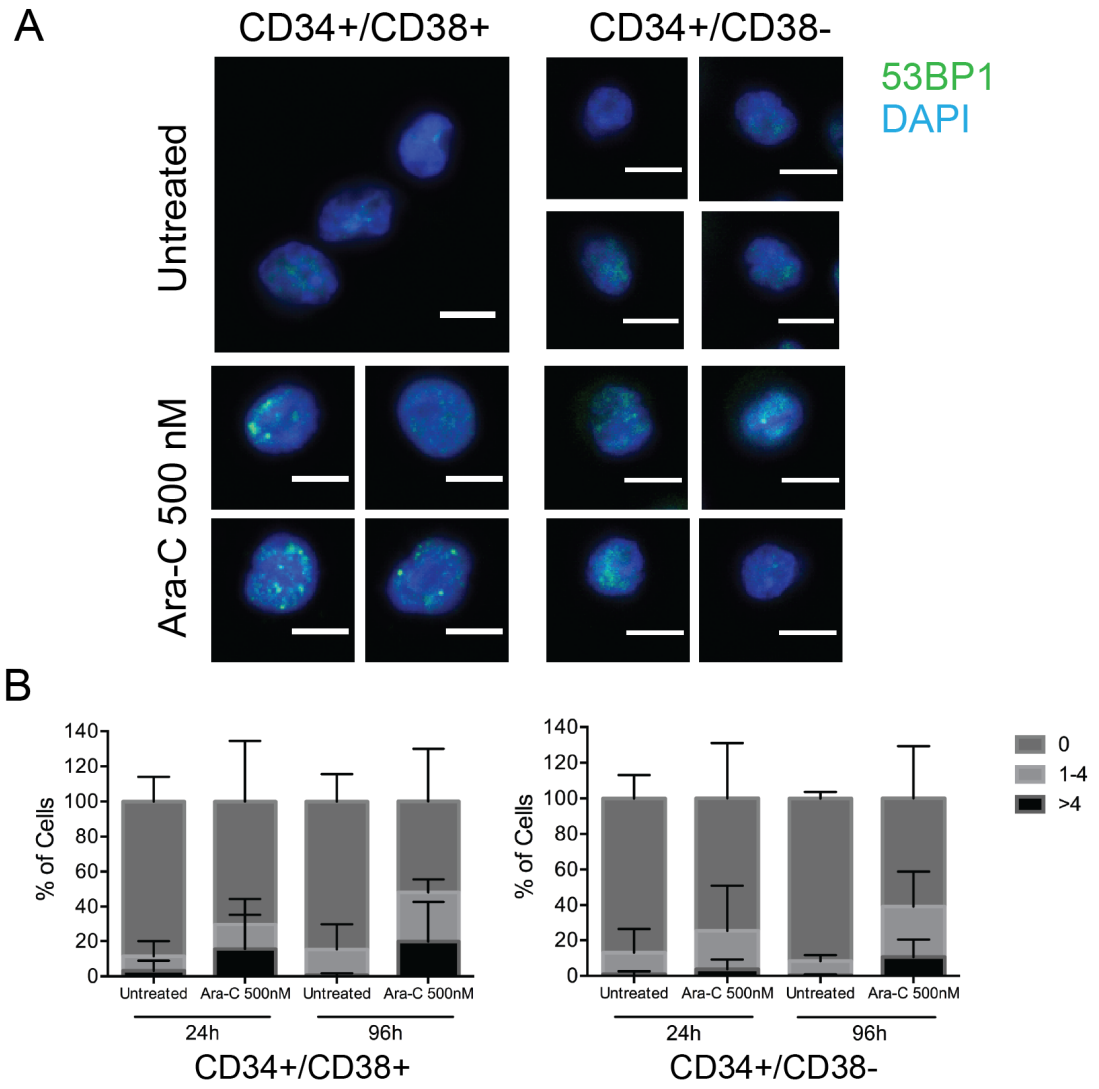

Figure 4.7 Foci counts of 53BP1 in CD34+ cells post Ara-C treatment *in vitro*.

(A) Representative immunofluorescence staining of 53BP1 foci (green) and DNA (blue) by DAPI in CD34+ CB HSPC and HPC populations post Ara-C treatment grown on MS-5 stromal cell layers *in vitro*. Scale bar, 10 μm. (B) Quantification of number of foci per cell represented as frequency of cells with either 0, 1-4 or >4.foci per cell. 100 cells were counted per condition (n=3). Error bars are ± S.D.

HPCs and HSPCs both showed increases in number of 53BP1 nuclear foci (Figure 4.7B). Again it can be seen that HSPCs display a weakened response to Ara-C when compared to HPCs, comparable to the γH2AX foci localization in Figure 4.5B.

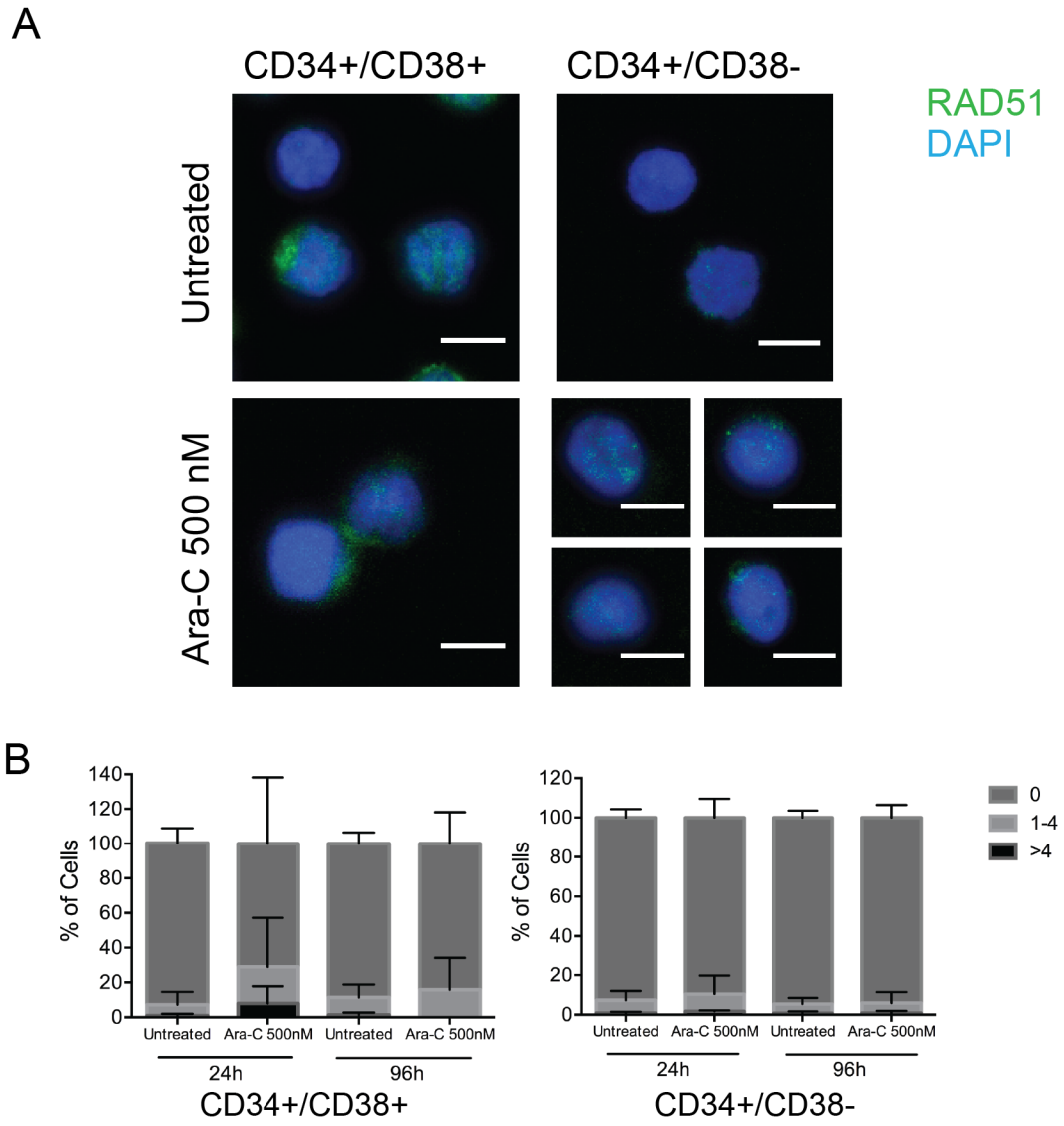

Figure 4.8 Foci counts of RAD51 in CD34+ cells post Ara-C treatment *in vitro.*

(A) Representative immunofluorescence staining of RAD51 foci (green) and DNA (blue) by DAPI in CD34+ CB HSPC and HPC populations post Ara-C treatment grown on MS-5 stromal cell layers *in vitro*. Scale bar, 10 μm (B) Quantification of number of foci per cell represented as frequency of cells with either 0, 1-4 or >4.foci per cell. 100 cells were counted per condition (n=3). Error bars are ± S.D.

On the other hand, nuclear foci formation of RAD51 was barely detected in response to Ara-C treatment (Figure 4.8B), especially in HSPCs. Only HPCs at 24 hours post Ara-C treatment showed a slight increase in number of cells displaying HR repair, most likely due to HR only being active in the cycling phase of the cell cycle.

Overall it appears that in the face of DNA damage by Ara-C normal human CD34+ populations will activate their repair mechanism, in a small frequency of cells, with a preference for NHEJ repair mechanism.

4.2.5 Response of normal CD34+ cells to DNA damage by irradiation.

It appears that although HSPC as a population receives less DNA damage from Ara-C over all than compared to HPC population, nevertheless HSPCs displayed a greater fold reduction in cell number and increase in apoptosis (Figure 4.2), suggesting that human stem containing populations are more sensitive to DNA damage than progenitors. Indeed, this similar finding was observed by Milyavsky et al. when using irradiation on human cord blood (Milyavsky et al., 2010). To test if DNA damage from irradiation reflected what was observed in our system with Ara-C, and was consistent with the literature, CD34+ CB cells were cultured on MS-5 stromal layers before irradiation with 2 Gy and analysed up to 48 hours later.

Analysis of cell number by FACS saw significant and comparable fold reductions of both HPCs and HSPCs, starting at 24 hours post irradiation and continuing to decrease with an approximate a 5-fold reduction in both populations by 48 hours (Figure 4.9A).

Although there appeared to be no differences in rate of decline of cell numbers between HSPCs and HPCs after treatment with irradiation, there were however evident differences in apoptosis (Figure 4.9B). Analysis of AnnexinV by 8 hours post irradiation in HPCs showed a slight increase but no significant induction of apoptosis ($p=0.15$), whereas HSPCs at the same time point had a 5-fold increase in apoptosis ($p=0.005$). Even beyond 8 hours, HSPCs maintained a significant

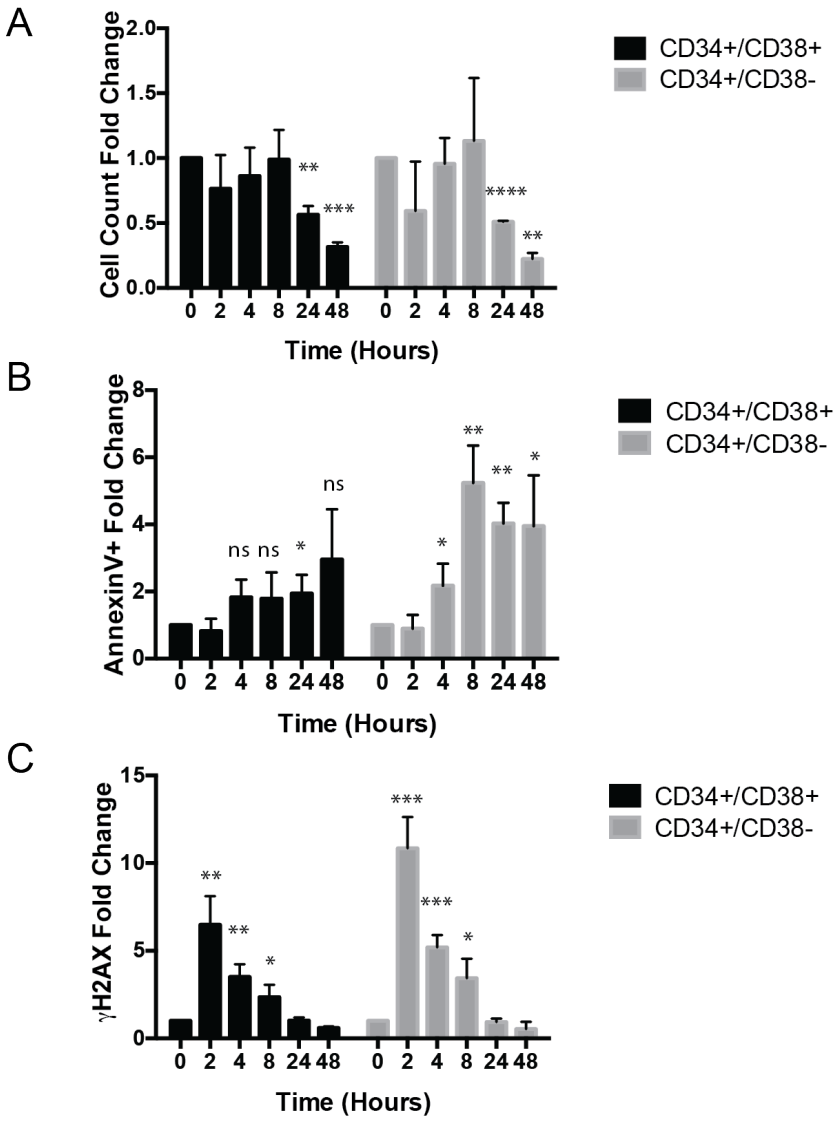

Figure 4.9 Response of CD34+ cells to DNA damage by irradiation.

CD34+ CB cells were grown *in vitro* on MS-5 stromal layers, irradiated with 2 Gy and analysed at 0, 2, 4, 8, 24 and 48 hours post irradiation. All results are represented as fold change compared to untreated. (A) Absolute cell counts by FACS (n=3) (B) Frequency of AnnexinV+ cells (n=3) (C) Intracellular FACS staining for γH2AX (n=3). *p<0.05, **p<0.005, ***p<0.0005, ****p<0.0001. Error bars are ± S.D.

AnnexinV expression (48 hours p=0.02), compared to HPCs, which throughout only maintained an approximate 2-fold increase in AnnexinV expression.

Invariably, as HSPCs demonstrated higher apoptosis than HPCs after irradiation, HSPCs showed a 11-fold increase in DNA damage by γH2AX compared with HPCs at 2 hours, which only had a 6-fold increase, nearly half of that of the HSPCs

(Figure 4.9C). Although the timing of apoptosis did not directly correlate with the γH2AX levels, indeed these findings were similar to what Milyavsky et al. reported. In that although most DNA damage was resolved in between the 8 and 24 hour time points in both populations, there was still a marked and persistent apoptosis in the remaining more primitive HSPC compartment. Showing an increased intolerance to DNA damage in the more primitive HSPCs.

Overall it appears that any DNA damaged incurred, be it through Ara-C or irradiation, HSPC populations are less able to tolerate the damage and can hypothetically be deemed more sensitive.

4.3 Results – *in vivo*

While *in vitro* assays are an extremely useful and straightforward tool for experiments involving drug treatments, for a more physiological setting, use of the xenograft model is routinely used in the study of human haematopoiesis. The mouse bone marrow provides an enhanced microenvironment for long-term maintenance of the HSPCs, with a full array of niche components for proper regulation of the primitive cells. Whereas the 2-D culture system, with MS-5 stromal layers, provides support, but not a full physiological maintenance of the HSPCs.

Therefore to examine response of Ara-C to normal human HPCs and HSPCs *in vivo,* sub-lethally irradiated NSG mice were injected intravenously with human CD34+ cells, left to engraft for 12 weeks, before treatment with Ara-C as outlined in Figure 4.10.

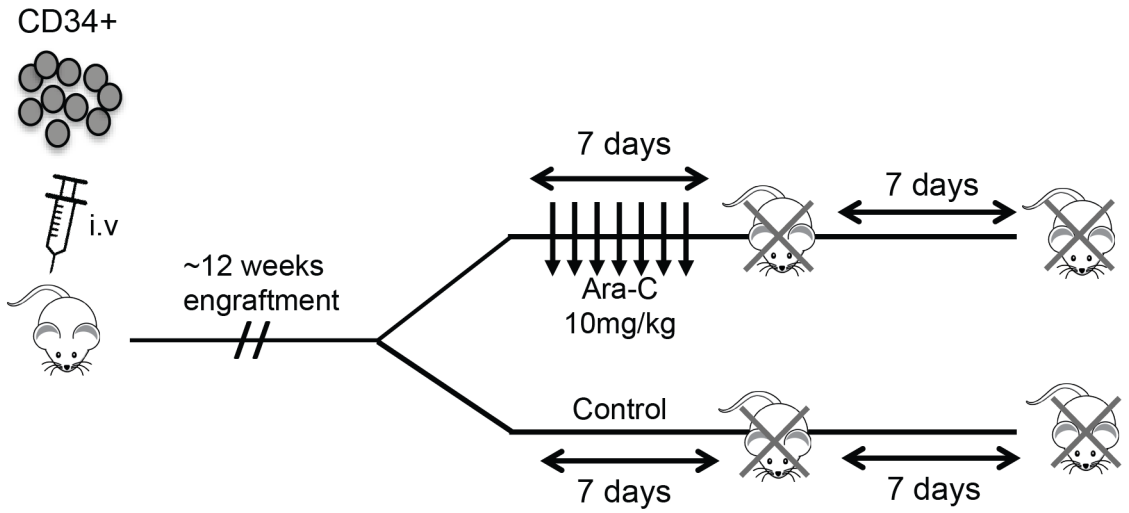

Figure 4.10 Schematic of *in vivo* Ara-C treatment protocol.

NSG mice were transplanted with 50,000 CD34+ purified cord blood cells. Engraftment was analysed at 12 weeks before treatment with 10mg/kg per day for 7 days. A cohort of mice were sacrificed 24 hours post the final injection and another cohort 7 days post the final injection after a recovery period.

To maintain clinical relevance a dose regime of 10 mg/kg Ara-C for 7 consecutive days was administered (Robles et al., 2000). This imitates a low-dose regime often

used to treat older patients to reduce toxicity. Mice were sacrificed 24 hours and 7 days post final injection for early and late time points of analysis.

4.3.1 Ara-C causes reduction in human engraftment.

Following Ara-C treatment of CD34+ engrafted NSG mice, human bone marrow chimerism was analysed by assessing the frequency of expression of hCD45 in the total CD45 fraction of the murine bone marrow (Figure 4.11A). Significant decreases in human CD45 engraftment could be seen at 24 hours; with further significant reductions 7 days post Ara-C treatment, showing the diminishing effect of Ara-C on human haematopoietic cells *in vivo*.

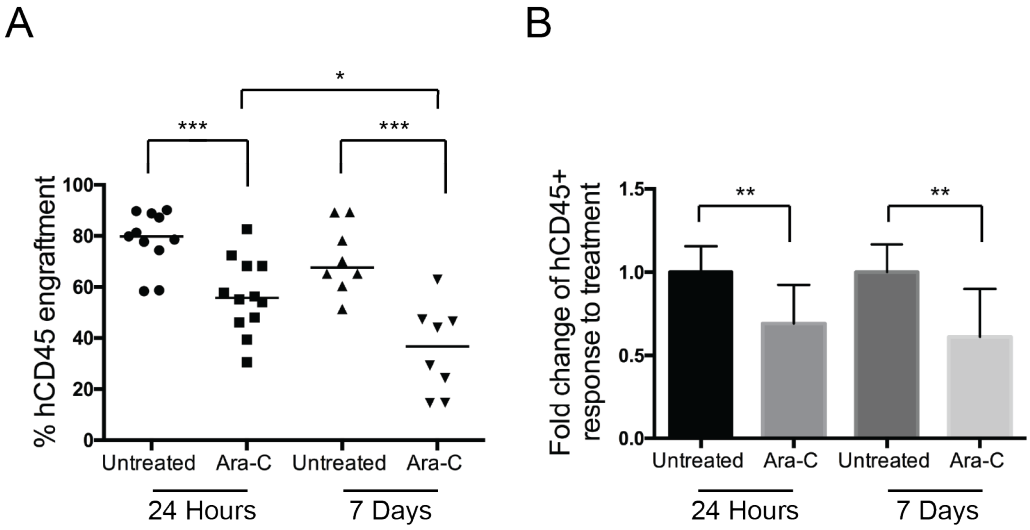

Figure 4.11 Human CD45+ cells response to Ara-C treatment *in vivo*.

(A) Analysis of human engraftment at 24 hours and 7 days post final Ara-C treatment by measuring frequency of hCD45+ expressing cells by FACS within the total CD45+ fraction of the murine bone marrow (hCD45+/mCD45+). Median bars are shown. (B) Fold change response of the frequency of human CD45+ cells within the murine bone marrow to Ara-C treatment. *p<0.05, **p<0.005, ***p<0.0005 (n=5).

Indeed there are significant fold reductions in the frequencies of human cells compared to murine within the bone marrow at both 24 hours and 7 days (Figure 4.11B), showing a significant response of the human cells to Ara-C treatment.

4.3.2 Normal stem and progenitor cell numbers are reduced by Ara-C treatment.

While there is significant reduction in frequency of human cells by examination of the whole CD45+ haematopoietic populations after Ara-C treatment, a closer analysis of actual cell numbers is needed. Observing specific populations within the bone marrow will determine if one population is more affected from Ara-C treatment than the other *in vivo.*

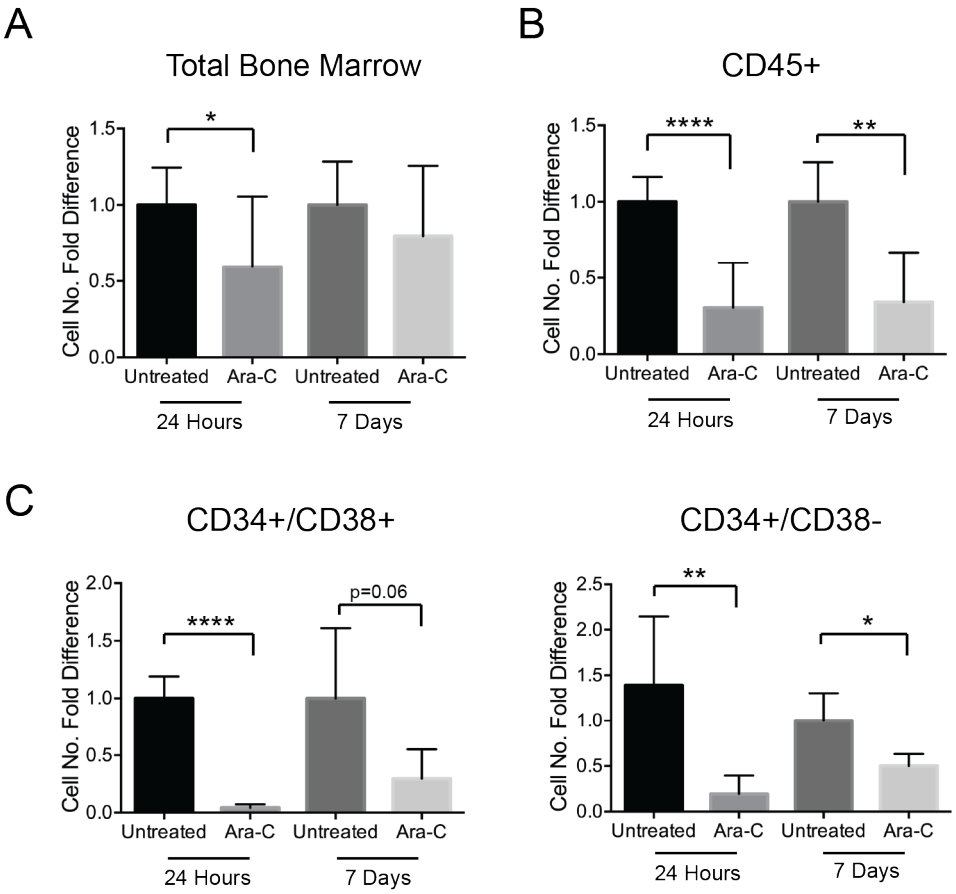

Figure 4.12 Cell counts of total bone marrow and human cells *in vivo* post Ara-C treatment.

FACS analysis of absolute cell counts post Ara-C treatment *in vivo*. Data is represented as fold change compared to untreated. (A) Cell counts of the total bone marrow. (B) Cell counts of the human CD45+ population. (C) Cell counts of HPCs (CD34+/CD38+) and HSPCs (CD34+/CD38-). *p<0.05, **p<0.005, ****p<0.0001 (n=3). Error bars are ± S.D.

Analysis of the total bone marrow by FACs showed a significant ($p=0.04$) two-fold reduction in cellularity at 24 hours, which began to rise slightly by 7 days (Figure 4.12A). The reductions in cell numbers were more marked when examining the total human CD45+ fraction of cells, which displayed a significant 3-fold reduction; this was maintained up to 7 days post Ara-C treatment (Figure 4.12B). This suggests the haematopoietic compartment is more sensitive to the effect of Ara-C than other bone marrow populations.

Indeed this observation was even more exacerbated when analysis of the more primitive haematopoietic populations showed that Ara-C treatment incurred a 10-fold reduction in HPC cell number compared to 4-fold in HSPC at 24 hours (Figure 4.12C). 7 days after the final treatment, there were still significant reductions in cell numbers for both populations, however there was evidence that the cells had begun to regenerate as the fold reduction was not as marked compared to 24 hours.

Analysis of AnnexinV showed a significant 2-fold increase in apoptosis of HPC populations (p=0.001) at 24 hours (Figure 4.13), corresponding to the greater reduction in cell number observed. At 7 days apoptosis was still observed in HPCs (p=0.053). Unusually, HSPCs did not show any significant increase in apoptosis at 24 hours or 7 days 7 days post Ara-C *in vivo* (Figure 4.13).

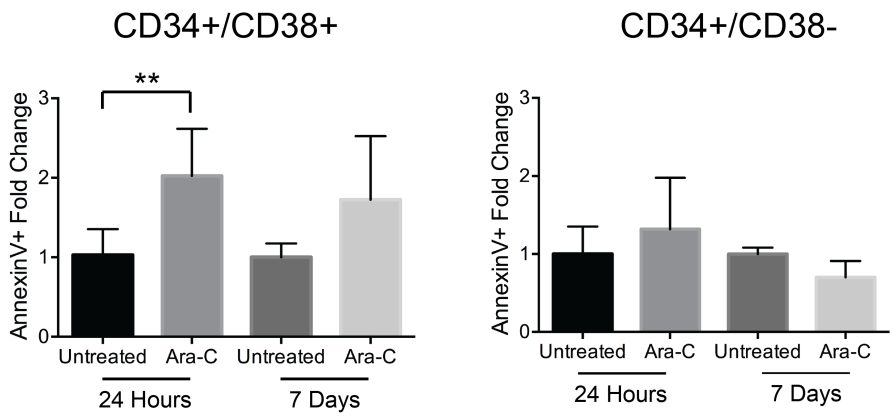

Figure 4.13 Apoptosis analysis by AnnexinV+ staining of CD34+ cells *in vivo* post Ara-C treatment.

Analysis of apoptosis by AnnexinV staining by FACS of HSPCs (CD34+/CD38-) and HPCs (CD34+/CD38+) post Ara-C treatment *in vivo.* Data is represented as fold change compared to mean of the untreated. **p<0.01 (n=3). Error bars are ± S.D.

4.3.3 Ara-C causes changes in cell cycle of progenitors *in vivo*.

Analysis of cell cycle status of CD34+ populations *in vivo* was undertaken by examining Ki67 and DAPI profiles. HPCs and HSPCs were both shown to have approximately 40% of cells within G0 in the untreated condition (Figure 4.14).

Remarkably HSPCs appeared to show no perturbations in cell cycle at 24 hours post Ara-C treatment, seemingly contrary to the cell loss observed. HPCs however, showed a significant decrease in frequency of cells in G0 ($p=0.02$) and a significant increase of cells in S-phase ($p=0.008$), reminiscent of the cell cycle profiles seen *in vitro*.

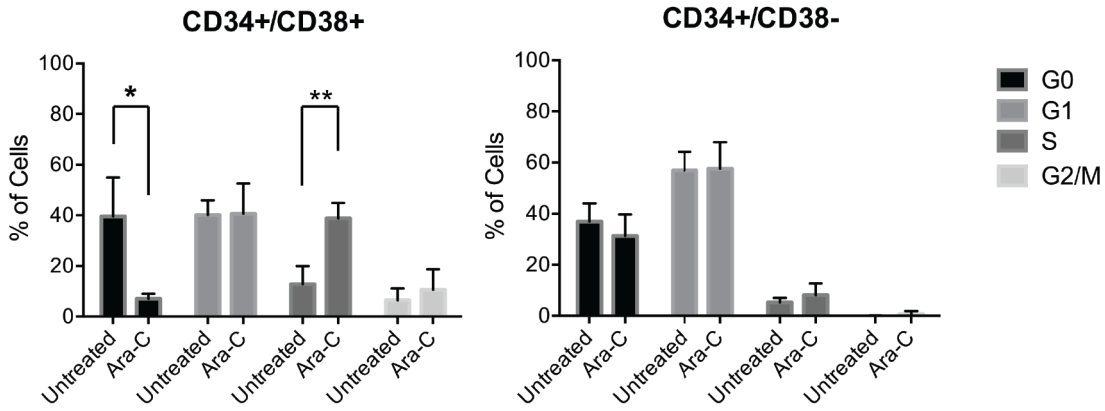

Figure 4.14 Analysis of cell cycle by intracellular FACS of Ki67 in CD34+ cells *in vivo* post Ara-C treatment.

Analysis of cell cycle by FACS of Ki67 and DAPI stained HSPCs (CD34+/CD38-) and HPCs (CD34+/CD38+) cells post Ara-C treatment *in vivo.* Represented as frequency of cells. *$p<0.05$, **$p<0.01$. Error bars are ± S.D.

4.3.4 DNA Damage post Ara-C treatment *in vivo*.

Considering the HSPC population appeared to endure a cell loss without alterations in cell cycle in response to Ara-C treatment *in vivo,* as compared to HPC, assessment of DNA damage was utilised post-treatment to determine whether Ara-C is acting sufficiently upon the different populations.

Assessment of DNA damage by γH2AX using FACS showed both HPCs and HSPCs increased levels of γH2AX at 24 hours post Ara-C treatment (Figure 4.15A).

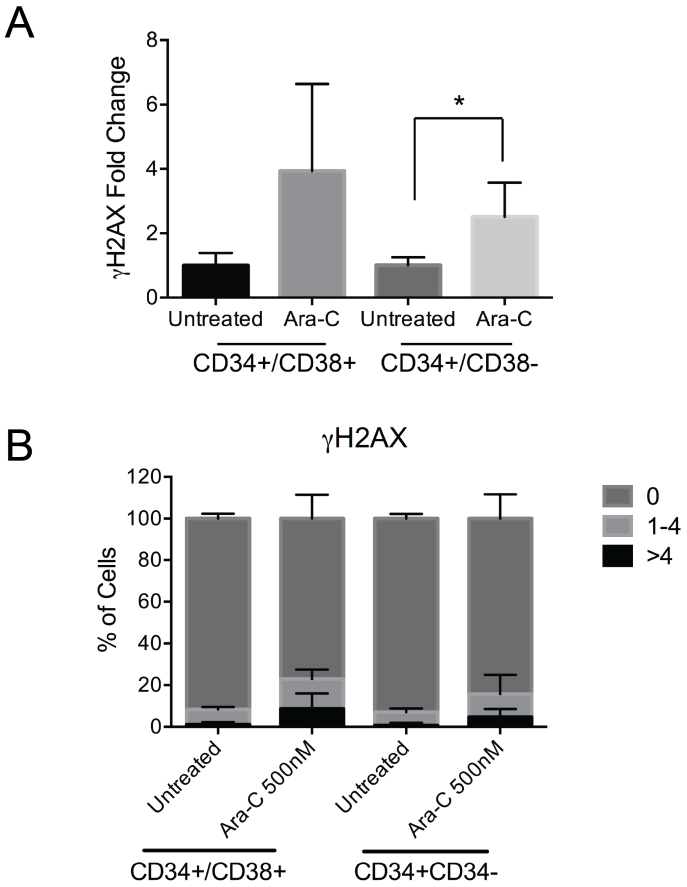

Figure 4.15 Quantification of γH2AX in CD34+ cells by FACS and IF post Ara-C treatment.

(A) Quantification of γH2AX by fold difference of MFI by geometric mean normalized to mean of the untreated condition. CD34+ cells were engrafted *in vivo* and analysed at 24 hours post-final Ara-C treatment. *p<0.05, (n=3). Error bars are ± S.D. (B) Immunofluorescence staining of γH2AX staining 24 hours post final Ara-C treatment *in vivo*. Quantification of number of foci per cell represented as frequency of cells with either 0, 1-4 or >4.foci per cell. 100 cells were counted per condition (n=3). Error bars are ± S.D.

HPC showed a 4-fold, yet statistically insignificant increase (p=0.07) and HSPC showed 2-fold induction of γH2AX (p=0.017). When γH2AX foci were quantified by IF, there seemed to be a slight increases in DNA damage in both populations (Figure 4.15B).

Measurement of direct DNA damage by alkaline comet assay showed significant increases in olive tail moment in HPC (Figure 4.16A), however HSPC appeared to display no differences in DNA damage post Ara-C treatment (Figure 4.16B).

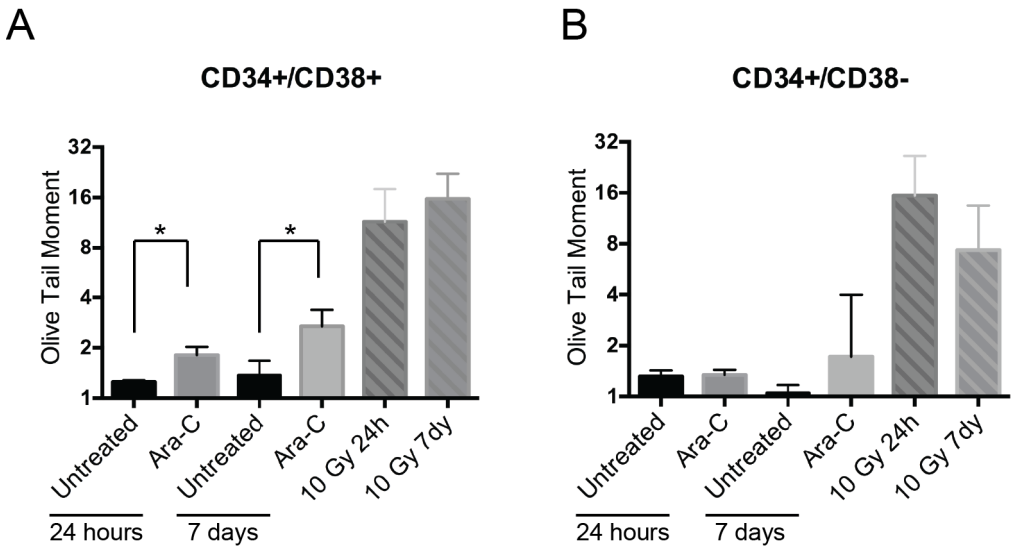

Figure 4.16 Alkaline comet assay of CD34+ cells treated with Ara-C *in vivo*.

Quantification of direct damage by olive tail moment, a measurement of DNA tail migration x comet tail DNA density. (A) HPC (CD34+/CD38+) and (B) HSPC (CD34+/CD38-) populations were sorted from CD34+ engrafted NSG mice at 24 hours and 7 days post Ara-C treatment *in vivo*. 100 cells were scored per slide where possible. *p<0.05 (n=3). Error bars are ± S.D.

HPC populations behaved as expected in response to Ara-C treatment *in vivo*, showing reduction in cell numbers; increase in frequency of cells in S-phase and increases in DNA damage. However, HSPC populations although showing a significant reduction in cell number, displayed no apoptosis or adaptations of cell cycle status with slight evidence of DNA damage by γH2AX. This perhaps suggests that any HSPC that come into contact with Ara-C die at a quicker rate and are lost before detection, whereas HPC are able to persist longer with damage. HSPC numbers were then able to revive after the 7-day recovery as Ara-C is cleared from the system.

4.3.5 DNA repair post Ara-C treatment *in vivo*.

As seen *in vitro* normal haematopoietic cells are able to show evidence of initiation of DNA repair mechanisms in response to Ara-C. Again, using IF staining for nuclear localisation of 53BP1 and RAD51, there was almost undetectable evidence of DNA repair by either mechanisms in both HSPCs and HPCs (Figure 4.17).

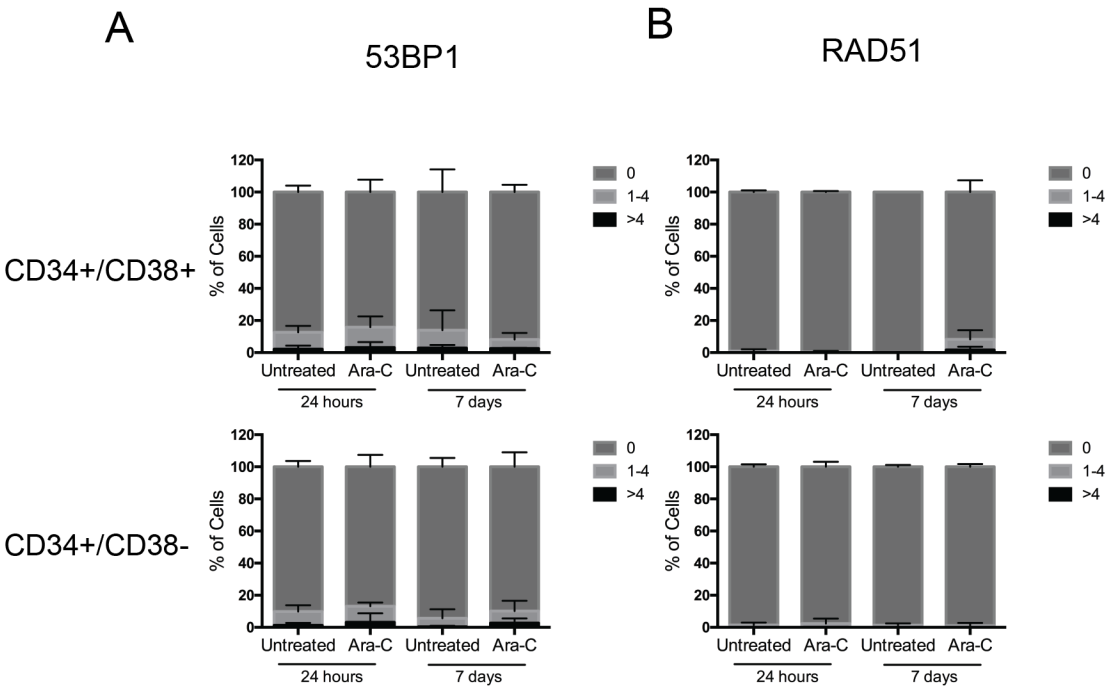

Figure 4.17 Analysis of DNA Repair by NHEJ and RAD51 in CD34+ treated with Ara-C *in vivo*.

Immunofluorescence staining of (A) 53BP1 nuclear foci and (B) RAD51 nuclear foci 24 hours and 7 days post final Ara-C treatment *in vivo*. Quantification of number of foci per cell represented as frequency of cells with either 0, 1-4 or >4.foci per cell. 100 cells were counted per condition (n=3). Error bars are ± S.D.

4.4 Discussion

In this chapter the effect of chemotherapeutic treatment by Ara-C was determined on normal haematopoietic cells. Using the *in vitro* model it was shown that HSPCs had a greater fold reduction in cell numbers, compared to HPCs, as well as a higher induction of apoptosis in response to Ara-C. However, as described previously, Ara-C works by incorporating into proliferating cells and analysis of cell cycle status showed that HPCs had a greater frequency of cells within the cycling phases. This suggested that HPCs should be the most effected. Indeed, when DNA damage was assessed it was shown that HPC had a greater amount of DNA damage in response to Ara-C when compared to HSPC. Taking this into consideration, even though HPCs are cycling more than HSPCs *in vitro*, thus receiving more DNA damage from Ara-C, HPCs appear to be more tolerant of Ara-C treatment than HSPCs. As well, analysis of activation of DNA repair mechanisms showed a greater frequency of HPCs with 53BP1 localisation, consistent to the amount of damage incurred. Interestingly, CD34+ CB cells showed a preference for NHEJ repair post Ara-C treatment, as also evidenced in the last chapter with AML cell lines.

While *in vitro* assessments of drug treatments are extremely useful, in the human haematopoietic field *in vivo* analysis using the xenograft model is the gold standard. After engrafting mice with CD34+ CB cells and treating with Ara-C there was reduction in human engraftment in the mouse bone marrow. When observing actual cell numbers of HPCs and HSPCs it was shown that HPCs had a greater fold reduction than HSPCs, coupled with a higher induction of apoptosis after Ara-C treatment. Paired with this, a perturbation in the cell cycle of HPCs was also observed. However the cell cycle of HSPCs remaining unchanged, as the majority of HSPCs were in the G0/G1 phases of the cell cycle, allowing greater evasion of the action of Ara-C. HPCs also showed a higher degree of DNA damage post Ara-C. However, contrary to what has previously been shown *in vitro*, there appeared to be no activation of DNA repair mechanisms in response to Ara-C in either HPCs or HSPCs. This could be due to the differences in the time points analysed and doses of Ara-C used.

The comparison of *in vitro* and *in vivo* data however should be taken with some caution. As alluded previously, the physiological interactions governing the regulation of the haematopoietic cells in both models is vastly different. It is known that the bone marrow niche is comprised of many different compartments of cells such as mesenchymal, osteoblastic and endothelial cells, each playing their own role in maintenance of the HSC *in vivo* (Morrison and Scadden, 2014). As well, the different dosages and treatment regimes of Ara-C used makes the direct comparison between the models even more difficult. *In vitro*, Ara-C is exposed directly to the haematopoietic cells and is added in a single dose. When the cells are analysed 96 hours later, Ara-C is still within the system, as the effect of the drug is more exacerbated than the early 24-hour time point. Whereas *in vivo*, Ara-C is dosed over several days into a full biological system where the drug has more boundaries to cross before reaching the bone marrow and taking its effect. By 7 days post the final treatment; most of the Ara-C appears to have cleared from the system as cell numbers show signs of recovery, with reductions in apoptosis. Therefore it was understandable that although there are differences in the models used and the observed outcomes, valuable insights can still be gained about the effect of Ara-C on normal CD34+ cells from *in vitro* and *in vivo* analysis.

One of the more pronounced changes that Ara-C inflicted was in the cell cycle. *In vitro* there was an initial enrichment of both HPCs and HSPCs cells within G0 at 24 hours post Ara-C treatment. This suggested that any cells in cycle when Ara-C was added were cleared by the treatment relatively quickly. By 96 hours however, cells that had come out of G0 and into cycle and were enriched in the S-phase compared to untreated. This was most pronounced in HPCs, whereas HSPCs seemed to be slower to exit quiescence and there was a substantial decrease in G2/M phase cells, showing they were unable to get passed the S-phase, suggestive of an S-phase block after long-term exposure to Ara-C and induction of DNA damage. The same could be seen *in vivo* in the HPC population. However HSPCs *in vivo* showed no observable differences in cell cycle post Ara-C, with most of the cells staying in G0/G1. To assess if this was indeed a true arrest at the G1/S-phase, molecular characterisation of levels of $p21^{CIP1}$ (encoded by *CDKN1A*) (Niculescu et al., 1998) and Cyclin E (Ohtsubo et al., 1995), as well as the analysis of activation of p53 (Meek, 2009) would be useful to dissect the cell fate decisions

happening between HPCs and HSPCs in response to DNA damage inflicted by Ara-C.

Overall, it could be suggested that in the treatment of HPCs and HSPCs with Ara-C, they show different dynamics of response. *In vitro* analysis shows that when CD34+ cells do come into contact with Ara-C they incur DNA damage and initiate NHEJ repair. However HSPCs appear to perish more readily, whereas HPCs are blocked in G1/S-phase arrest seeming to tolerate the effect of Ara-C longer. On the other hand, the *in vivo* analysis provides a bigger picture in what could be happening clinically. As Ara-C treatment comes to an end, the quiescent HSPCs have been spared and they remain to help regenerate the bone marrow.

Chapter 5. Results 3: DNA Damage response of Primary Acute Myeloid leukaemia Samples to Ara-C Treatment.

5.1 Introduction

The DNA damage response (DDR) in normal human haematopoiesis still remains somewhat controversial. Yet currently, perhaps more is known about the DNA damage and repair mechanisms in AML, due to their role in pathogenesis of the disease and responses to therapies. While mutations in DNA damage response and repair genes are rare in AML (CancerGenomeAtlasResearch, 2013), it is apparent that the many epigenetic abnormalities observed in AML, can cause deregulation of the gene expression of the many DDR genes. Briefly, this can range from certain complex karyotype AMLs overexpressing genes such as *RAD21* and *MSH6* (Schoch et al., 2005) causing enhanced DNA repair activity by HR or MMR respectively. In addition, fusion onco-proteins, such as PML-RARA, can inhibit the expression of numerous DNA repair genes including *DNA-PK* involved in NHEJ repair (Casorelli et al., 2006). These alterations in DDR are heterogeneous, as is the very nature of AML, often depending on their karyotype and gene mutations.

Previously in this study it was shown that when normal haematopoietic cells come into contact with Ara-C, DNA damage is incurred and NHEJ repair is activated in both HSPCs and HPCs. However, the more mature progenitor populations appeared to be more tolerant of the Ara-C treatment. The literature certainly shows that there are differences in the DNA damage responses between progenitor and stem cell populations. Therefore could the same be said for AML when comparing LICs and bulk tumour populations? The final part of this study will be to ascertain the response of primary human AML samples to treatment with Ara-C, again with key focus on activation of DNA damage and repair mechanisms.

5.2 Results

For this investigation a panel of six primary AML patient samples was selected based on their ability to engraft into NSG mice. From the clinical data available there was a mixture of karyotypes, however most patient samples that are able to engraft come with a intermediate to poor risk group (Table 1). Although requested, clinical outcome data for the samples was unattainable at the on going time of the study. All samples were negative for NPM1 mutation (Taussig et al., 2010).

	Karyotype/FAB Subtype	Risk Group
AML1	M0 - Inv(3)(q21;q26)t(8;13)	Poor
AML2	Normal	Intermediate
AML3	Normal - FLT3-ITD	Intermediate
AML4	M5 – t(9;11)(p21q23) MLL/AF9	Intermediate
AML5	M1	Intermediate
AML6	N/A	N/A

Table 5.1 Karyotypes and risk groups of the cohort of primary AML patient samples.

To provide the best comparison to normal haematopoiesis, only CD34 expressing AML samples were used, where pre-screening had been done to determine that LICs were within the CD34+ compartment. AML6 was the only sample where LICs were undetermined therefore it can be said that LICs are highly enriched, but perhaps not exclusively, within the CD34+ compartment (Taussig et al., 2008).

Samples were injected i.v. and when high engraftment (~80% hCD45) was attained Ara-C was administered as described previously (Chapter 4), 10mg/kg daily for 7 days. Again, samples were analysed at 24 hours and 7 days post the final injection. As seen in Figure 5.1 the phenotypic expression of CD34 and CD38 post engraftment is diverse across the samples and to assure that a leukaemic engraftment was obtained expression of CD33 versus CD19 was always assessed. For this study CD34+ and CD34- populations were analysed separately to correspond with LIC containing and bulk tumour populations respectively.

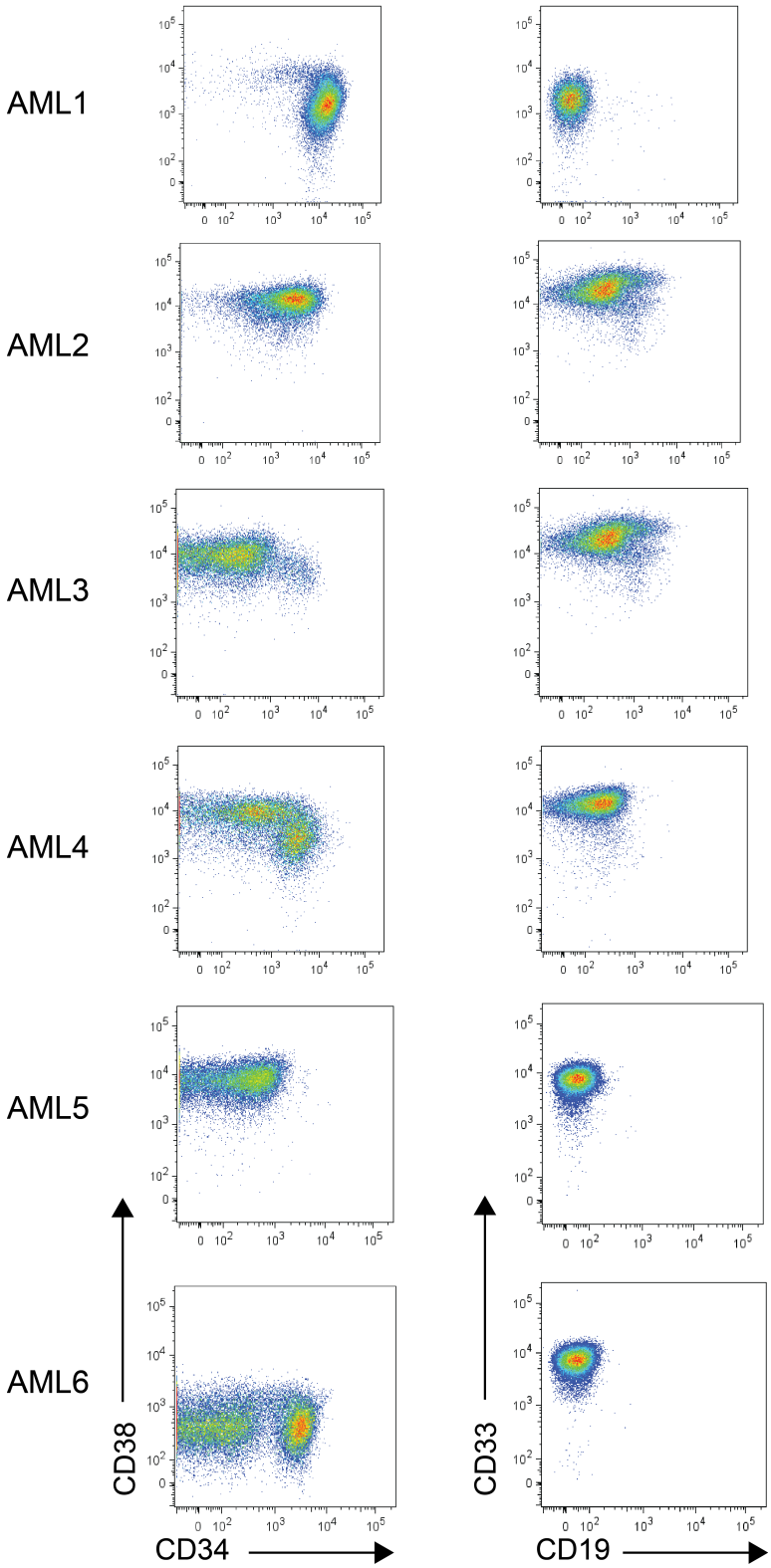

Figure 5.1 Phenotypic profiles of primary AML patient samples.

FACS plots showing the expression profiles of CD34/CD38 and CD33/CD19 (gated from total CD45) post engraftment for the cohort of primary AML patient samples.

5.2.1 Effect of Ara-C on AML CD45 engraftment *in vivo*.

Following Ara-C treatment of AML engrafted mice, human bone marrow chimerism was analysed by assessing the frequency of human CD45 expression in the total CD45 fraction of the murine bone marrow (Figure 5.2). Significant decreases in AML engraftment were seen at 24 hours post Ara-C treatment in 50% of the samples (AML1 p=0.002, AML2 p=0.03 and AML3 p=0.006). Human engraftment was even further diminished at 7 days, for samples AML2 (p=0.006) and AML3 (p=0.0002). There was no data for sample AML1 at the 7-day time point due to the aggressiveness of the leukaemia sample weakening the animals and causing premature death after challenge from Ara-C. Frequency of AML engraftment for samples AML4 and AML6 however remained relatively unchanged.

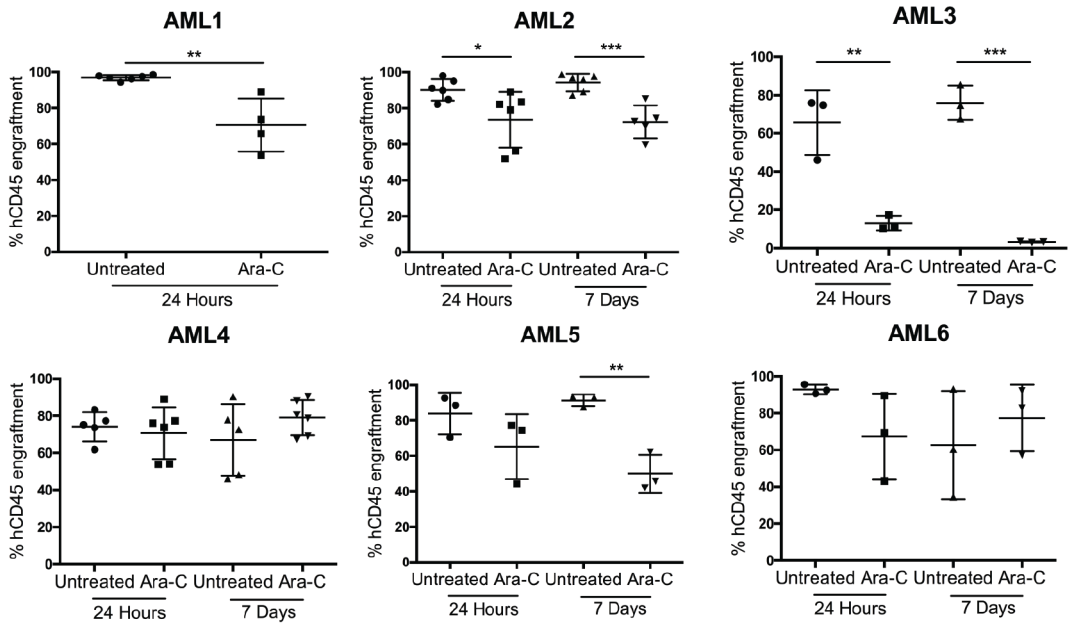

Figure 5.2 Human CD45+ engraftment of primary AML samples post Ara-C treatment.

Analysis of human engraftment at 24 and 7 days post final Ara-C treatment by measuring frequency of hCD45+ expressing cells by FACS within the total CD45 fraction of the murine bone marrow. *p<0.05, **p<0.005, ***p<0.0005. Error bars are ± S.D. (n=3-6 mice).

5.2.2 Reduction in the number of AML cells post Ara-C treatment *in vivo*.

As there were differences in the reduction of engraftment between AML samples an examination of actual cell numbers was undertaken to ascertain whether CD34+ populations, compared to CD34- were more affected by the Ara-C treatment.

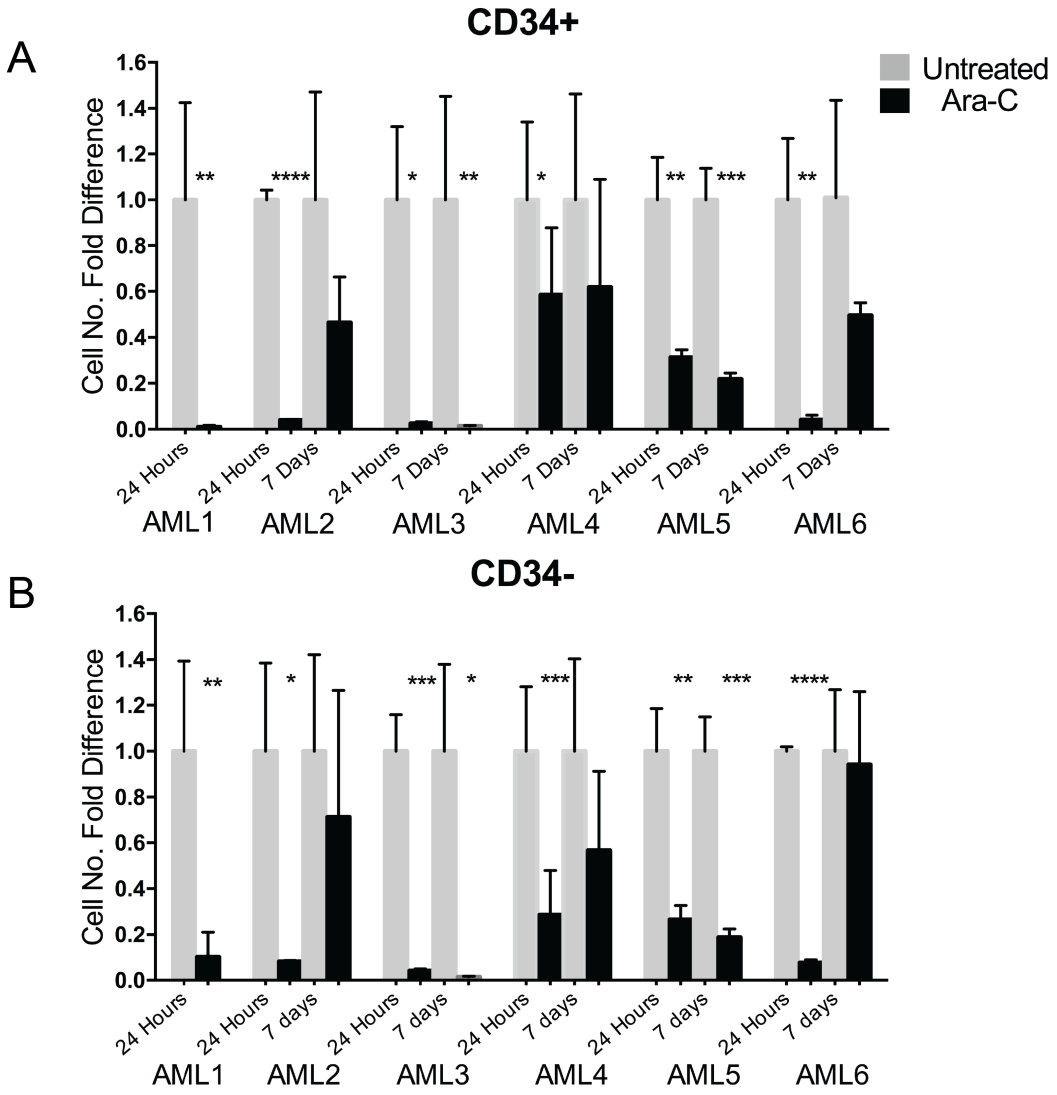

Figure 5.3 Cell counts of human AML cells *in vivo* post Ara-C treatment.

FACS analysis of cell counts of (A) CD34+ and (B) CD34- populations post Ara-C treatment *in vivo*. Data is represented as fold change compared to mean of untreated samples. *p<0.05, **p<0.005, ***p<0.001, ****p<0.0001. Error bars are ± S.D (n=3-6 mice).

CD34+ LIC containing populations showed a dramatic fold reduction in the number of cells at 24 hours post Ara-C treatment compared to untreated, with all but sample AML4 showing a significant decline in numbers (Figure 5.3A). By 7 days

there was evidence of recovery of cell numbers in samples AML2 and AML6 however samples AML3 and AML5 appeared to decline even further.

The CD34- populations at 24 hours, although showing hugely significant reductions, they were not as marked at the corresponding CD34+ populations (Figure 5.3B). CD34+ populations of sample AML1 were decreased by approximately 100-fold in response to Ara-C, whereas CD34- populations were only reduced 10-fold. Another example is sample AML6, where the CD34+ population was reduced on average 25-fold and the CD34- population 14-fold. The only sample to buck this trend was AML4, which showed a significant reduction in CD34- cell numbers ($p=0.0007$) by 5-fold compared to untreated, whereas the CD34+ population was approximately 1.5-fold reduced. By 7 days post Ara-C treatment 50% of the samples appeared to have regained numbers of CD34- cells back to levels comparable with untreated. While samples AML3 and AML5 again showed further declines in cell number.

Ara-C was extremely effective on the majority of samples, with sample AML4 being the least responsive to treatment. Sample AML3 was particularly sensitive being almost completely diminished with no recovery at 7 days. Overall the samples showed a mixed response to treatment, with CD34- populations showing the lowest reduction in cell number and the quickest recovery by 7 days post Ara-C treatment.

5.2.3 Induction of apoptosis by Ara-C treatment of AML samples in vivo.

Analysis of apoptosis was done by staining for AnnexinV expression post Ara-C treatment *in vivo.* Analogous with the reduction in cell numbers, CD34+ populations showed greater fold-increases in apoptosis than compared to CD34- populations from the same samples (Figure 5.4A). Sample AML3 had a 5-fold increase in apoptosis in CD34+ cells ($p=0.0001$), yet only a 2.5-fold increase in CD34- cells ($p=0.002$) at 24 hours.

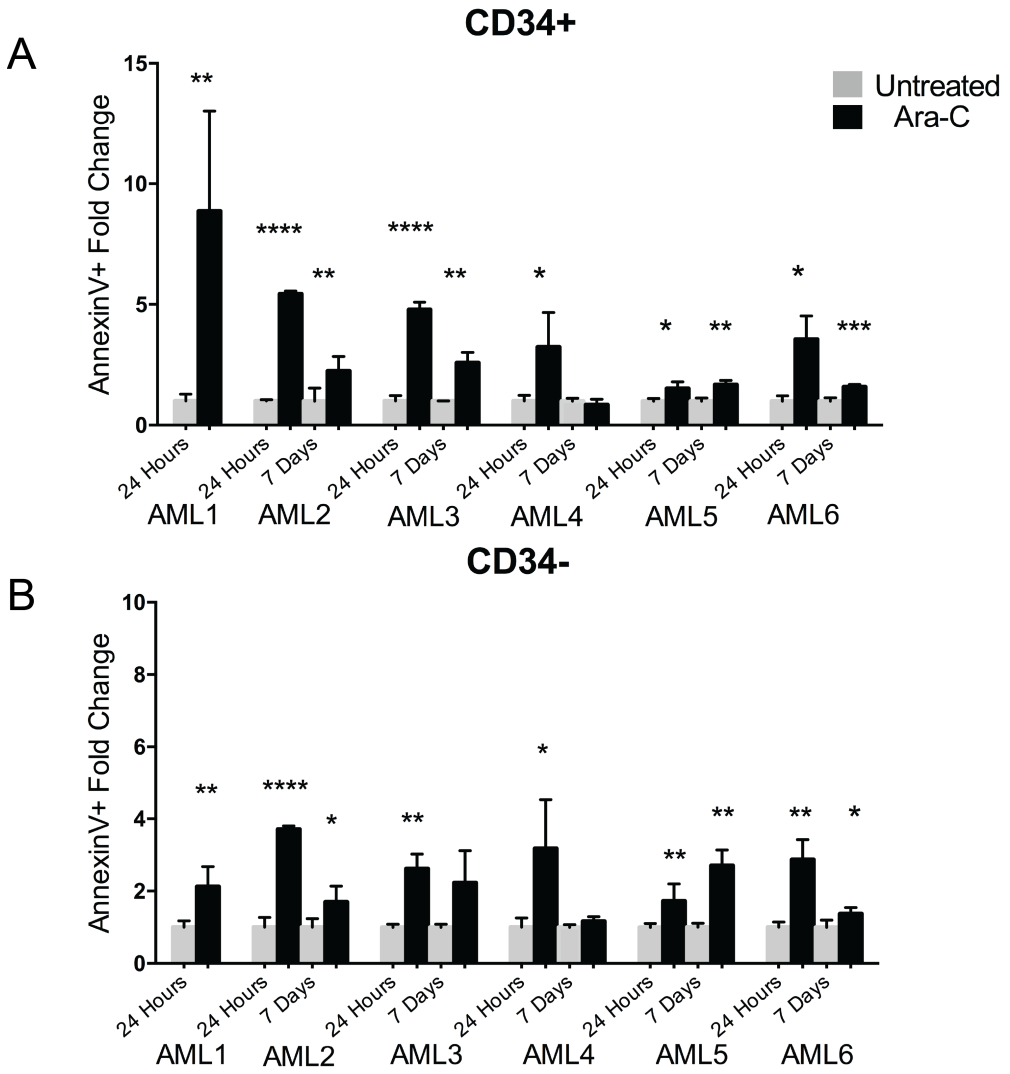

Figure 5.4 Apoptosis analysis by AnnexinV+ staining of primary AML samples *in vivo* post Ara-C treatment.

Analysis of apoptosis by AnnexinV staining by FACS of (A) CD34+ and (B) CD34- fractions post Ara-C treatment in vivo. Data is represented of fold change compared to mean of untreated. *p<0.05, **p<0.005, ***p<0.0005, ****p<0.0001. Error bars are ± S.D. (n=3-6 mice).

By 7 days most CD34+ populations had reduced apoptosis compared to 24 hours, yet there was still evidence of significant differences compared to untreated. Only sample AML5 maintained the same frequency of AnnexinV positive cells, comparable to the further reductions in cell number seen at 7 days for this sample.

CD34- populations by 7 days post Ara-C treatment as well showed levels of apoptosis beginning to return to that of untreated, yet still had significant

frequencies of cells staining for AnnexinV (Figure 5.4B). Sample AML4 was the only samples that had completely reduced its apoptosis by 7 days post Ara-C treatment, again showing a quick recovery.

5.2.4 Cell cycle status of AML patents samples post Ara-C treatment *in vivo*.

To investigate if the differences in reduction of cell numbers and apoptosis observed correlated with proliferation status, analysis of the cell cycle status of CD34+ and CD34- AML populations was undertaken by examining Ki67 and DAPI profiles by FACS.

As evidenced in Figure 5.5, the frequency of the cell cycle phases between each of the samples at the untreated level is vastly different. Especially when comparing the frequency of G0 cells in samples AML4 and AML5 which are 40% and 80% respectively. At 24 hours post Ara-C treatment samples AML3 and AML5 show significant enrichment of G0 cells in both CD34+ and CD34- populations. This G0 enrichment was continued up to 7 days, with sample AML5 as well showing significant reductions in the S and G2/M cycling phases. Sample AML6, and partially sample AML2, showed the stalling of cells at the G1/S phases in response to Ara-C treatment in both CD34 populations over both the time points analysed. Sample AML4 did not appear to react to the treatment of Ara-C.

Overall CD34- populations had a greater proportion of cells within G0, comparable to their lower reduction in cell numbers and lower induction of apoptosis compared to CD34+ populations. As well there was a mixture of responses with some samples stalling in the cycling phases and other samples enriching for G0 cells.

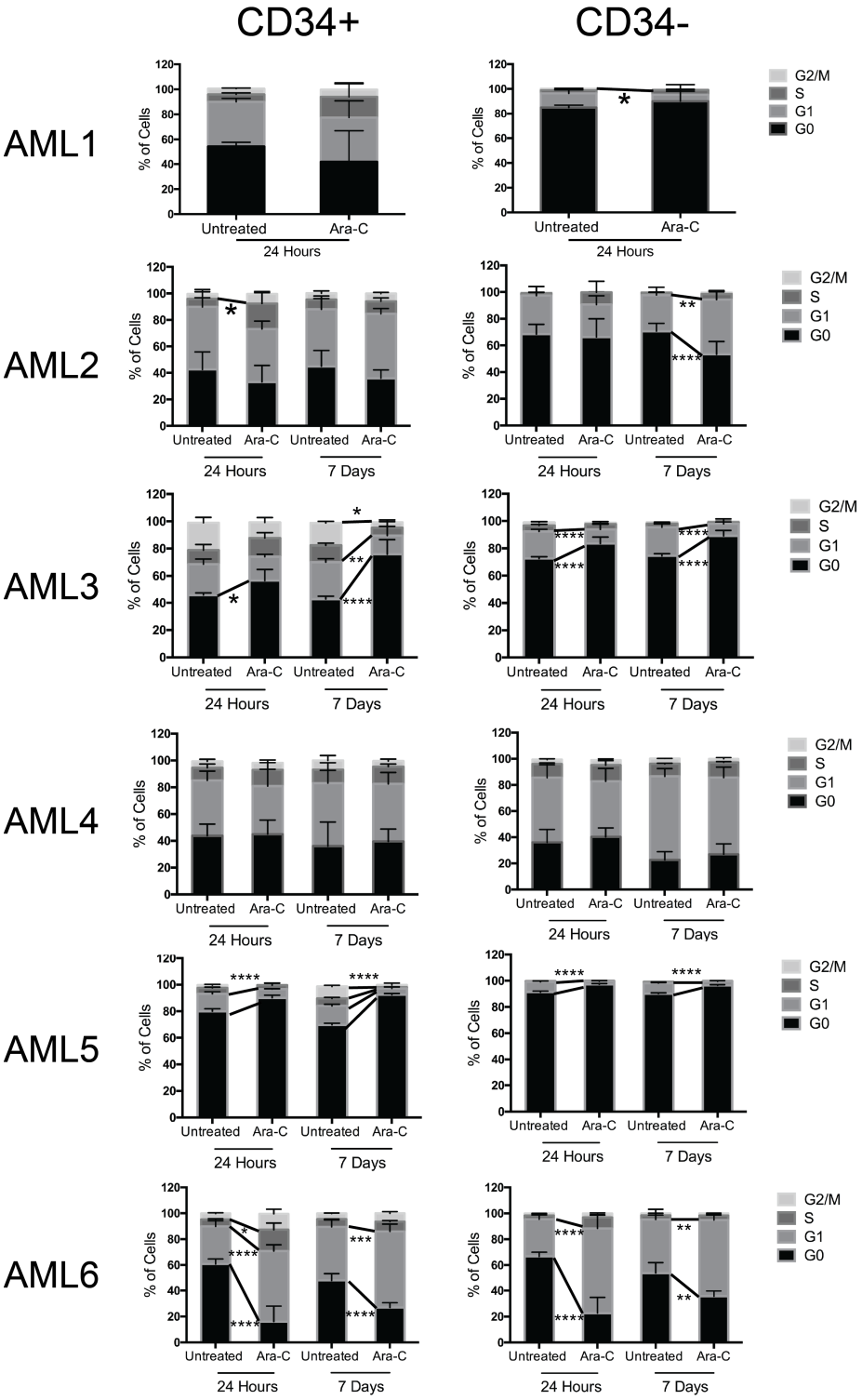

Figure 5.5 Cell cycle profiles by Ki67 staining of AML patient samples post Ara-C treatment *in vivo*.

Analysis of cell cycle by FACS of Ki67 and DAPI intracellularly stained primary AML patient samples *in vivo*. CD34+ and CD34- populations are represented as frequency of cells within the cell cycle phases. *p<0.05, **p<0.005, ***p<0.0005, ****p<0.0001. Error bars are ± S.D (n=3-6 mice).

5.2.5 DNA Damage post Ara-C in primary AML samples *in vivo*.

As CD34+ cells were shown to be more proliferative and effected by Ara-C *in vivo* than CD34- populations, assessment of DNA damage was employed to determine whether the AML samples were being sufficiently exposed to the drug. Overall levels of γH2AX by FACS showed mild differences post Ara-C treatment compared to untreated (Figure 5.6) in both CD34 populations.

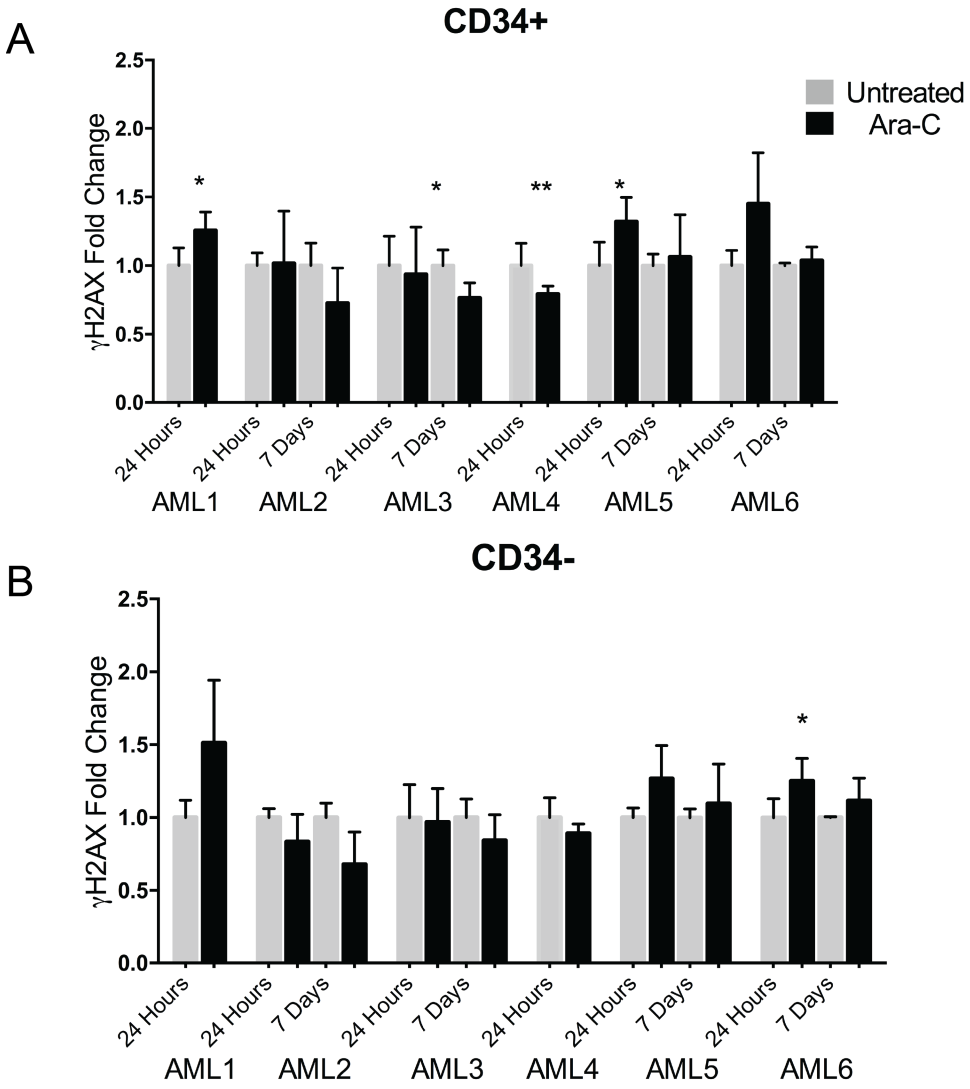

Figure 5.6 Analysis of DNA damage by γH2AX FACS in primary AML patient samples post Ara-C treatment.

Quantification of γH2AX by fold difference of MFI by geometric mean normalised to the mean of the untreated condition. Cells analysed 24 and 7 days after the final dose of Ara-C and were fractioned into CD34+ and CD34- populations. *p<0.05, **p<0.005. Error bars are ± S.D (n=3-6 mice).

Comparing CD34+ (Figure 5.6A) and CD34- (Figure 5.6B) populations between the same samples showed comparable changes in fold-change of γH2AX, with all samples at 7 days post Ara-C treatment displaying reduced levels of DNA damage. Interestingly, samples AML1, AML5 and AML6 showed increases in DNA damage, yet samples AML2, AML3 and AML4 all showed decreases across both the CD34 populations analysed.

When γH2AX was quantified by foci counting (Figure 5.7A) at 24 hours final treatment, again there was only evidence of mild changes in the level of DNA damage in the majority of samples (Figure 5.7B) after Ara-C treatment. Analysis of the CD34+ for sample AML5 could not be performed for this or subsequent IF experiments due to lack of available cells. Sample AML1 showed the largest increase in number of foci per cell in the CD34- compartment in response to Ara-C ($p=0.009$), in parallel with the largest fold increase of γH2AX by FACS (Figure 5.6A). Most AML samples showed evidence of an increase in DNA damage, with sample AML4 as usual showing no response. Samples AML1, AML3 and AML6 also showed differences in DNA damage between CD34+ and CD34- populations, showing heterogeneous responses within samples.

Again overall it can be seen that each AML sample displays a differential response to Ara-C when analysing DNA damage.

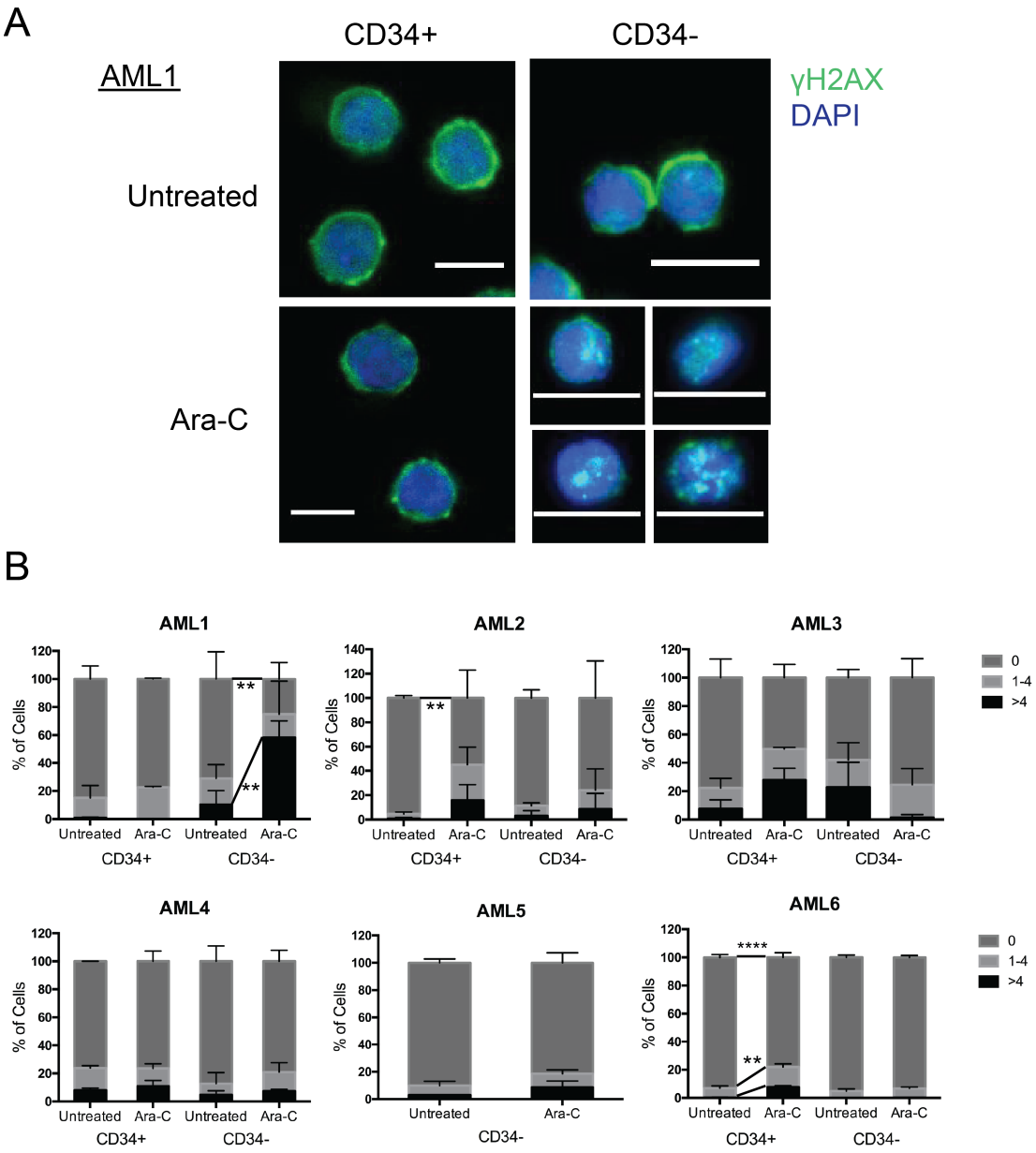

Figure 5.7 γH2AX foci counts post Ara-C treatment in AML patient samples *in vivo.*

(A) Representative immunofluorescence staining of γH2AX foci (green) and DNA (blue) in CD34+ and CD34- populations of engrafted primary AML patient *in vivo,* 24 hours post final Ara-C treatment. Scale bar, 10 μm. (B) Quantification of the number of foci per nuclei represented as frequency of cells with either 0, 1-4 or >4 foci per cell. 100 cells were counted per condition. **p<0.005, ****p<0.0001 (n=3). Error bars are ± S.D. (n=3-6 mice).

5.2.6 DNA repair post Ara-C treatment *in vivo*.

As performed previously, analysis of activation of DNA repair pathways in response to Ara-C in primary AML samples was done by the quantification of localisation of nuclear foci by IF.

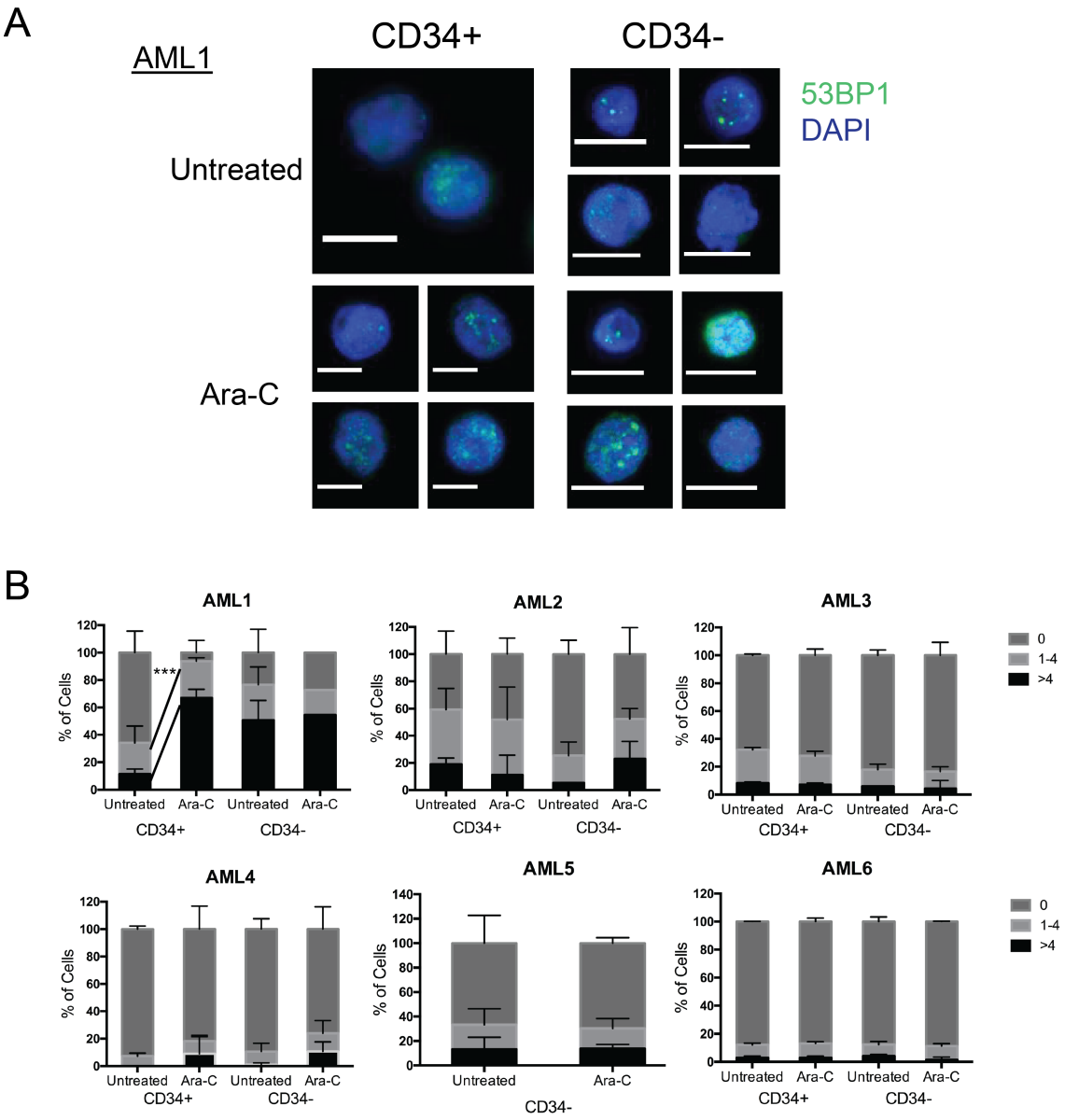

Figure 5.8 53BP1 foci counts post Ara-C treatment in AML patient samples *in vivo* for analysis of NHEJ repair.

(A) Representative immunofluorescence staining of 53BP1 foci (green) and DNA (blue) in CD34+ and CD34- populations of engrafted primary AML patient *in vivo,* 24 hours post final Ara-C treatment. Scale bar, 10 μm. (B) Quantification of the number of foci per nuclei represented as frequency of cells with either 0, 1-4 or >4 foci per cell. 100 cells were counted per condition. ****p<0.0001. Error bars are ± S.D. (n=3-6 mice).

Observation of 53BP1 nuclear foci for the activation of NHEJ repair was done for all AML samples post Ara-C treatment (Figure 5.8A). Comparing between patients it can be seen that sample AML1 is the only sample with significant increases in frequency of cells with 53BP1 foci after Ara-C treatment, however mild increases in foci counts could be seen in samples AML2 and AML4 (Figure 5.8B).

Comparison of CD34+ and CD34- populations in sample AML1 showed that the CD34- compartment had constitutively localised foci in up to 80% of cells, which did not change upon Ara-C treatment. As well sample AML2 showed a higher frequency of CD34- cells with 53BP1 than compared to the CD34+ population. Overall in the majority of samples there was an apparent basal level of 53BP1 foci in approximately 10-30% of all cells.

Analysis of RAD51 foci localisation for the activation of HR repair was preformed in parallel (Figure 5.9A). Across all the samples, except for AML1, there was barely evidence of RAD51 foci formation (Figure 5.9B). 50% of CD34+ cells of patient sample AML1 showed evidence of HR repair in response to Ara-C treatment, with significant increases seen as well in the CD34- compartment of frequency of cells with1-4 foci per cell.

In conclusion it would appear that generally the AML patient samples activate NHEJ repair within a small frequency of cells, in both the CD34+ and CD34- populations in response to Ara-C treatment.

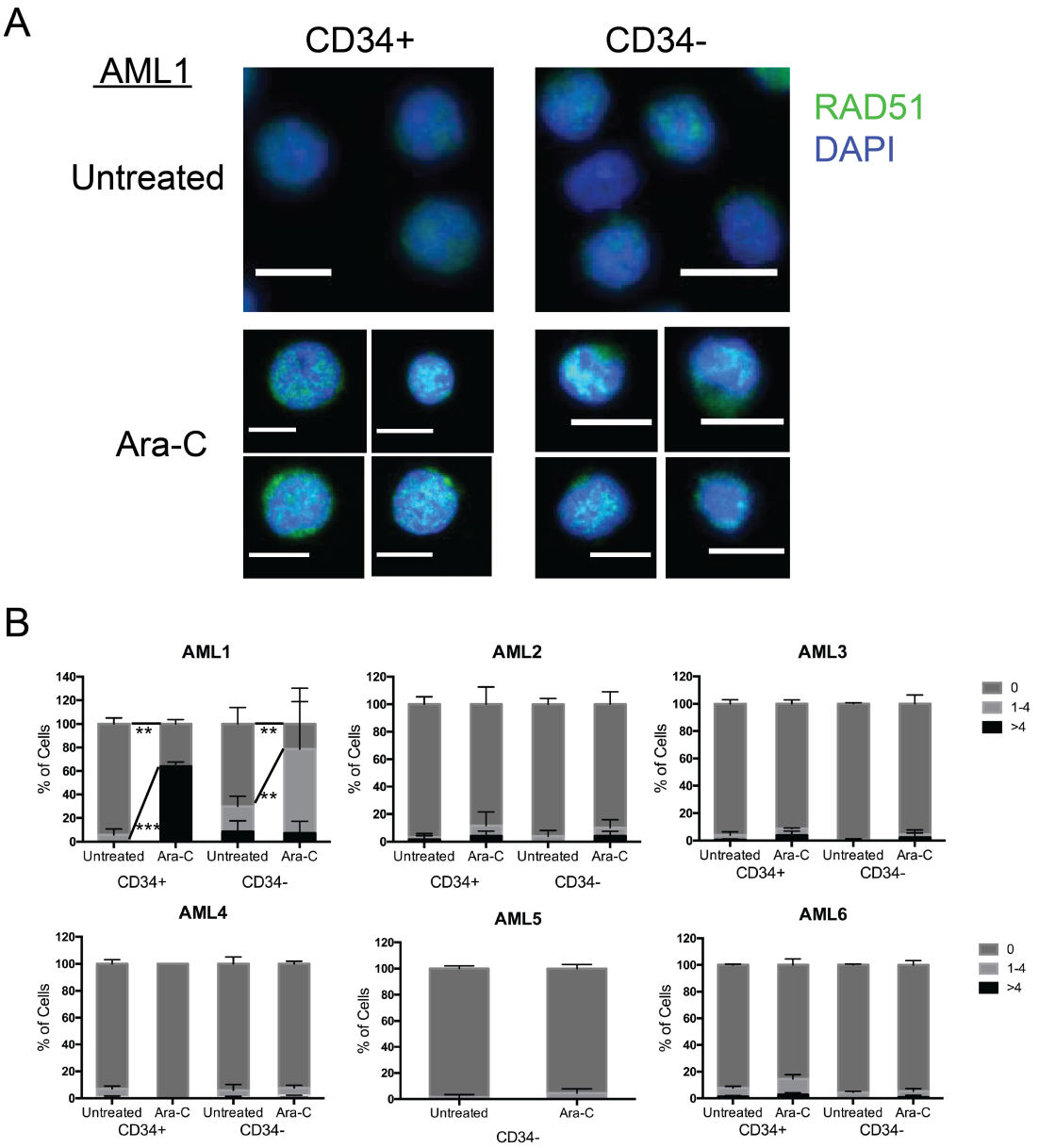

Figure 5.9 RAD51 foci counts post Ara-C treatment in AML patient samples *in vivo* for analysis of HR repair.

(A) Representative immunofluorescence staining of RAD51 foci (green) and DNA (blue) in CD34+ and CD34- populations of engrafted primary AML patient *in vivo*, 24 hours post final Ara-C treatment. Scale bar, 10 μm. (B) Quantification of the number of foci per nuclei represented as frequency of cells with either 0, 1-4 or >4 foci per cell. 100 cells were counted per condition. **p<0.005. Error bars are ± S.D. (n=3-6 mice).

5.2.7 Gene expression profiling of key DNA damage response and repair components.

As described in the literature there are frequently aberrations of epigenetic modulators in AML such as DNMT3a and EZH2, causing changes in gene

expression (Ernst et al., 2010, Mayle et al., 2015). Although the mutation status of such epigenetic regulators is unknown for the samples used in this study, perhaps the heterogeneous response shown to Ara-C could be explained by difference in expression of DDR effectors. To assess if there were any differences in gene expression of different DNA damage and repair components between CD34+ and CD34- compartments, an RT^2 Profiler PCR array was preformed for the detection of specific targets involved in human DNA repair pathways.

Directly after thawing, AML patient samples were sorted by FACS into CD34+ and CD34- populations, with the exclusion of any lymphocytic cells expressing CD3 or CD19, before RNA extraction. Both CD34+ and CD34- populations for each sample were run on the same PCR plate. The samples analysed were unchallenged by Ara-C as the aim was to detect any differences in the level of expression of genes in the AMLs natural state.

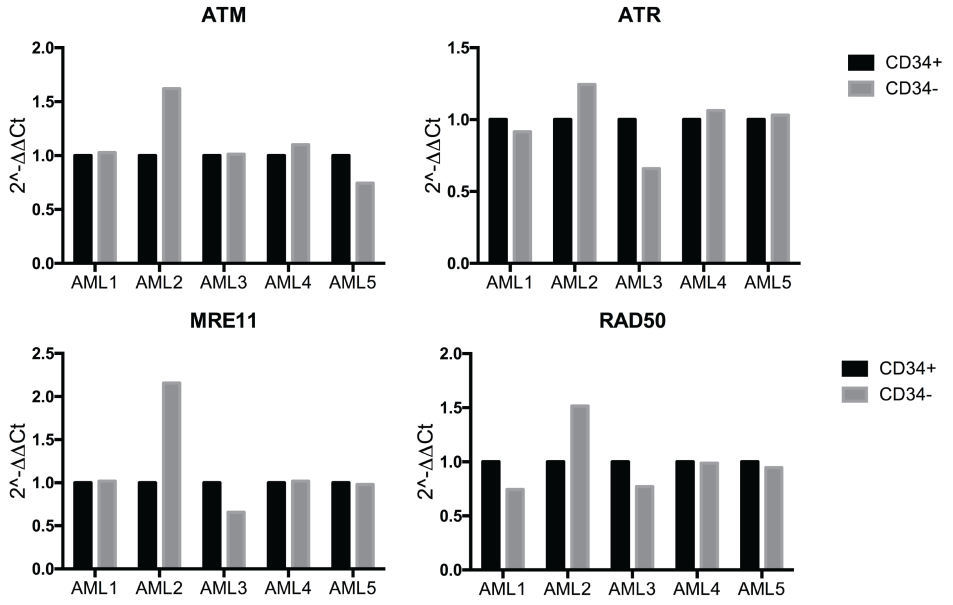

Figure 5.10 Gene expression of DNA damage response components in primary AML samples.

Primary AML samples were sorted into CD34+ and CD34- populations. Gene expression was quantified by normalising to housekeeping controls. Data shown is relative to the CD34+ population in each individual sample. Data represents one experiment with the mean of duplicated samples.

Focusing on genes that are involved in the initial recognition of DNA damage, it was clear that sample AML2 had differential expression of *ATM*, *MRE11* and

RAD50 between CD34+ and CD34- populations (Figure 5.10). *MRE11* and *RAD50* code for subunits of the MRN complex, which recognises DSBs and recruits factors, such as ATM, to begin co-ordinating a DNA damage response (Uziel et al., 2003).

If a population were to have less of any of these genes they may not be able to properly recognise DNA damage. The rest of the patient samples did not have as marked differences in gene expressions, however sample AML3 appeared to have the opposite result of sample AML2, with relative expression of *MRE11* and *RAD50* apparently now less in the CD34- compartment as compared to CD34+ (Figure 5.10).

Analysis of genes involved in NHEJ repair again highlighted sample AML2 as having differential expression between the populations of the genes *LIG3* and *LIG4* (Figure 5.11). These genes encode DNA Ligase III and DNA Ligase IV respectively, and work to join the DNA back together at the final stage of NHEJ (Lieber, 2010a).

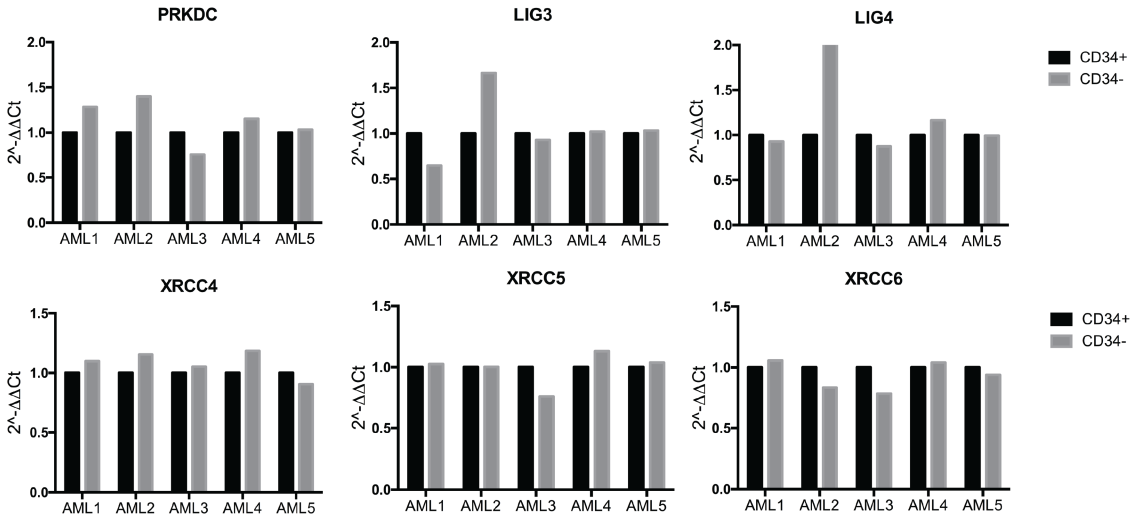

Figure 5.11 Gene expression of NHEJ genes in primary AML samples.

Primary AML samples were sorted into CD34+ and CD34- populations. Gene expression was quantified by normalising to housekeeping controls. Data shown is relative to the CD34+ population in each individual sample. Data represents one experiment with the mean of duplicated samples.

The majority of the samples again have similar expression levels between their CD34+ and CD34- compartments in most of the targets analysed. Interestingly however, sample AML3 had reduced *XRCC5* and *XRCC6* expression in their

CD34- cells compared to CD34+. These genes encode the two subunits for the heterodimer Ku70/Ku80 which hold the two ends of the DNA break together during NHEJ (Lieber, 2010a). This could suggest that the CD34- population of sample AML3 has a less effective NHEJ.

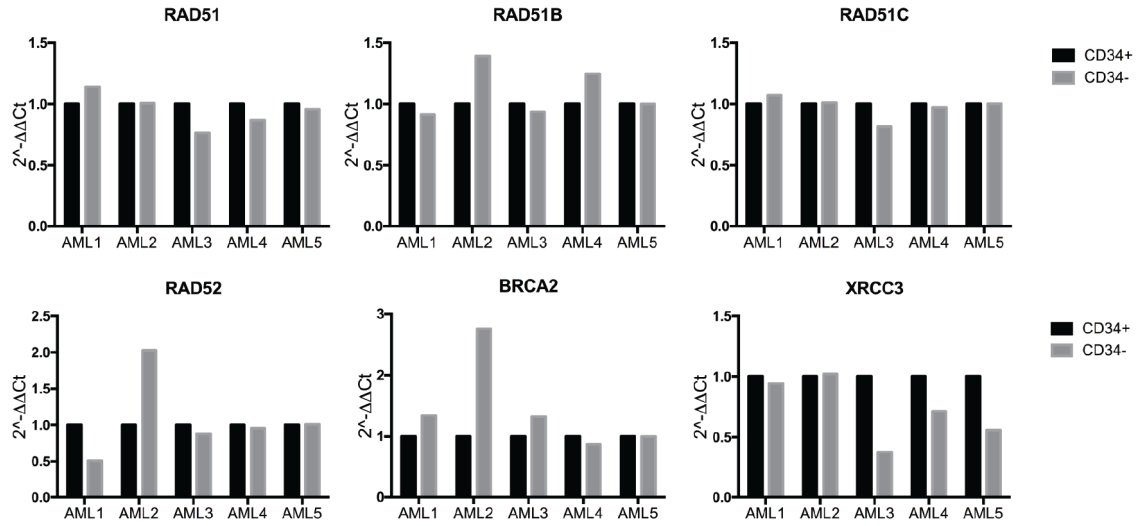

Figure 5.12 Gene expression of HR genes in primary AML samples.

Primary AML samples were sorted into CD34+ and CD34- populations. Gene expression was quantified by normalising to housekeeping controls. Data shown is relative to the CD34+ population in each individual sample. Data represents one experiment with the mean of duplicated samples.

Finally several genes involved in HR repair were analysed, again with sample AML2 and AML3 showing some of the largest differences in expression between their CD34+ and CD34- populations. *RAD51B, RAD51C, RAD52, BRCA2* and *XRCC3* all function to ensure the proper recruitment of RAD51, which is the crucial catalytic component of HR (Li and Heyer, 2008). A difference in expression of any of these components could potentially cause perturbations of HR repair. Interestingly the CD34+ population sample AML1 had higher expression of *RAD52* and was the only population to show significant activation of HR in response to Ara-C. As well, CD34+ AML1 cells had lower expression of *BRCA2*. RAD52 has been shown to be regulate RAD51 in the absence of BRCA2, thus making it a potential target for synthetic lethality in the presence of BRCA2 deficiency (Feng et al., 2011). Overall it could be suggested that there is differences in the gene expression of DNA damage response and repair genes between the LIC containing CD34+ populations and the CD34- compartments.

5.3 Discussion

In this chapter the effect of Ara-C on human primary AML samples was determined using the *in vivo* model. The cohort of AML samples were selected based on their expression of the CD34 antigen and their ability to engraft into immunodeficient mice. As seen in the previous chapter than normal HSPCs and HPCs show differential responses to Ara-C both *in vivo* and *in vitro*, it was to be determined whether the CD34+ LIC containing populations and the CD34- bulk tumour compartment responded differently to Ara-C also.

Overall it was shown that CD34+ populations showed the greatest decrease in cell number and higher activation of apoptosis in response to Ara-C treatment as compared to CD34-, corresponding to what was seen in the HSPC population in Chapter 4. In samples AML1 and AML3 this was most apparent with an almost complete depletion of human leukaemic cells from the bone marrow, however a small CD34- population was still maintained. Sample AML4 showed the least reduction in cell numbers and by 7 days there was no significant induction of apoptosis in either CD34+ or CD34- populations, suggesting a quick recovery from Ara-C treatment. Samples AML2 and AML6 also show quiet rapid recovery of their cell numbers, whereas samples AML3 and AML5 continued to even further their cell loss in both populations. It is evident to see that Ara-C is indeed an effective drug, yet there appears to be subtle differences in sensitivities between samples.

Analysis of cell cycle showed that overall CD34- populations had a higher frequency of cells in G0 compared to CD34+, suggesting they had less exposure to Ara-C. As CD34- populations do not contain LICs, they correspond to a more differentiated population, which would conceivably have more cells in quiescence. Thus this would explain the differences in cell numbers post Ara-C treatment between the two populations. Interestingly samples AML2 and AML6, the two samples that showed recovery of cell numbers 7 days after Ara-C treatment, both displayed evidence of enrichment of cells at the G1/S phases, in CD34+ and CD34- population. Sample AML4 on the other hand showed no evidence of any changes in cell cycle. Whereas samples AML3 and AML5, who showed continual reduction in cell number up to 7 days, exhibited huge enrichment of cells within G0, with an

almost complete abolishment of cells in the cycling phases. It appears that differences in reduction of cell number between the two populations could be due to the fact that CD34- populations were generally more quiescent. Overall, CD34+ and CD34- populations reacted in a similar manner to Ara-C. However AML1 was the only sample seeming to go against this trend as the CD34+ compartment showed the beginnings of an S-phase block and CD34- cells showed a reduction in the cycling phases. Indeed there are evidently differential responses to Ara-C between the AML samples when regarding cell cycle status.

This trend of samples AML2 and AML6 reacting in a similar manner was continued when they both showed significant increases in DNA damage in the CD34+ population in response to Ara-C. AML1 was the only sample that showed the CD34- compartment inducing any DNA damage in response to Ara-C. These mild inductions of DNA damage were similar to what was seen *in vivo* for the normal haematopoietic cells. When DNA repair was analysed it was evident that there was a basal level of NHEJ but the only sample that showed significant activation of either NHEJ or HR repair mechanisms in response to Ara-C was sample AML1, especially within the CD34+ compartment. Sample AML4, which appeared to be the most refractory to Ara-C treatment, showed a small frequency of cells with activation of NHEJ, but no HR.

Overall these heterogeneous responses to Ara-C treatment could be due to their differences in karyotype. Sample AML1 was the only complex karyotype sample with a poor prognosis, yet it was seemingly highly sensitive to Ara-C treatment and was one of the only samples to initiate DNA repair mechanisms. Sample AML4 has the MLL-AF9 fusion onco-protein, which is also associated with an adverse prognosis (Krivtsov and Armstrong, 2007). The expression of the fusion partner MLL1 is lost during the translocation and therefore its activity in DNA methylation is abrogated causing changes in chromatin structure and gene expression profiles. Horton et al. showed that MLL-AF9 enriched for gene signatures in chemotherapeutic resistance, which perhaps correlates with sample AML4 appearing to be the sample most refractory to Ara-C treatment (Horton et al., 2013). Samples AML2 and AML3 had normal karyotype associated with an intermediate risk, however sample AML3 held a FLT3-ITD mutation which has been shown to

have a drug-resistance phenotype due to up-regulation of expression of *RAD51* causing enhanced HR repair activity (Seedhouse et al., 2006). Indeed in sample AML3 it was shown that the CD34+ population had a higher expression of *RAD51* from analysis by the PCR arrays. However sample AML3 showed only slight activation of HR repair in response to Ara-C and was extremely sensitive to treatment, with cell numbers and engraftment almost completely diminished, seemingly contrary to its expected drug resistant phenotype.

Overall the cohort of AML samples showed heterogeneous responses to Ara-C treatment. There were not many apparent differences between the CD34+ and CD34- populations apart from an increased amount of quiescent cells, and sample AML1 showing a substantial activation of HR. It was again apparent, just like the AML cell lines and normal haematopoietic cells, that NHEJ was preferred over HR in response to Ara-C induced DNA damage and that there was a basal level of activation of NHEJ. Although it cannot be said for certain whether DNA repair mechanisms have an effect on the outcome to Ara-C in AML samples, but it can be seen that there are differential responses to the DNA damage incurred by Ara-C treatment and more investigation into the pathways involved could be key to dissecting these responses.

Chapter 6. Discussion

This thesis set forth to determine whether differences in DNA repair mechanisms in AML patients, compared to normal haematopoietic cells, could be responsible for any adverse responses to the chemotherapeutic agent Ara-C. The aim was to observe any potential differences in response to Ara-C of CD34+ LIC containing compartments and the more differentiated CD34- compartments of AML primary samples, as compared to normal haematopoietic stem and progenitor cells. Using *in vitro* and *in vivo* approaches, responses to Ara-C, focusing on DNA damage and repair, were assessed in AML cell lines, UCB cells and primary AML patient samples.

It is well established that normal haematopoietic stem and progenitor cell populations react inversely to DNA damage, and indeed normal HSPCs appeared to show an increased sensitivity compared to HPC when exposed to Ara-C. This falls in line with what Milyavsky et al., showed in that in response to irradiation the HSC (which in this study they established as CD34+CD38-CD45RA-CD90+) displayed greater apoptosis than compared to progenitor cells (Milyavsky et al., 2010, Yamashita et al., 2015). This mechanism is believed to help maintain the integrity of the stem cell pool and protect from DNA damage causing mutations, which could cause malignant transformations.

As outlined in Chapter 4 the studies in normal haematopoiesis were performed using the UCB model. While this provides a rich source of HSCs, cells from UCB represent a young haematopoietic system, which has been shown to differ in the DDR compared to the aged haematopoietic system (Rossi et al., 2007, Beerman et al., 2014). However, while cells from adult bone marrow (BM) samples would be a more age-appropriate model for this study, due to the expense and scarcity of available adult BM, UCB is often used in studies of human HSC biology.

For the studies in leukaemia, AML cell lines provided a good starting point as they displayed varying sensitivities to Ara-C treatment, while all receiving similar amounts of DNA damage *in vitro*. However, AML cell lines don't present with much phenotypic heterogeneity, unlike primary AML samples, so different populations

within the cell lines could not be analysed against the CD34+ CB HPC and HSPC populations.

The analyses on primary AML samples were performed *in vivo* using CD34 expressing samples, with diverse karyotypes, comparing their CD34+ LIC containing and CD34- tumour populations. While it initially seemed that the CD34+ populations were more sensitive to Ara-C treatment, based on cell counts and activation of apoptosis, the influence of cell cycle status appeared to be a contributing factor to their response.

When examining normal HSPCs and HPCs for their cell cycle statuses post Ara-C treatment, differences between the populations were revealed. By the later time points of exposure to Ara-C *in vitro,* most of the HPCs were stalled at the G1/S phase, whereas HSPCs showed a G0 enrichment and reduction in the G2/M cycling phases. For the HPCs, the same results were reflected *in vivo,* however HSPCs appeared to show no difference in cell cycle status. The AML patient samples reacted in a similar manner to Ara-C treatment displaying either a G1/S phase accumulation, G0 enrichment or no alteration. While there were no major observable differences between CD34+ and CD34- AML populations, within each sample in response to Ara-C, it appeared that AML patient samples as a whole either reacted like normal HPCs or HSPCs. Assessment of BrdU incorporation would add another layer of knowledge onto the cell cycle differences. If added to the system at the same time as Ara-C, any cells that have BrdU in their DNA and are in G0 at the time of analysis may have been able to preform a full cycle of cell division without consequence from Ara-C.

LICs from CD34+ AMLs have been shown to arise from early progenitor populations such as LMPP (Goardon et al., 2011b) and also from CD38+ progenitors (Taussig et al., 2008, Sarry et al., 2011, Eppert et al., 2011) which may include mature GMPs. Therefore, this suggests that perhaps the AML patient samples, based on the phenotypic origin of their LIC, may be being influenced in their responses to chemotherapy as it can be seen that AML samples either act in a HPC like manner, or like HSPCs.

Overall in response to Ara-C AML cell lines, normal CB cells and AML patient samples all displayed preferential activation of NHEJ repair over HR repair. Many studies observing DNA damage responses in the HSC have utilised ionising radiation as the main source of DNA damage. These studies show that due to the quiescent nature of the stem cells NHEJ is favoured, however when cells are pushed to cycle they induce HR repair (Mohrin et al., 2010, Beerman et al., 2014). While NHEJ repair can take place at any point in the cell cycle, HR repair is specific to the cycling S/G2/M phases (Sancar et al., 2004). The mode of action of Ara-C requires the cell to be within the S-phase of the cell cycle and for DNA to be replicating to enforce its effect, therefore it could have been speculated that HR should have occurred and not NHEJ repair.

Whilst *in vitro* there was clear evidence of a proportion of cells activating NHEJ repair after Ara-C treatment, disappointingly *in vivo* this was less evident. As was suggested in the discussion of Chapter 4, this may be due to the differences in dosage of Ara-C and time points analysed between the models. *In vivo*, instead of analysing cells after the full dose regime had been administered, examination following a couple of doses of Ara-C could have feasibly captured any on-going DNA damage responses as Ara-C was beginning to take effect. Although the seven-day dose regime was perhaps too harsh for the kinetics of DNA damage analysis, it helped gain an insight into the landscape post Ara-C of any remaining cells.

What is chronically understudied is the effect Ara-C has on normal haematopoietic cells within the bone marrow, particularly primitive CD34+ populations. Indeed, Ara-C would not typically be administered to a healthy patient with a healthy haematopoiesis. However, in cases of haematological disease, such as AML or lymphoma, there is still a residual normal haematopoietic system that comes into contact with the drug. Post induction therapy, with a treatment regime utilising Ara-C, most patients are able to achieve a remission with the return of a functional haematopoietic system. Thus it could be speculated that normal haematopoietic cells could be more resilient and evasive to chemotherapy than their malignant counterparts. Indeed, this could be due to the highly quiescent phenotype of the LT-HSC (Foudi et al., 2009, Bradford et al., 1997, Cheshier et al., 1999), or the

high expression of drug efflux transporters, known to be active on primitive stem populations (McKenzie et al., 2007, Chaudhary and Roninson, 1991, Scharenberg et al., 2002). Simply meaning, they potentially have a greater ability to evade the action of Ara-C compared to more differentiated cells and thus can remain latent in the bone marrow during treatment. As well, these same characteristics have been postulated as mechanisms of chemoresistance for the LIC, where the primitive malignant cells can remain quiescent and protected before leading to an eventual relapse. As with any cancer treatment, analysis of their effect on the normal cells is paramount to helping provide more targeted therapies. Therefore, this study helps shed some light onto how human CD34+ may behave when coming into contact with chemotherapeutic agents. Indeed, as Ara-C is routinely not solely used for treatment regimes, assessing the effect of other chemotherapeutic agents used in combination with Ara-C, such as daunorubicin and fludarabine would also be beneficial.

To further elucidate the mechanisms surrounding the variable cell cycle control post Ara-C treatment between the normal stem and progenitor populations and the AML patient samples, it would be advantageous to investigate the molecular decisions surrounding the response to Ara-C. At the onset of DNA damage there is a concerted activation of multiple pathways, all defined under the umbrella of the DNA damage response. Cell cycle checkpoints are an important part of this process and are intimately linked with DNA repair, therefore analysis of the key molecular entities involved in G1 and S phase checkpoints would be beneficial to understanding why Ara-C causes G0 enrichment in some AML samples and the HSPC populations, yet a apparent G1/S block in other AML samples and HPCs, with abolishment of G2/M phases. Examination of the p53/p21 axis could potentially be key to unravelling this and how this could lead to downstream decisions of initiation of DNA repair mechanisms in response to DNA damage. Indeed these molecular queues would shed light on the decisions that carry the cell into the preference for NHEJ repair.

Study of DDR mechanisms within normal human HSCs and LICs poses quite the challenge, mainly due to the rarity of the populations and therefore shortage of material to work with. Indeed, after Ara-C treatment this problem is even more

exacerbated. DDR mechanisms are primarily controlled by protein-protein interactions and phosphorylation events, which often require abundant amounts of cells to analyse. Yet the majority of DNA damage studies in human haematopoiesis so far have had to rely on genomic and transcriptome approaches due to greater reliability and effectiveness with low cell numbers. The targeted PCR array on CD34+ and CD34- populations from the panel of AML samples performed in this study was one such approach. There was evidence of differential expressions of DNA repair genes between LIC and tumour populations of some of the samples, however as gene expression signatures can be karyotype dependent, a larger cohort of samples would be needed for validation.

While this study focuses on the DNA repair pathways as a possible reason for differential responses to Ara-C treatment, resistance to Ara-C is most likely a mixture of different contributing factors. Although these works provide evidence of activation of DNA repair pathways in response to Ara-C it was hard to conclude from this data whether it was a true contributor in the response to Ara-C. After all, DNA repair is by no means the full story when assessing the responses to the cytotoxic drug. In early studies of chemoresistance to Ara-C much of the focus was on how the drug was metabolised and transported in and out of the cell. To first transform Ara-C into its active and functional form Ara-CTP, a number of phosphorylation steps are needed. The down regulation in the expression of one of the key enzymes involved in this process, deoxycytidine kinase (DCK), or presence of mutations effecting its activity, have been correlated to a poorer response to Ara-C in AML patients and *in vitro* studies (Bhalla et al., 1984, Song et al., 2009, Veuger et al., 2000). Or conversely, up regulation of cytidine deaminase (CDA), which transforms Ara-C into the inactive Ara-U (uracil arabinoside), again correlates with an increased resistance to Ara-C treatment (Schroder et al., 1996). Both these mechanisms would contribute to reducing the amount of active Ara-C available to incorporate into the DNA thus causing DNA damage.

Another means that by which levels of Ara-C within the cell could be affected to contribute to chemoresistance, is by alterations in the influx of the drug by the human equalibrative nucleotide transporter hENT1 (Hubeek et al., 2005, Wiley et al., 1982), or increased expression of efflux transporters from the ABC family such

as MRP8 (encoded by ABCC11), which is has particular affinity for Ara-C transport (Efferth et al., 2001, Guo et al., 2009). By their very nature, stem cells have a higher expression of efflux transporters to protect from damage by toxic agents (Scharenberg et al., 2002). Taking this into account it is believed that LIC populations may also hold this characteristic, giving them enhanced chemoresistance than compared to bulk tumour populations (Wulf et al., 2001, de Grouw et al., 2006). However, frustratingly inhibitors of drug transporters have preformed poorly with limited success in the clinic for treatment of AML (Peck et al., 2001, Greenberg et al., 2004, Fisher and Sikic, 1995).

Despite the many associations afforded over the years, which provide evidence for different mechanisms contributing to chemoresistance, this study has shown that Ara-C is still able to effectively incorporate in DNA and inflict damage, suggesting there is still a potential mechanism downstream of Ara-C metabolism and cellular transport for chemoresistance.

Stepping back and assessing chemoresistance in AML from a broader perspective it can be seen that perhaps one of the biggest challenges facing effective treatment of AML is the inherent clonal heterogeneity of the disease and the clonal evolution observed during treatment. A key study, using whole genome sequencing to track mutations in AML patient samples at diagnosis and relapse, showed that during treatment, specific clones may be selected which can arise again after remission to cause relapse (Ding et al., 2012). Subsequent work showed that the LIC frequency was significantly increased at relapse when compared to matched diagnostic samples, as well as showing an overall diverse physiological change to the original disease presented (Ho et al., 2016). The subsequent relapsed clone always harbours an increased mutational burden, compared to its founding clone at diagnosis, and has acquired chemoresistance to the treatments previously used. These new mutations observed at relapse are most likely created from the harsh cytotoxic treatments used causing DNA damage, and may be providing the transformed clones a survival advantage.

To corroborate the clonal dynamics observed in AML patient samples during treatment with the work done here, it would be beneficial to compare the

characteristics of the clones, which are present at diagnosis with the clones that persist after Ara-C treatment into relapse. Specifically analysing if there are any differences in activity and kinetics of the DNA damage and repair pathways. Indeed in this study it is seen that leukaemic cells prefer NHEJ repair in response to Ara-C treatment. Therefore one possible outcome could be that a particular subset of clones has a higher capacity for DNA repair in response to cytotoxic treatments and with the preference for the inaccurate NHEJ repair, this could help generate the additional mutations observed at relapse.

How DNA damage and repair mechanisms play a part in adverse responses to Ara-C treatment in AML requires further exploration as addressed in this study. As well, understanding how normal haematopoietic cells may be affected by the chemotherapeutic agent are important in the bigger picture of Ara-C response. Ultimately, a collaborative analysis of the molecular mechanisms governing LIC and HSC DNA repair, quiescence and drug metabolism may be key to providing better understanding about their role in disease progression and chemoresistance.

Chapter 7. Appendix

7.1 Buffers

Annexin Binding Buffer

Supplier: BD Pharmingen

10 mM HEPES

140 mM NaCl

2.5 mM$CaCl_2$

Electrophoresis Buffer

300 mM NaOH

1 mM EDTA

Make to pH 13

Immunofluorescence Blocking Solution

10% Normal goat serum

2% BSA

0.1% Triton-X100

10 mM Sodium Azide,

PBS

Lysing Solution

2.5 M NaCl

100 mM EDTA

10 mM Tris

10% DMSO

0.1% Triton-X,

Make to pH 10

Neutralisation Buffer

0.4 M Tris

pH 7.5 to with conc. HCl

PBS (Phosphate buffered saline)

100 mM sodium phosphate

150 mM NaCl

7.2 Antibodies

Antibody	Company	Clone/Reference	Application
Phospho-histone H2A.X (Ser139)	Cell Signalling	20E3	FACS
Phospho-histone H2A.X (Ser139)	Millipore	JBW301	IF
Rabbit mAb IgG XP™ Isotype Control	Cell Signalling	DAE1	FACS
Alexa Flour® 594 goat anti-mouse IgG	Molecular Probes	A11005	IF
Alexa Flour® 488 goat anti-rabbit IgG	Molecular Probes	A11008	IF
AnnexinV	BD Pharmingen	BMS306	FACS
53BP1	Santa Cruz	H-300	IF
RAD51	Santa Cruz	H-92	IF
Ki67	BD Pharmingen	B-56	FACS
IgG1, kappa Isotype Control	BD Pharmingen	MOPC-21	IF
hCD45	eBioscience	HI30	FACS
mCD45	eBioscience	30-F11	FACS
CD34	BD Pharmingen	8G12	FACS
CD38	eBioscience	HIT2	FACS
CD45RA	eBioscience	HI100	FACS
CD90	eBioscience	Ebio5310	FACS
Lineage Cocktail 1	BD Pharmingen	340546	FACS
CD19	BD Pharmingen	555415	FACS
CD33	BD Pharmingen	555450	FACS
CD3	BD Pharmingen	555339	FACS

Reference List

ABRAHAM, R. T. 2001. Cell cycle checkpoint signaling through the ATM and ATR kinases. *Genes Dev,* 15**,** 2177-96.

ADOLFSSON, J., BORGE, O. J., BRYDER, D., THEILGAARD-MONCH, K., ASTRAND-GRUNDSTROM, I., SITNICKA, E., SASAKI, Y. & JACOBSEN, S. E. 2001. Upregulation of Flt3 expression within the bone marrow Lin(-)Sca1(+)c-kit(+) stem cell compartment is accompanied by loss of self-renewal capacity. *Immunity,* 15**,** 659-69.

ADOLFSSON, J., MANSSON, R., BUZA-VIDAS, N., HULTQUIST, A., LIUBA, K., JENSEN, C. T., BRYDER, D., YANG, L., BORGE, O. J., THOREN, L. A., ANDERSON, K., SITNICKA, E., SASAKI, Y., SIGVARDSSON, M. & JACOBSEN, S. E. 2005. Identification of Flt3+ lympho-myeloid stem cells lacking erythro-megakaryocytic potential a revised road map for adult blood lineage commitment. *Cell,* 121**,** 295-306.

AHNESORG, P., SMITH, P. & JACKSON, S. P. 2006. XLF interacts with the XRCC4-DNA ligase IV complex to promote DNA nonhomologous end-joining. *Cell,* 124**,** 301-13.

ALCALAY, M., MEANI, N., GELMETTI, V., FANTOZZI, A., FAGIOLI, M., ORLETH, A., RIGANELLI, D., SEBASTIANI, C., CAPPELLI, E., CASCIARI, C., SCIURPI, M. T., MARIANO, A. R., MINARDI, S. P., LUZI, L., MULLER, H., DI FIORE, P. P., FROSINA, G. & PELICCI, P. G. 2003. Acute myeloid leukemia fusion proteins deregulate genes involved in stem cell maintenance and DNA repair. *J Clin Invest,* 112**,** 1751-61.

ANJOS-AFONSO, F., CURRIE, E., PALMER, HECTOR G., FOSTER, KATIE E., TAUSSIG, DAVID C. & BONNET, D. 2013. CD34− Cells at the Apex of the Human Hematopoietic Stem Cell Hierarchy Have Distinctive Cellular and Molecular Signatures. *Cell Stem Cell,* 13**,** 161-174.

BAGRINTSEVA, K., GEISENHOF, S., KERN, R., EICHENLAUB, S., REINDL, C., ELLWART, J. W., HIDDEMANN, W. & SPIEKERMANN, K. 2005. FLT3-ITD-TKD dual mutants associated with AML confer resistance to FLT3 PTK inhibitors and cytotoxic agents by overexpression of Bcl-x(L). *Blood,* 105**,** 3679-85.

BARBOZA, J. A., LIU, G., JU, Z., EL-NAGGAR, A. K. & LOZANO, G. 2006. p21 delays tumor onset by preservation of chromosomal stability. *Proc Natl Acad Sci U S A,* 103**,** 19842-7.

BARNETT, M. J., SUTHERLAND, H. J., EAVES, A. C., HOGGE, D. E., HUMPHRIES, R. K., KLINGEMANN, H. G., LANSDORP, P. M., PHILLIPS, G. L., REECE, D. E., SHEPHERD, J. D. & ET AL. 1991. Human hematopoietic stem cells in long-term culture: quantitation and manipulation. *Bone Marrow Transplant,* 7 Suppl 1**,** 70.

BARTEK, J. & LUKAS, J. 2007. DNA damage checkpoints: from initiation to recovery or adaptation. *Current Opinion in Cell Biology,* 19**,** 238-245.

BAUM 1993. Expression of Thy-1 on human hematopoietic progenitor cells. *The Journal of Experimental Medicine,* 177**,** 1331-1342.

BECKER, A. J., MCCULLOCH, E. A. & TILL, J. E. 1963. Cytological Demonstration of the Clonal Nature of Spleen Colonies Derived from Transplanted Mouse Marrow Cells. *Nature,* 197**,** 452-454.

BEERMAN, I., SEITA, J., INLAY, M. A., WEISSMAN, I. L. & ROSSI, D. J. 2014. Quiescent hematopoietic stem cells accumulate DNA damage during aging that is repaired upon entry into cell cycle. *Cell stem cell,* 15**,** 37-50.

BENVENISTE, P., FRELIN, C., JANMOHAMED, S., BARBARA, M., HERRINGTON, R., HYAM, D. & ISCOVE, N. N. 2010. Intermediate-term hematopoietic stem cells with extended but time-limited reconstitution potential. *Cell Stem Cell,* 6**,** 48-58.

BHALLA, K., NAYAK, R. & GRANT, S. 1984. Isolation and characterization of a deoxycytidine kinase-deficient human promyelocytic leukemic cell line highly resistant to 1-beta-D- arabinofuranosylcytosine. *Cancer Res,* 44**,** 5029-37.

BHATIA, M., WANG, J. C., KAPP, U., BONNET, D. & DICK, J. E. 1997. Purification of primitive human hematopoietic cells capable of repopulating immune-deficient mice. *Proc Natl Acad Sci U S A,* 94**,** 5320-5.

BOICHUK, S., HU, L., MAKIELSKI, K., PANDOLFI, P. P. & GJOERUP, O. V. 2011. Functional connection between Rad51 and PML in homology-directed repair. *PLoS One,* 6**,** e25814.

BONNET, D. & DICK, J. E. 1997. Human acute myeloid leukemia is organized as a hierarchy that originates from a primitive hematopoietic cell. *Nature Medicine,* 3**,** 730-737.

BOUWMAN, P. & JONKERS, J. 2012. The effects of deregulated DNA damage signalling on cancer chemotherapy response and resistance. *Nat Rev Cancer,* 12**,** 587-598.

BRADFORD, G. B., WILLIAMS, B., ROSSI, R. & BERTONCELLO, I. 1997. Quiescence, cycling, and turnover in the primitive hematopoietic stem cell compartment. *Exp Hematol,* 25**,** 445-53.

BYRD, J. C., MROZEK, K., DODGE, R. K., CARROLL, A. J., EDWARDS, C. G., ARTHUR, D. C., PETTENATI, M. J., PATIL, S. R., RAO, K. W., WATSON, M. S., KODURU, P. R., MOORE, J. O., STONE, R. M., MAYER, R. J., FELDMAN, E. J., DAVEY, F. R., SCHIFFER, C. A., LARSON, R. A. & BLOOMFIELD, C. D. 2002. Pretreatment cytogenetic abnormalities are predictive of induction success, cumulative incidence of relapse, and overall survival in adult patients with de novo acute myeloid leukemia: results from Cancer and Leukemia Group B (CALGB 8461). *Blood,* 100**,** 4325-36.

CABEZAS-WALLSCHEID, N., KLIMMECK, D., HANSSON, J., LIPKA, D. B., REYES, A., WANG, Q., WEICHENHAN, D., LIER, A., VON PALESKE, L., RENDERS, S., WUNSCHE, P., ZEISBERGER, P., BROCKS, D., GU, L., HERRMANN, C., HAAS, S., ESSERS, M. A., BRORS, B., EILS, R., HUBER, W., MILSOM, M. D., PLASS, C., KRIJGSVELD, J. & TRUMPP, A. 2014. Identification of regulatory networks in HSCs and their immediate progeny via integrated proteome, transcriptome, and DNA methylome analysis. *Cell Stem Cell,* 15**,** 507-22.

CAIRNS, R. A. & MAK, T. W. 2013. Oncogenic isocitrate dehydrogenase mutations: mechanisms, models, and clinical opportunities. *Cancer Discov,* 3**,** 730-41.

CANCERGENOMEATLASRESEARCH 2013. Genomic and Epigenomic Landscapes of Adult De Novo Acute Myeloid Leukemia. *New England Journal of Medicine,* 368**,** 2059-2074.

CASORELLI, I., TENEDINI, E., TAGLIAFICO, E., BLASI, M. F., GIULIANI, A., CRESCENZI, M., PELOSI, E., TESTA, U., PESCHLE, C., MELE, L., DIVERIO, D., BRECCIA, M., LO-COCO, F., FERRARI, S. & BIGNAMI, M. 2006. Identification of a molecular signature for leukemic promyelocytes and their normal counterparts: Focus on DNA repair genes. *Leukemia,* 20**,** 1978-88.

CAVELIER, C., DIDIER, C., PRADE, N., MANSAT-DE MAS, V., MANENTI, S., RECHER, C., DEMUR, C. & DUCOMMUN, B. 2009. Constitutive activation of the DNA damage signaling pathway in acute myeloid leukemia with complex karyotype: potential importance for checkpoint targeting therapy. *Cancer Res,* 69**,** 8652-61.

CHAUDHARY, P. M. & RONINSON, I. B. 1991. Expression and activity of P-glycoprotein, a multidrug efflux pump, in human hematopoietic stem cells. *Cell,* 66**,** 85-94.

CHEN, Q., KHOURY, M. & CHEN, J. 2009. Expression of human cytokines dramatically improves reconstitution of specific human-blood lineage cells in humanized mice. *Proc Natl Acad Sci U S A,* 106**,** 21783-8.

CHENG, K., SPORTOLETTI, P., ITO, K., CLOHESSY, J. G., TERUYA-FELDSTEIN, J., KUTOK, J. L. & PANDOLFI, P. P. 2010. The cytoplasmic NPM mutant induces myeloproliferation in a transgenic mouse model. *Blood,* 115**,** 3341-5.

CHESHIER, S. H., MORRISON, S. J., LIAO, X. & WEISSMAN, I. L. 1999. In vivo proliferation and cell cycle kinetics of long-term self-renewing hematopoietic stem cells. *Proc Natl Acad Sci U S A,* 96**,** 3120-5.

CHESON, B. D., BENNETT, J. M., KOPECKY, K. J., BUCHNER, T., WILLMAN, C. L., ESTEY, E. H., SCHIFFER, C. A., DOEHNER, H., TALLMAN, M. S., LISTER, T. A., LO-COCO, F., WILLEMZE, R., BIONDI, A., HIDDEMANN, W., LARSON, R. A., LOWENBERG, B., SANZ, M. A., HEAD, D. R., OHNO, R. & BLOOMFIELD, C. D. 2003. Revised recommendations of the International Working Group for Diagnosis, Standardization of Response Criteria, Treatment Outcomes, and Reporting Standards for Therapeutic Trials in Acute Myeloid Leukemia. *J Clin Oncol,* 21**,** 4642-9.

CHEUNG, N. & SO, C. W. 2011. Transcriptional and epigenetic networks in haematological malignancy. *FEBS Lett,* 585**,** 2100-11.

CHOU, W. C., CHOU, S. C., LIU, C. Y., CHEN, C. Y., HOU, H. A., KUO, Y. Y., LEE, M. C., KO, B. S., TANG, J. L., YAO, M., TSAY, W., WU, S. J., HUANG, S. Y., HSU, S. C., CHEN, Y. C., CHANG, Y. C., KUO, Y. Y., KUO, K. T., LEE, F. Y., LIU, M. C., LIU, C. W., TSENG, M. H., HUANG, C. F. & TIEN, H. F. 2011. TET2 mutation is an unfavorable prognostic factor in acute myeloid leukemia patients with intermediate-risk cytogenetics. *Blood,* 118**,** 3803-10.

CIMPRICH, K. A. & CORTEZ, D. 2008. ATR: an essential regulator of genome integrity. *Nat Rev Mol Cell Biol,* 9**,** 616-27.

CIVIN, C. I., STRAUSS, L. C., BROVALL, C., FACKLER, M. J., SCHWARTZ, J. F. & SHAPER, J. H. 1984. Antigenic analysis of hematopoiesis. III. A hematopoietic progenitor cell surface antigen defined by a monoclonal antibody raised against KG-1a cells. *Journal of Immunology,* 133**,** 157-165.

COOMBS, C. C., TALLMAN, M. S. & LEVINE, R. L. 2016. Molecular therapy for acute myeloid leukaemia. *Nat Rev Clin Oncol,* 13**,** 305-318.

COSTA, R. M., CHIGANCAS, V., GALHARDO RDA, S., CARVALHO, H. & MENCK, C. F. 2003. The eukaryotic nucleotide excision repair pathway. *Biochimie,* 85**,** 1083-99.

D'ANDREA, A. D. & GROMPE, M. 2003. The Fanconi anaemia/BRCA pathway. *Nat Rev Cancer,* 3**,** 23-34.

DANET, G. H., LUONGO, J. L., BUTLER, G., LU, M. M., TENNER, A. J., SIMON, M. C. & BONNET, D. A. 2002. C1qRp defines a new human stem cell population with hematopoietic and hepatic potential. *Proceedings of the National Academy of Sciences,* 99**,** 10441-10445.

DAVIS, J. N., MCGHEE, L. & MEYERS, S. 2003. The ETO (MTG8) gene family. *Gene,* 303**,** 1-10.

DE GROUW, E. P. L. M., RAAIJMAKERS, M. H. G. P., BOEZEMAN, J. B., VAN DER REIJDEN, B. A., VAN DE LOCHT, L. T. F., DE WITTE, T. J. M., JANSEN, J. H. & RAYMAKERS, R. A. P. 2006. Preferential expression of a high number of ATP binding cassette transporters in both normal and leukemic CD34+CD38- cells. *Leukemia,* 20**,** 750-754.

DESHPANDE, A. J., CHEN, L., FAZIO, M., SINHA, A. U., BERNT, K. M., BANKA, D., DIAS, S., CHANG, J., OLHAVA, E. J., DAIGLE, S. R., RICHON, V. M., POLLOCK, R. M. & ARMSTRONG, S. A. 2013. Leukemic transformation by the MLL-AF6 fusion oncogene requires the H3K79 methyltransferase Dot1l. *Blood,* 121**,** 2533-41.

DING, L., LEY, T. J., LARSON, D. E., MILLER, C. A., KOBOLDT, D. C., WELCH, J. S., RITCHEY, J. K., YOUNG, M. A., LAMPRECHT, T., MCLELLAN, M. D., MCMICHAEL, J. F., WALLIS, J. W., LU, C., SHEN, D., HARRIS, C. C., DOOLING, D. J., FULTON, R. S., FULTON, L. L., CHEN, K., SCHMIDT, H., KALICKI-VEIZER, J., MAGRINI, V. J., COOK, L., MCGRATH, S. D., VICKERY, T. L., WENDL, M. C., HEATH, S., WATSON, M. A., LINK, D. C., TOMASSON, M. H., SHANNON, W. D., PAYTON, J. E., KULKARNI, S., WESTERVELT, P., WALTER, M. J., GRAUBERT, T. A., MARDIS, E. R., WILSON, R. K. & DIPERSIO, J. F. 2012. Clonal evolution in relapsed acute myeloid leukaemia revealed by whole-genome sequencing. *Nature,* 481**,** 506-510.

DOHNER, H., ESTEY, E. H., AMADORI, S., APPELBAUM, F. R., BUCHNER, T., BURNETT, A. K., DOMBRET, H., FENAUX, P., GRIMWADE, D., LARSON, R. A., LO-COCO, F., NAOE, T., NIEDERWIESER, D., OSSENKOPPELE, G. J., SANZ, M. A., SIERRA, J., TALLMAN, M. S., LOWENBERG, B. & BLOOMFIELD, C. D. 2010. Diagnosis and management of acute myeloid leukemia in adults: recommendations

from an international expert panel, on behalf of the European LeukemiaNet. *Blood,* 115**,** 453-74.
DÖHNER, K., SCHLENK, R. F., HABDANK, M., SCHOLL, C., RÜCKER, F. G., CORBACIOGLU, A., BULLINGER, L., FRÖHLING, S. & DÖHNER, H. 2005. Mutant nucleophosmin (NPM1) predicts favorable prognosis in younger adults with acute myeloid leukemia and normal cytogenetics: interaction with other gene mutations. *Blood,* 106**,** 3740-3746.
DONZELLI, M. & DRAETTA, G. F. 2003. Regulating mammalian checkpoints through Cdc25 inactivation. *EMBO Reports,* 4**,** 671-677.
DOULATOV, S., NOTTA, F., EPPERT, K., NGUYEN, L. T., OHASHI, P. S. & DICK, J. E. 2010. Revised map of the human progenitor hierarchy shows the origin of macrophages and dendritic cells in early lymphoid development. *Nat Immunol,* 11**,** 585-593.
DOULATOV, S., NOTTA, F., LAURENTI, E. & DICK, JOHN E. 2012. Hematopoiesis: A Human Perspective. *Cell Stem Cell,* 10**,** 120-136.
DREYLING, M. H., MARTINEZ-CLIMENT, J. A., ZHENG, M., MAO, J., ROWLEY, J. D. & BOHLANDER, S. K. 1996. The t(10;11)(p13;q14) in the U937 cell line results in the fusion of the AF10 gene and CALM, encoding a new member of the AP-3 clathrin assembly protein family. *Proc Natl Acad Sci U S A,* 93**,** 4804-9.
EAVES, C. J. 2015. Hematopoietic stem cells: concepts, definitions, and the new reality. *Blood,* 125**,** 2605-2613.
EFFERTH, T., FUTSCHER, B. W. & OSIEKA, R. 2001. 5-Azacytidine Modulates the Response of Sensitive and Multidrug-Resistant K562 Leukemic Cells to Cytostatic Drugs. *Blood Cells, Molecules, and Diseases,* 27**,** 637-648.
EPPERT, K., TAKENAKA, K., LECHMAN, E. R., WALDRON, L., NILSSON, B., VAN GALEN, P., METZELER, K. H., POEPPL, A., LING, V., BEYENE, J., CANTY, A. J., DANSKA, J. S., BOHLANDER, S. K., BUSKE, C., MINDEN, M. D., GOLUB, T. R., JURISICA, I., EBERT, B. L. & DICK, J. E. 2011. Stem cell gene expression programs influence clinical outcome in human leukemia. *Nat Med,* 17**,** 1086-1093.
ERNST, T., CHASE, A. J., SCORE, J., HIDALGO-CURTIS, C. E., BRYANT, C., JONES, A. V., WAGHORN, K., ZOI, K., ROSS, F. M., REITER, A., HOCHHAUS, A., DREXLER, H. G., DUNCOMBE, A., CERVANTES, F., OSCIER, D., BOULTWOOD, J., GRAND, F. H. & CROSS, N. C. P. 2010. Inactivating mutations of the histone methyltransferase gene EZH2 in myeloid disorders. *Nat Genet,* 42**,** 722-726.
FAVERA, R. D., WONG-STAAL, F. & GALLO, R. C. 1982. onc gene amplification in promyelocytic leukaemia cell line HL-60 and primary leukaemic cells of the same patient. *Nature,* 299**,** 61-63.
FENG, Z., SCOTT, S. P., BUSSEN, W., SHARMA, G. G., GUO, G., PANDITA, T. K. & POWELL, S. N. 2011. Rad52 inactivation is synthetically lethal with BRCA2 deficiency. *Proceedings of the National Academy of Sciences of the United States of America,* 108**,** 686-691.
FISHER, G. A. & SIKIC, B. I. 1995. Clinical studies with modulators of multidrug resistance. *Hematol Oncol Clin North Am,* 9**,** 363-82.

FOUDI, A., HOCHEDLINGER, K., VAN BUREN, D., SCHINDLER, J. W., JAENISCH, R., CAREY, V. & HOCK, H. 2009. Analysis of histone 2B-GFP retention reveals slowly cycling hematopoietic stem cells. *Nat Biotechnol,* 27**,** 84-90.

FRITSCH, G., STIMPFL, M., KURZ, M., PRINTZ, D., BUCHINGER, P., FISCHMEISTER, G., HOECKER, P. & GADNER, H. 1996. The composition of CD34 subpopulations differs between bone marrow, blood and cord blood. *Bone Marrow Transplant,* 17**,** 169-78.

GALE, R. E., GREEN, C., ALLEN, C., MEAD, A. J., BURNETT, A. K., HILLS, R. K. & LINCH, D. C. 2008. The impact of FLT3 internal tandem duplication mutant level, number, size, and interaction with NPM1 mutations in a large cohort of young adult patients with acute myeloid leukemia. *Blood,* 111**,** 2776-84.

GATI, W. P., PATERSON, A. R., BELCH, A. R., CHLUMECKY, V., LARRATT, L. M., MANT, M. J. & TURNER, A. R. 1998. Es nucleoside transporter content of acute leukemia cells: role in cell sensitivity to cytarabine (araC). *Leuk Lymphoma,* 32**,** 45-54.

GATI, W. P., PATERSON, A. R., LARRATT, L. M., TURNER, A. R. & BELCH, A. R. 1997. Sensitivity of acute leukemia cells to cytarabine is a correlate of cellular es nucleoside transporter site content measured by flow cytometry with SAENTA-fluorescein. *Blood,* 90**,** 346-53.

GOARDON, N., MARCHI, E., ATZBERGER, A., QUEK, L., SCHUH, A., SONEJI, S., WOLL, P., MEAD, A., ALFORD, K. A., ROUT, R., CHAUDHURY, S., GILKES, A., KNAPPER, S., BELDJORD, K., BEGUM, S., ROSE, S., GEDDES, N., GRIFFITHS, M., STANDEN, G., STERNBERG, A., CAVENAGH, J., HUNTER, H., BOWEN, D., KILLICK, S., ROBINSON, L., PRICE, A., MACINTYRE, E., VIRGO, P., BURNETT, A., CRADDOCK, C., ENVER, T., JACOBSEN, S. E., PORCHER, C. & VYAS, P. 2011a. Coexistence of LMPP-like and GMP-like leukemia stem cells in acute myeloid leukemia. *Cancer Cell,* 19**,** 138-52.

GOARDON, N., MARCHI, E., ATZBERGER, A., QUEK, L., SCHUH, A., SONEJI, S., WOLL, P., MEAD, A., ALFORD, K. A., ROUT, R., CHAUDHURY, S., GILKES, A., KNAPPER, S., BELDJORD, K., BEGUM, S., ROSE, S., GEDDES, N., GRIFFITHS, M., STANDEN, G., STERNBERG, A., CAVENAGH, J., HUNTER, H., BOWEN, D., KILLICK, S., ROBINSON, L., PRICE, A., MACINTYRE, E., VIRGO, P., BURNETT, A., CRADDOCK, C., ENVER, T., JACOBSEN, S. E. W., PORCHER, C. & VYAS, P. 2011b. Coexistence of LMPP-like and GMP-like Leukemia Stem Cells in Acute Myeloid Leukemia. *Cancer Cell,* 19**,** 138-152.

GRAUBERT, T. & WALTER, M. J. 2011. Genetics of Myelodysplastic Syndromes: New Insights. *ASH Education Program Book,* 2011**,** 543-549.

GREENBERG, P. L., LEE, S. J., ADVANI, R., TALLMAN, M. S., SIKIC, B. I., LETENDRE, L., DUGAN, K., LUM, B., CHIN, D. L., DEWALD, G., PAIETTA, E., BENNETT, J. M. & ROWE, J. M. 2004. Mitoxantrone, etoposide, and cytarabine with or without valspodar in patients with relapsed or refractory acute myeloid leukemia and high-risk myelodysplastic syndrome: a phase III trial (E2995). *J Clin Oncol,* 22**,** 1078-86.

GRIMWADE, D., HILLS, R. K., MOORMAN, A. V., WALKER, H., CHATTERS, S., GOLDSTONE, A. H., WHEATLEY, K., HARRISON, C. J. & BURNETT, A. K. 2010. Refinement of cytogenetic classification in acute myeloid leukemia: determination of prognostic significance of rare recurring chromosomal abnormalities among 5876 younger adult patients treated in the United Kingdom Medical Research Council trials. *Blood,* 116**,** 354-365.

GUO, Y., KÖCK, K., RITTER, C. A., CHEN, Z.-S., GRUBE, M., JEDLITSCHKY, G., ILLMER, T., AYRES, M., BECK, J. F., SIEGMUND, W., EHNINGER, G., GANDHI, V., KROEMER, H. K., KRUH, G. D. & SCHAICH, M. 2009. Expression of ABCC-Type Nucleotide Exporters in Blasts of Adult Acute Myeloid Leukemia: Relation to Long-term Survival. *Clinical Cancer Research,* 15**,** 1762-1769.

HILLS, S. A. & DIFFLEY, J. F. 2014. DNA replication and oncogene-induced replicative stress. *Curr Biol,* 24**,** R435-44.

HITOMI, K., IWAI, S. & TAINER, J. A. 2007. The intricate structural chemistry of base excision repair machinery: implications for DNA damage recognition, removal, and repair. *DNA Repair (Amst),* 6**,** 410-28.

HO, T.-C., LAMERE, M., STEVENS, B. M., ASHTON, J. M., MYERS, J. R., O'DWYER, K. M., LIESVELD, J. L., MENDLER, J. H., GUZMAN, M., MORRISSETTE, J. D., ZHAO, J., WANG, E. S., WETZLER, M., JORDAN, C. T. & BECKER, M. W. 2016. Evolution of acute myelogenous leukemia stem cell properties after treatment and progression. *Blood,* 128**,** 1671-1678.

HORTON, S. J., JAQUES, J., WOOLTHUIS, C., VAN DIJK, J., MESURACA, M., HULS, G., MORRONE, G., VELLENGA, E. & SCHURINGA, J. J. 2013. MLL-AF9-mediated immortalization of human hematopoietic cells along different lineages changes during ontogeny. *Leukemia,* 27**,** 1116-1126.

HOWLADER N, N. A., KRAPCHO M, 2014. Table 13.16: Acute myeloid leukemia - 5-year relative and period survival by race, sex, diagnosis year and age. *SEER Cancer Statistics Review, 1975-2011*.

HUBEEK, I., STAM, R. W., PETERS, G. J., BROEKHUIZEN, R., MEIJERINK, J. P. P., WERING, E. R. V., GIBSON, B. E. S., CREUTZIG, U., ZWAAN, C. M., CLOOS, J., KUIK, D. J., PIETERS, R. & KASPERS, G. J. L. 2005. The human equilibrative nucleoside transporter 1 mediates in vitro cytarabine sensitivity in childhood acute myeloid leukaemia. *Br J Cancer,* 93**,** 1388-1394.

INOUE, S., LI, W. Y., TSENG, A., BEERMAN, I., ELIA, A. J., BENDALL, S. C., LEMONNIER, F., KRON, K. J., CESCON, D. W., HAO, Z., LIND, E. F., TAKAYAMA, N., PLANELLO, A. C., SHEN, S. Y., SHIH, A. H., LARSEN, D. M., LI, Q., SNOW, B. E., WAKEHAM, A., HAIGHT, J., GORRINI, C., BASSI, C., THU, K. L., MURAKAMI, K., ELFORD, A. R., UEDA, T., STRALEY, K., YEN, K. E., MELINO, G., CIMMINO, L., AIFANTIS, I., LEVINE, R. L., DE CARVALHO, D. D., LUPIEN, M., ROSSI, D. J., NOLAN, G. P., CAIRNS, R. A. & MAK, T. W. 2016. Mutant IDH1 Downregulates ATM and Alters DNA Repair and Sensitivity to DNA Damage Independent of TET2. *Cancer Cell,* 30**,** 337-48.

INSINGA, A., CICALESE, A., FARETTA, M., GALLO, B., ALBANO, L., RONZONI, S., FURIA, L., VIALE, A. & PELICCI, P. G. 2013. DNA damage in stem cells activates p21, inhibits p53, and induces symmetric self-renewing divisions. *Proc Natl Acad Sci U S A,* 110**,** 3931-6.

ISHII, M., MATSUOKA, Y., SASAKI, Y., NAKATSUKA, R., TAKAHASHI, M., NAKAMOTO, T., YASUDA, K., MATSUI, K., ASANO, H., UEMURA, Y., TSUJI, T., FUKUHARA, S. & SONODA, Y. 2011. Development of a high-resolution purification method for precise functional characterization of primitive human cord blood-derived CD34-negative SCID-repopulating cells. *Exp Hematol,* 39**,** 203-213.e1.

ISSAAD, C., CROISILLE, L., KATZ, A., VAINCHENKER, W. & COULOMBEL, L. 1993. A murine stromal cell line allows the proliferation of very primitive human CD34++/CD38- progenitor cells in long-term cultures and semisolid assays. *Blood,* 81**,** 2916-24.

ITO, M., HIRAMATSU, H., KOBAYASHI, K., SUZUE, K., KAWAHATA, M., HIOKI, K., UEYAMA, Y., KOYANAGI, Y., SUGAMURA, K., TSUJI, K., HEIKE, T. & NAKAHATA, T. 2002. NOD/SCID/gamma(c)(null) mouse: an excellent recipient mouse model for engraftment of human cells. *Blood,* 100**,** 3175-82.

JACOBSON, L., SIMMONS, E., MARKS, E., ROBSON, M., BETHARD, W. & GASTON, E. 1950. The role of the spleen in radiation injury and recovery. *The Journal of laboratory and clinical medicine,* 35**,** 746-770.

JAN, M., SNYDER, T. M., CORCES-ZIMMERMAN, M. R., VYAS, P., WEISSMAN, I. L., QUAKE, S. R. & MAJETI, R. 2012. Clonal evolution of preleukemic hematopoietic stem cells precedes human acute myeloid leukemia. *Sci Transl Med,* 4**,** 149ra118.

KANAI, M., HIRAYAMA, F., YAMAGUCHI, M., OHKAWARA, J., SATO, N., FUKAZAWA, K., YAMASHITA, K., KUWABARA, M., IKEDA, H. & IKEBUCHI, K. 2000. Stromal cell-dependent ex vivo expansion of human cord blood progenitors and augmentation of transplantable stem cell activity. *Bone Marrow Transplant,* 26**,** 837-44.

KELLY, L. M., LIU, Q., KUTOK, J. L., WILLIAMS, I. R., BOULTON, C. L. & GILLILAND, D. G. 2002. FLT3 internal tandem duplication mutations associated with human acute myeloid leukemias induce myeloproliferative disease in a murine bone marrow transplant model. *Blood,* 99**,** 310-318.

KIEL, M. J., YILMAZ, O. H., IWASHITA, T., YILMAZ, O. H., TERHORST, C. & MORRISON, S. J. 2005. SLAM family receptors distinguish hematopoietic stem and progenitor cells and reveal endothelial niches for stem cells. *Cell,* 121**,** 1109-21.

KOCABAS, F., ZHENG, J., THET, S., COPELAND, N. G., JENKINS, N. A., DEBERARDINIS, R. J., ZHANG, C. & SADEK, H. A. 2012. Meis1 regulates the metabolic phenotype and oxidant defense of hematopoietic stem cells. *Blood,* 120**,** 4963-72.

KOHN, L. A., HAO, Q.-L., SASIDHARAN, R., PAREKH, C., GE, S., ZHU, Y., MIKKOLA, H. K. A. & CROOKS, G. M. 2012. Lymphoid Priming in Human Bone Marrow Begins Prior to CD10 Expression with Up-Regulation of L-selectin. *Nature immunology,* 13**,** 963-971.

KONOPLEVA, M. 2002. Stromal cells prevent apoptosis of AML cells by up-regulation of anti-apoptotic proteins. *Leukemia,* 16**,** 1713-1724.
KRESO, A. & DICK, J. E. 2014. Evolution of the cancer stem cell model. *Cell Stem Cell,* 14**,** 275-91.
KRIVTSOV, A. V. & ARMSTRONG, S. A. 2007. MLL translocations, histone modifications and leukaemia stem-cell development. *Nat Rev Cancer,* 7**,** 823-33.
KUFE, D. W., MAJOR, P. P., EGAN, E. M. & BEARDSLEY, G. P. 1980. Correlation of cytotoxicity with incorporation of ara-C into DNA. *J Biol Chem,* 255**,** 8997-900.
LANE, D. P. 1992. p53, guardian of the genome. *Nature,* 358**,** 15-16.
LANSDORP, P. M., SUTHERLAND, H. J. & EAVES, C. J. 1990. Selective expression of CD45 isoforms on functional subpopulations of CD34+ hemopoietic cells from human bone marrow. *Journal of Experimental Medicine,* 172**,** 363-366.
LI, G. M. 2008. Mechanisms and functions of DNA mismatch repair. *Cell Res,* 18**,** 85-98.
LI, X. & HEYER, W. D. 2008. Homologous recombination in DNA repair and DNA damage tolerance. *Cell Res,* 18**,** 99-113.
LIEBER, M. R. 2010a. The Mechanism of Double-Strand DNA Break Repair by the Nonhomologous DNA End Joining Pathway. *Annual review of biochemistry,* 79**,** 181-211.
LIEBER, M. R. 2010b. The mechanism of double-strand DNA break repair by the nonhomologous DNA end-joining pathway. *Annu Rev Biochem,* 79**,** 181-211.
LINDVALL, C., FURGE, K., BJORKHOLM, M., GUO, X., HAAB, B., BLENNOW, E., NORDENSKJOLD, M. & TEH, B. T. 2004. Combined genetic and transcriptional profiling of acute myeloid leukemia with normal and complex karyotypes. *Haematologica,* 89**,** 1072-81.
MAJETI, R., PARK, C. Y. & WEISSMAN, I. L. 2007a. Identification of a Hierarchy of Multipotent Hematopoietic Progenitors in Human Cord Blood. *Cell Stem Cell,* 1**,** 635-645.
MAJETI, R., PARK, C. Y. & WEISSMAN, I. L. 2007b. Identification of a hierarchy of multipotent hematopoietic progenitors in human cord blood. *Cell Stem Cell,* 1**,** 635-45.
MANZ, M. G. 2007. Human-hemato-lymphoid-system mice: opportunities and challenges. *Immunity,* 26**,** 537-41.
MANZ, M. G., MIYAMOTO, T., AKASHI, K. & WEISSMAN, I. L. 2002. Prospective isolation of human clonogenic common myeloid progenitors. *Proc Natl Acad Sci U S A,* 99**,** 11872-7.
MARCUCCI, G., METZELER, K. H., SCHWIND, S., BECKER, H., MAHARRY, K., MROZEK, K., RADMACHER, M. D., KOHLSCHMIDT, J., NICOLET, D., WHITMAN, S. P., WU, Y. Z., POWELL, B. L., CARTER, T. H., KOLITZ, J. E., WETZLER, M., CARROLL, A. J., BAER, M. R., MOORE, J. O., CALIGIURI, M. A., LARSON, R. A. & BLOOMFIELD, C. D. 2012. Age-related prognostic impact of different types of DNMT3A mutations in adults with primary cytogenetically normal acute myeloid leukemia. *J Clin Oncol,* 30**,** 742-50.

MARTELLI, M. P., PETTIROSSI, V., THIEDE, C., BONIFACIO, E., MEZZASOMA, F., CECCHINI, D., PACINI, R., TABARRINI, A., CIURNELLI, R., GIONFRIDDO, I., MANES, N., ROSSI, R., GIUNCHI, L., OELSCHLAGEL, U., BRUNETTI, L., GEMEI, M., DELIA, M., SPECCHIA, G., LISO, A., DI IANNI, M., DI RAIMONDO, F., FALZETTI, F., DEL VECCHIO, L., MARTELLI, M. F. & FALINI, B. 2010. CD34+ cells from AML with mutated NPM1 harbor cytoplasmic mutated nucleophosmin and generate leukemia in immunocompromised mice. *Blood,* 116**,** 3907-22.

MATHEW, C. G. 2006. Fanconi anaemia genes and susceptibility to cancer. *Oncogene,* 25**,** 5875-5884.

MAXIMOW 1909. *Fol. Haematol.,* 8**,** 125-134.

MAYLE, A., YANG, L., RODRIGUEZ, B., ZHOU, T., CHANG, E., CURRY, C. V., CHALLEN, G. A., LI, W., WHEELER, D., REBEL, V. I. & GOODELL, M. A. 2015. Dnmt3a loss predisposes murine hematopoietic stem cells to malignant transformation. *Blood,* 125**,** 629-638.

MCCUNE, J. M., NAMIKAWA, R., KANESHIMA, H., SHULTZ, L. D., LIEBERMAN, M. & WEISSMAN, I. L. 1988. The SCID-hu mouse: murine model for the analysis of human hematolymphoid differentiation and function. *Science,* 241**,** 1632-9.

MCKENZIE, J. L., TAKENAKA, K., GAN, O. I., DOEDENS, M. & DICK, J. E. 2007. Low rhodamine 123 retention identifies long-term human hematopoietic stem cells within the Lin-CD34+CD38- population. *Blood,* 109**,** 543-5.

MEEK, D. W. 2009. Tumour suppression by p53: a role for the DNA damage response? *Nat Rev Cancer,* 9**,** 714-23.

METZELER, K. H., MAHARRY, K., RADMACHER, M. D., MROZEK, K., MARGESON, D., BECKER, H., CURFMAN, J., HOLLAND, K. B., SCHWIND, S., WHITMAN, S. P., WU, Y. Z., BLUM, W., POWELL, B. L., CARTER, T. H., WETZLER, M., MOORE, J. O., KOLITZ, J. E., BAER, M. R., CARROLL, A. J., LARSON, R. A., CALIGIURI, M. A., MARCUCCI, G. & BLOOMFIELD, C. D. 2011. TET2 mutations improve the new European LeukemiaNet risk classification of acute myeloid leukemia: a Cancer and Leukemia Group B study. *J Clin Oncol,* 29**,** 1373-81.

MILYAVSKY, M., GAN, O. I., TROTTIER, M., KOMOSA, M., TABACH, O., NOTTA, F., LECHMAN, E., HERMANS, K. G., EPPERT, K., KONOVALOVA, Z., ORNATSKY, O., DOMANY, E., MEYN, M. S. & DICK, J. E. 2010. A Distinctive DNA Damage Response in Human Hematopoietic Stem Cells Reveals an Apoptosis-Independent Role for p53 in Self-Renewal. *Cell Stem Cell,* 7**,** 186-197.

MOEHRLE, BETTINA M., NATTAMAI, K., BROWN, A., FLORIAN, MARIA C., RYAN, M., VOGEL, M., BLIEDERHAEUSER, C., SOLLER, K., PROWS, DANIEL R., ABDOLLAHI, A., SCHLEIMER, D., WALTER, D., MILSOM, MICHAEL D., STAMBROOK, P., PORTEUS, M. & GEIGER, H. 2015. Stem Cell-Specific Mechanisms Ensure Genomic Fidelity within HSCs and upon Aging of HSCs. *Cell Reports,* 13**,** 2412-2424.

MOHRIN, M., BOURKE, E., ALEXANDER, D., WARR, M. R., BARRY-HOLSON, K., LE BEAU, M. M., MORRISON, C. G. & PASSEGUÉ, E. 2010.

Hematopoietic Stem Cell Quiescence Promotes Error-Prone DNA Repair and Mutagenesis. *Cell Stem Cell,* 7**,** 174-185.
MOLINARI, M., MERCURIO, C., DOMINGUEZ, J., GOUBIN, F. & DRAETTA, G. F. 2000. Human Cdc25 A inactivation in response to S phase inhibition and its role in preventing premature mitosis. *EMBO Rep,* 1**,** 71-9.
MORRISON, S. J. & SCADDEN, D. T. 2014. The bone marrow niche for haematopoietic stem cells. *Nature,* 505**,** 327-334.
MORRISON, S. J. & WEISSMAN, I. L. 1994. The long-term repopulating subset of hematopoietic stem cells is deterministic and isolatable by phenotype. *Immunity,* 1**,** 661-73.
MULLER, P. A. J. & VOUSDEN, K. H. 2013. p53 mutations in cancer. *Nat Cell Biol,* 15**,** 2-8.
NICOLINI, F. E., CASHMAN, J. D., HOGGE, D. E., HUMPHRIES, R. K. & EAVES, C. J. 2004. NOD/SCID mice engineered to express human IL-3, GM-CSF and Steel factor constitutively mobilize engrafted human progenitors and compromise human stem cell regeneration. *Leukemia,* 18**,** 341-7.
NICULESCU, A. B., 3RD, CHEN, X., SMEETS, M., HENGST, L., PRIVES, C. & REED, S. I. 1998. Effects of p21(Cip1/Waf1) at both the G1/S and the G2/M cell cycle transitions: pRb is a critical determinant in blocking DNA replication and in preventing endoreduplication. *Mol Cell Biol,* 18**,** 629-43.
NIELSEN, J. S. & MCNAGNY, K. M. 2009. CD34 is a key regulator of hematopoietic stem cell trafficking to bone marrow and mast cell progenitor trafficking in the periphery. *Microcirculation,* 16**,** 487-96.
NOTTA, F., DOULATOV, S., LAURENTI, E., POEPPL, A., JURISICA, I. & DICK, J. E. 2011. Isolation of single human hematopoietic stem cells capable of long-term multilineage engraftment. *Science,* 333**,** 218-21.
NOTTA, F., ZANDI, S., TAKAYAMA, N., DOBSON, S., GAN, O. I., WILSON, G., KAUFMANN, K. B., MCLEOD, J., LAURENTI, E., DUNANT, C. F., MCPHERSON, J. D., STEIN, L. D., DROR, Y. & DICK, J. E. 2016. Distinct routes of lineage development reshape the human blood hierarchy across ontogeny. *Science,* 351**,** aab2116.
OHTSUBO, M., THEODORAS, A. M., SCHUMACHER, J., ROBERTS, J. M. & PAGANO, M. 1995. Human cyclin E, a nuclear protein essential for the G1-to-S phase transition. *Mol Cell Biol,* 15**,** 2612-24.
OKADA, S., NAKAUCHI, H., NAGAYOSHI, K., NISHIKAWA, S., MIURA, Y. & SUDA, T. 1992. In vivo and in vitro stem cell function of c-kit- and Sca-1-positive murine hematopoietic cells. *Blood,* 80**,** 3044-50.
OSAWA, M., HANADA, K., HAMADA, H. & NAKAUCHI, H. 1996. Long-term lymphohematopoietic reconstitution by a single CD34-low/negative hematopoietic stem cell. *Science,* 273**,** 242-5.
PANIER, S. & BOULTON, S. J. 2014. Double-strand break repair: 53BP1 comes into focus. *Nat Rev Mol Cell Biol,* 15**,** 7-18.
PECK, R. A., HEWETT, J., HARDING, M. W., WANG, Y. M., CHATURVEDI, P. R., BHATNAGAR, A., ZIESSMAN, H., ATKINS, F. & HAWKINS, M. J. 2001. Phase I and pharmacokinetic study of the novel MDR1 and MRP1 inhibitor biricodar administered alone and in combination with doxorubicin. *J Clin Oncol,* 19**,** 3130-41.

PFLUMIO, F., IZAC, B., KATZ, A., SHULTZ, L. D., VAINCHENKER, W. & COULOMBEL, L. 1996. Phenotype and function of human hematopoietic cells engrafting immune-deficient CB17-severe combined immunodeficiency mice and nonobese diabetic-severe combined immunodeficiency mice after transplantation of human cord blood mononuclear cells. *Blood,* 88**,** 3731-40.

PIETRAS, E. M., REYNAUD, D., KANG, Y.-A., CARLIN, D., CALERO-NIETO, F. J., LEAVITT, A. D., STUART, J. M., GÖTTGENS, B. & PASSEGUÉ, E. 2015. Functionally distinct subsets of lineage-biased multipotent progenitors control blood production in normal and regenerative conditions. *Cell stem cell,* 17**,** 35-46.

POPAT, U., DE LIMA, M. J., SALIBA, R. M., ANDERLINI, P., ANDERSSON, B. S., ALOUSI, A. M., HOSING, C., NIETO, Y., PARMAR, S., KHOURI, I. F., KEBRIAEI, P., QAZILBASH, M., CHAMPLIN, R. E. & GIRALT, S. A. 2012. Long-term outcome of reduced-intensity allogeneic hematopoietic SCT in patients with AML in CR. *Bone Marrow Transplant,* 47**,** 212-6.

PRATCORONA, M., BRUNET, S., NOMDEDEU, J., RIBERA, J. M., TORMO, M., DUARTE, R., ESCODA, L., GUARDIA, R., QUEIPO DE LLANO, M. P., SALAMERO, O., BARGAY, J., PEDRO, C., MARTI, J. M., TORREBADELL, M., DIAZ-BEYA, M., CAMOS, M., COLOMER, D., HOYOS, M., SIERRA, J. & ESTEVE, J. 2013. Favorable outcome of patients with acute myeloid leukemia harboring a low-allelic burden FLT3-ITD mutation and concomitant NPM1 mutation: relevance to post-remission therapy. *Blood,* 121**,** 2734-8.

PROCHAZKA, M., GASKINS, H. R., SHULTZ, L. D. & LEITER, E. H. 1992. The nonobese diabetic scid mouse: model for spontaneous thymomagenesis associated with immunodeficiency. *Proc Natl Acad Sci U S A,* 89**,** 3290-4.

PROKOCIMER, M., SHAKLAI, M., BASSAT, H. B., WOLF, D., GOLDFINGER, N. & ROTTER, V. 1986. Expression of p53 in human leukemia and lymphoma. *Blood,* 68**,** 113-8.

ROBAK, T. 2003. Purine Nucleoside Analogues in the Treatment of Myleoid Leukemias. *Leukemia & Lymphoma,* 44**,** 391-409.

ROBLES, C., KIM, K. M., OKEN, M. M., BENNETT, J. M., LETENDRE, L., WIERNIK, P. H., O'CONNELL, M. J. & CASSILETH, P. A. 2000. Low-dose cytarabine maintenance therapy vs observation after remission induction in advanced acute myeloid leukemia: an Eastern Cooperative Oncology Group Trial (E5483). *Leukemia,* 14**,** 1349-53.

ROSSI, D. J., SEITA, J., CZECHOWICZ, A., BHATTACHARYA, D., BRYDER, D. & WEISSMAN, I. L. 2007. Hematopoietic stem cell quiescence attenuates DNA damage response and permits DNA damage accumulation during aging. *Cell Cycle,* 6**,** 2371-6.

RUBE, C. E., FRICKE, A., WIDMANN, T. A., FURST, T., MADRY, H., PFREUNDSCHUH, M. & RUBE, C. 2011. Accumulation of DNA damage in hematopoietic stem and progenitor cells during human aging. *PLoS One,* 6**,** e17487.

SANCAR, A., LINDSEY-BOLTZ, L. A., UNSAL-KACMAZ, K. & LINN, S. 2004. Molecular mechanisms of mammalian DNA repair and the DNA damage checkpoints. *Annu Rev Biochem,* 73**,** 39-85.

SARRY, J.-E., MURPHY, K., PERRY, R., SANCHEZ, P. V., SECRETO, A., KEEFER, C., SWIDER, C. R., STRZELECKI, A.-C., CAVELIER, C., XE, CHER, C., MANSAT-DE MAS, V., XE, RONIQUE, DELABESSE, E., DANET-DESNOYERS, G. & CARROLL, M. 2011. Human acute myelogenous leukemia stem cells are rare and heterogeneous when assayed in NOD/SCID/IL2Rγc-deficient mice. *The Journal of Clinical Investigation,* 121**,** 384-395.

SAVIC, V., YIN, B., MAAS, N. L., BREDEMEYER, A. L., CARPENTER, A. C., HELMINK, B. A., YANG-IOTT, K. S., SLECKMAN, B. P. & BASSING, C. H. 2009. Formation of dynamic gamma-H2AX domains along broken DNA strands is distinctly regulated by ATM and MDC1 and dependent upon H2AX densities in chromatin. *Mol Cell,* 34**,** 298-310.

SCHARENBERG, C. W., HARKEY, M. A. & TOROK-STORB, B. 2002. The ABCG2 transporter is an efficient Hoechst 33342 efflux pump and is preferentially expressed by immature human hematopoietic progenitors. *Blood,* 99**,** 507-12.

SCHOCH, C., KERN, W., KOHLMANN, A., HIDDEMANN, W., SCHNITTGER, S. & HAFERLACH, T. 2005. Acute myeloid leukemia with a complex aberrant karyotype is a distinct biological entity characterized by genomic imbalances and a specific gene expression profile. *Genes Chromosomes Cancer,* 43**,** 227-38.

SCHRODER, J. K., KIRCH, C., FLASSHOVE, M., KALWEIT, H., SEIDELMANN, M., HILGER, R., SEEBER, S. & SCHUTTE, J. 1996. Constitutive overexpression of the cytidine deaminase gene confers resistance to cytosine arabinoside in vitro. *Leukemia,* 10**,** 1919-24.

SEEDHOUSE, C. H., HUNTER, H. M., LLOYD-LEWIS, B., MASSIP, A. M., PALLIS, M., CARTER, G. I., GRUNDY, M., SHANG, S. & RUSSELL, N. H. 2006. DNA repair contributes to the drug-resistant phenotype of primary acute myeloid leukaemia cells with FLT3 internal tandem duplications and is reversed by the FLT3 inhibitor PKC412. *Leukemia,* 20**,** 2130-2136.

SELUANOV, A., MAO, Z. & GORBUNOVA, V. 2010. Analysis of DNA Double-strand Break (DSB) Repair in Mammalian Cells. *Journal of Visualized Experiments : JoVE***,** 2002.

SHIEH, S. Y., AHN, J., TAMAI, K., TAYA, Y. & PRIVES, C. 2000. The human homologs of checkpoint kinases Chk1 and Cds1 (Chk2) phosphorylate p53 at multiple DNA damage-inducible sites. *Genes Dev,* 14**,** 289-300.

SHILOH, Y. 2003. ATM and related protein kinases: safeguarding genome integrity. *Nat Rev Cancer,* 3**,** 155-68.

SHLUSH, L. I., ZANDI, S., MITCHELL, A., CHEN, W. C., BRANDWEIN, J. M., GUPTA, V., KENNEDY, J. A., SCHIMMER, A. D., SCHUH, A. C., YEE, K. W., MCLEOD, J. L., DOEDENS, M., MEDEIROS, J. J. F., MARKE, R., KIM, H. J., LEE, K., MCPHERSON, J. D., HUDSON, T. J., PAN-LEUKEMIA GENE PANEL CONSORTIUM, T. H., BROWN, A. M. K., TRINH, Q. M., STEIN, L. D., MINDEN, M. D., WANG, J. C. Y. & DICK, J. E. 2014. Identification of pre-leukaemic haematopoietic stem cells in acute leukaemia. *Nature,* 506**,** 328-333.

SHORT, N. J. & RAVANDI, F. 2016. Acute Myeloid Leukemia: Past, Present, and Prospects for the Future. *Clinical Lymphoma Myeloma and Leukemia,* 16, Supplement**,** S25-S29.

SHULTZ, L. D., LYONS, B. L., BURZENSKI, L. M., GOTT, B., CHEN, X., CHALEFF, S., KOTB, M., GILLIES, S. D., KING, M., MANGADA, J., GREINER, D. L. & HANDGRETINGER, R. 2005. Human lymphoid and myeloid cell development in NOD/LtSz-scid IL2R gamma null mice engrafted with mobilized human hemopoietic stem cells. *J Immunol,* 174**,** 6477-89.

SMARDOVA, J., PAVLOVA, S., SVITAKOVA, M., GROCHOVA, D. & RAVCUKOVA, B. 2005. Analysis of p53 status in human cell lines using a functional assay in yeast: detection of new non-sense p53 mutation in codon 124. *Oncol Rep,* 14**,** 901-7.

SONG, J. H., KIM, S. H., KWEON, S. H., LEE, T. H., KIM, H. J., KIM, H. J. & KIM, T. S. 2009. Defective expression of deoxycytidine kinase in cytarabine-resistant acute myeloid leukemia cells. *Int J Oncol,* 34**,** 1165-71.

SOUSSI, T., ISHIOKA, C., CLAUSTRES, M. & BEROUD, C. 2006. Locus-specific mutation databases: pitfalls and good practice based on the p53 experience. *Nat Rev Cancer,* 6**,** 83-90.

SPANGRUDE, G. J., HEIMFELD, S. & WEISSMAN, I. L. 1988. Purification and characterization of mouse hematopoietic stem cells. *Science,* 241**,** 58-62.

STEGMANN, A. P., HONDERS, M. W., KESTER, M. G., LANDEGENT, J. E. & WILLEMZE, R. 1993. Role of deoxycytidine kinase in an in vitro model for AraC- and DAC-resistance: substrate-enzyme interactions with deoxycytidine, 1-beta-D-arabinofuranosylcytosine and 5-aza-2'-deoxycytidine. *Leukemia,* 7**,** 1005-11.

STROUT, M. P., MRÓZEK, K., HEINONEN, K., SAIT, S. N. J., SHOWS, T. B. & APLAN, P. D. 1996. ML-1 cell line lacks a germline MLL locus. *Genes, Chromosomes and Cancer,* 16**,** 204-210.

SUDA, T., TAKUBO, K. & SEMENZA, G. L. 2011. Metabolic regulation of hematopoietic stem cells in the hypoxic niche. *Cell Stem Cell,* 9**,** 298-310.

SUGIMOTO, K., TOYOSHIMA, H., SAKAI, R., MIYAGAWA, K., HAGIWARA, K., ISHIKAWA, F., TAKAKU, F., YAZAKI, Y. & HIRAI, H. 1992. Frequent mutations in the p53 gene in human myeloid leukemia cell lines. *Blood,* 79**,** 2378-83.

SUGIYAMA, T. & KOWALCZYKOWSKI, S. C. 2002. Rad52 Protein Associates with Replication Protein A (RPA)-Single-stranded DNA to Accelerate Rad51-mediated Displacement of RPA and Presynaptic Complex Formation. *Journal of Biological Chemistry,* 277**,** 31663-31672.

SUNDSTROM, C. & NILSSON, K. 1976. Establishment and characterization of a human histiocytic lymphoma cell line (U-937). *Int J Cancer,* 17**,** 565-77.

SUTHERLAND, H. J., EAVES, C. J., EAVES, A. C., DRAGOWSKA, W. & LANSDORP, P. M. 1989. Characterization and partial purification of human marrow cells capable of initiating long-term hematopoiesis in vitro. *Blood,* 74**,** 1563-70.

TAKAHASHI, M., MATSUOKA, Y., SUMIDE, K., NAKATSUKA, R., FUJIOKA, T., KOHNO, H., SASAKI, Y., MATSUI, K., ASANO, H., KANEKO, K. &

SONODA, Y. 2014. CD133 is a positive marker for a distinct class of primitive human cord blood-derived CD34-negative hematopoietic stem cells. *Leukemia,* 28**,** 1308-15.

TAUSSIG, D. C., MIRAKI-MOUD, F., ANJOS-AFONSO, F., PEARCE, D. J., ALLEN, K., RIDLER, C., LILLINGTON, D., OAKERVEE, H., CAVENAGH, J., AGRAWAL, S. G., LISTER, T. A., GRIBBEN, J. G. & BONNET, D. 2008. Anti-CD38 antibody–mediated clearance of human repopulating cells masks the heterogeneity of leukemia-initiating cells. *Blood,* 112**,** 568-575.

TAUSSIG, D. C., VARGAFTIG, J., MIRAKI-MOUD, F., GRIESSINGER, E., SHARROCK, K., LUKE, T., LILLINGTON, D., OAKERVEE, H., CAVENAGH, J., AGRAWAL, S. G., LISTER, T. A., GRIBBEN, J. G. & BONNET, D. 2010. Leukemia-initiating cells from some acute myeloid leukemia patients with mutated nucleophosmin reside in the CD34(−) fraction. *Blood,* 115**,** 1976-1984.

TILL, J. E. & MCCULLOCH, E. A. 1961. A Direct Measurement of the Radiation Sensitivity of Normal Mouse Bone Marrow Cells. *Radiation Research,* 14**,** 213-222.

TRECCA, D., LONGO, L., BIONDI, A., CRO, L., CALORI, R., GRIGNANI, F., MAIOLO, A. T., PELICCI, P. G. & NERI, A. 1994. Analysis of p53 gene mutations in acute myeloid leukemia. *Am J Hematol,* 46**,** 304-9.

UZIEL, T., LERENTHAL, Y., MOYAL, L., ANDEGEKO, Y., MITTELMAN, L. & SHILOH, Y. 2003. Requirement of the MRN complex for ATM activation by DNA damage. *The EMBO Journal,* 22**,** 5612-5621.

VAN PELT, K., DE HAAN, G., VELLENGA, E. & DAENEN, S. M. G. J. 2005. Administration of low-dose cytarabine results in immediate S-phase arrest and subsequent activation of cell cycling in murine stem cells. *Experimental Hematology,* 33**,** 226-231.

VEUGER, M. J. T., HONDERS, M. W., LANDEGENT, J. E., WILLEMZE, R. & BARGE, R. M. Y. 2000. High incidence of alternatively spliced forms of deoxycytidine kinase in patients with resistant acute myeloid leukemia. *Blood,* 96**,** 1517-1524.

VIALE, A., DE FRANCO, F., ORLETH, A., CAMBIAGHI, V., GIULIANI, V., BOSSI, D., RONCHINI, C., RONZONI, S., MURADORE, I., MONESTIROLI, S., GOBBI, A., ALCALAY, M., MINUCCI, S. & PELICCI, P. G. 2009. Cell-cycle restriction limits DNA damage and maintains self-renewal of leukaemia stem cells. *Nature,* 457**,** 51-6.

WEINSTEIN, H. J., GRIFFIN, T. W., FEENEY, J., COHEN, H. J., PROPPER, R. D. & SALLAN, S. E. 1982. Pharmacokinetics of continuous intravenous and subcutaneous infusions of cytosine arabinoside. *Blood,* 59**,** 1351-3.

WIEDERSCHAIN, D., KAWAI, H., SHILATIFARD, A. & YUAN, Z. M. 2005. Multiple mixed lineage leukemia (MLL) fusion proteins suppress p53-mediated response to DNA damage. *J Biol Chem,* 280**,** 24315-21.

WILEY, J. S., JONES, S. P., SAWYER, W. H. & PATERSON, A. R. 1982. Cytosine arabinoside influx and nucleoside transport sites in acute leukemia. *J Clin Invest,* 69**,** 479-89.

WILL, B., ZHOU, L., VOGLER, T. O., BEN-NERIAH, S., SCHINKE, C., TAMARI, R., YU, Y., BHAGAT, T. D., BHATTACHARYYA, S., BARREYRO, L.,

HEUCK, C., MO, Y., PAREKH, S., MCMAHON, C., PELLAGATTI, A., BOULTWOOD, J., MONTAGNA, C., SILVERMAN, L., MACIEJEWSKI, J., GREALLY, J. M., YE, B. H., LIST, A. F., STEIDL, C., STEIDL, U. & VERMA, A. 2012. Stem and progenitor cells in myelodysplastic syndromes show aberrant stage-specific expansion and harbor genetic and epigenetic alterations. *Blood,* 120**,** 2076-86.

WILLINGER, T., RONGVAUX, A., STROWIG, T., MANZ, M. G. & FLAVELL, R. A. 2011. Improving human hemato-lymphoid-system mice by cytokine knock-in gene replacement. *Trends Immunol,* 32**,** 321-7.

WILSON, A., LAURENTI, E., OSER, G., VAN DER WATH, R. C., BLANCO-BOSE, W., JAWORSKI, M., OFFNER, S., DUNANT, C. F., ESHKIND, L., BOCKAMP, E., LIO, P., MACDONALD, H. R. & TRUMPP, A. 2008. Hematopoietic stem cells reversibly switch from dormancy to self-renewal during homeostasis and repair. *Cell,* 135**,** 1118-29.

WULF, G. G., WANG, R. Y., KUEHNLE, I., WEIDNER, D., MARINI, F., BRENNER, M. K., ANDREEFF, M. & GOODELL, M. A. 2001. A leukemic stem cell with intrinsic drug efflux capacity in acute myeloid leukemia. *Blood,* 98**,** 1166-73.

YAMAMOTO, R., MORITA, Y., OOEHARA, J., HAMANAKA, S., ONODERA, M., RUDOLPH, KARL L., EMA, H. & NAKAUCHI, H. 2013. Clonal Analysis Unveils Self-Renewing Lineage-Restricted Progenitors Generated Directly from Hematopoietic Stem Cells. *Cell,* 154**,** 1112-1126.

YAMASHITA, M., NITTA, E. & SUDA, T. 2015. Aspp1 Preserves Hematopoietic Stem Cell Pool Integrity and Prevents Malignant Transformation. *Cell Stem Cell,* 17**,** 23-34.

YANG, L., BRYDER, D., ADOLFSSON, J., NYGREN, J., MANSSON, R., SIGVARDSSON, M. & JACOBSEN, S. E. 2005. Identification of Lin(-)Sca1(+)kit(+)CD34(+)Flt3- short-term hematopoietic stem cells capable of rapidly reconstituting and rescuing myeloablated transplant recipients. *Blood,* 105**,** 2717-23.

YU, J. & ZHANG, L. 2003. No PUMA, no death: implications for p53-dependent apoptosis. *Cancer Cell,* 4**,** 248-9.

ZHOU, T., HASTY, P., WALTER, C. A., BISHOP, A. J., SCOTT, L. M. & REBEL, V. I. 2013. Myelodysplastic syndrome: an inability to appropriately respond to damaged DNA? *Exp Hematol,* 41**,** 665-74.

ZOU, L. & ELLEDGE, S. J. 2003. Sensing DNA damage through ATRIP recognition of RPA-ssDNA complexes. *Science,* 300**,** 1542-8.